Thanh-Phong Mai

Experimental Investigation of Heterogeneously Catalyzed Hydrolysis of Esters

Experimental Investigation of Heterogeneously Catalyzed Hydrolysis of Esters

Dissertation

zur Erlangung des akademischen Grades

Doktoringenieur
(Dr.-Ing.)

von M. Eng. **Thanh-Phong Mai**

geb. am 03/02/1972 in Ha-Tinh, Vietnam

genehmigt durch die Fakultät für Verfahrens- und Systemtechnik
der Otto-von-Guericke-Universität Magdeburg

Gutachter:
> Prof. Dr.-Ing. Andreas Seidel-Morgenstern
> Prof. Dr.-Ing. Achim Kienle

Promotionskolloquium am 19. Dezember 2006

Abstract

The thermodynamics and kinetics of the hydrolysis of four esters (methyl formate, methyl acetate, ethyl formate, and ethyl acetate) were investigated experimentally and theoretically. An acidic ion-exchange resin was used as heterogeneous catalyst and adsorbent. Alternatively, hydrochloric acid was used as a homogeneous catalyst.

The chemical reaction equilibrium was measured for various temperatures and initial concentrations of the reactants using conventional batch reactor runs. The influence of the absence and presence of the solid catalyst on the liquid-phase equilibrium composition was also studied in a batch reactor. The relevant distribution equilibria of the components involved were quantified based on pulse chromatographic experiments. To investigate the kinetics of the four reactions, a reaction calorimeter was employed. Systematic experiments to measure heat flows due to reaction were carried out with catalyst suspensions in the calorimeter. Reaction rate constants were quantified from the measured heat flows. The four hydrolysis reactions were found to proceed with very different reaction rates. The fastest reaction was the hydrolysis of methyl formate. The slowest was the hydrolysis of ethyl acetate. For comparison, reaction rate constants were also quantified from concentration-time profiles recorded in conventional batch experiments.

A simplified pseudo-homogeneous model and the determined parameters were found to be capable of describing the heat flows measured in the reaction calorimeter for all reactions studied under diverse operating conditions.

The thermodynamic and kinetic parameters determined in this work form a platform to design and optimize chromatographic reactors for the hydrolysis reactions investigated and the corresponding esterifications.

Zusammenfassung

In dieser Arbeit wurde die Thermodynamik und Kinetik der homogen und heterogen katalysierten Hydrolyse von vier Estern (Methylformiat, Methylacetat, Ethylformiat und Ethylacetat) theoretisch und experimentell untersucht. Ein saurer Ionenaustauscher wurde als fester Katalysator und gleichzeitig als Adsorbent verwendet. Außerdem wurde alternativ Salzsäure als homogener Katalysator eingesetzt.

Das Reaktionsgleichgewicht wurde für verschiedene Temperaturen und Ausgangskonzentrationen der Reaktanten experimentell untersucht. Der Einfluss des Feststoffkatalysators auf die Gleichgewichtskonzentrationen in der flüssigen Phase wurde analysiert. Für die Ermittlung der Reaktionskinetik der vier Reaktionen wurde ein Reaktionskalorimeter eingesetzt in dem Katalysatorsuspensionen vorgelegt werden konnten. Die Gleichgewichtsverteilung der Komponenten zwischen der flüssigen und festen Phase wurde mittels chromatographischer Pulsexperimente quantifiziert. Zur Bestimmung der Reaktionsgeschwindigkeitskonstanten dienten gemessene Wärmeströme. Es wurde festgestellt, dass die Reaktionsraten der vier untersuchten Reaktionen sehr unterschiedlichen sind. Die schnellste Reaktion ist die Hydrolyse von Methylformiat, die langsamste ist die Hydrolyse von Ethylacetat. Darüber hinaus wurden die Reaktionsraten auch in konventionellen Batch-Versuchen durch Messung von Konzentrations-Zeit-Profilen quantifiziert. Eine gute Übereinstimmung der Ergebnisse aus kalorimetrichen Messungen und Batch-Versuchen wurde festgestellt.

Für die quantitative Beschreibung der Wärmeströme im Reaktionskalorimeter konnte erfolgreich ein vereinfachtes pseudohomogenes Modell eingesetzt werden.

Die in dieser Arbeit ermittelten Parameter (Reaktionsgleichgewichtskonstanten und Reaktionsgeschwindigkeitskonstanten) konnten durch unabhängige Versuche validiert werden. Diese Parameter können für die Auslegung und Optimierung chromatographischer Reaktoren zur effizienten Durchführung dieser reversiblen Hydrolysereaktionen bzw. der korrespondierenden Veresterungen verwendet werden.

Acknowledgements

Contents

Introduction

Information and knowledge from thermodynamics and chemical kinetics are of great importance to properly predict chemical reactions and to design chemical reactors. Thermodynamics tell us in which direction a reaction system will develop and how far it is from its equilibrium state. Analyses of kinetics provide information about the rate with which the system will approach equilibrium.

In recent years, several new and more sophisticated reactor types have been suggested and attract interest from researchers all over the world [Sund05]. One of these new reactor types is the so-called chromatographic reactor. Before introducing the principle of chromatographic reactors, which need to be understood better to apply them successfully, a short introduction into thermodynamics and kinetics will be given.

1.1 Thermodynamics

The science of thermodynamics was born in the nineteenth century in order to describe the operation of steam engines and to set forth the limits of what they can accomplish. However, the principles observed to be valid for engines were soon generalized into postulates now known as the first and second laws of thermodynamics [Smith96]. Extensive introductions to thermodynamics can be found in many textbooks (e.g., [Smith96], [Sand99]). Thermodynamics is a study of energy changes accompanying physical and chemical changes. It is based on macroscopic-property formulations dealing with the average changes that occur among larger numbers of molecules, rather than with detailed (microscopic) changes that occur in a single molecule. On the other hand,

knowledge of microscopic behavior of matter can be useful in the calculation of thermodynamic properties. The region of the universe under study, which may be a specified volume in space or a quantity of matter, is typically called the *system*. A system is separated from the rest of the universe, called the surroundings, by a boundary which may be imaginary or not, but which by convention defines a finite volume. The possible exchanges of work, heat, or matter between the system and the surroundings take place across this boundary. A system is said to be *isolated*, if matter and energy can not cross the boundary, i.e., the system does not change as a result of changes in its surroundings. An *adiabatic* system is one that is thermally isolated from its surroundings; that is, heat can not cross the boundary. If matter can flow into or out of a thermodynamic system, the system is said to be *open*; if not, the system is *closed*.

The state of a system characterized by properties such as temperature, pressure, density, composition, etc. is referred to the *thermodynamic state* of the system. These properties do not depend on the past history of the system nor on the means by which it has reached a given state. They depend only on the present conditions. The corresponding properties are known as *state properties* or *functions*.

An important concept in thermodynamics is the equilibrium state. General characteristics of an equilibrium state are that (1) the state does not vary with time; (2) the system is uniform (i.e., there are no internal temperature, pressure, velocity, or concentration gradients) or is composed of subsystems each of which is uniform; (3) all flows of heat, mass or work between the system and its surroundings are zero; and (4) the net rate of all chemical reactions is zero [Sand99].

There is a comprehensive theoretical framework available to predict many essential thermodynamic properties of systems containing several components (or species) [Smith96]. This toolbox provides e.g., enthalpies of phase transition and reaction, and allows to predict the distribution of the components between several phases [O´con05].

Equilibrium requires that the rates of all possible reactions between the components of the system are zero. This state is often not reached in industrially applied chemical reactors.

1.2 Kinetics of Chemical Reactions

Chemical kinetics is concerned with the rates of chemical reactions (i.e., with the quantitative description of how fast the reactions occur) and the factors affecting these rates [Miss99]. In contrast to thermodynamics these rates can be often determined only

experimentally. Typically, a laboratory scale reactor is used to carry out the reaction to quantify the dependences of rates on various factors, such as concentrations of species and temperature. The primary goal of chemical kinetics is the development and validation of a rate law (for a single system) or a set of rate laws (for complex reaction systems). Approaches to study a reaction are normally based on the following aspects (not necessarily in the order listed) [Miss99]:

1. Choice of type of reactor to be used and certain features relating to its mode of operation (e.g., a batch reactor operated at constant volume).
2. Choice of species (reactant or product) to follow during the experiments (e.g., by chemical analysis).
3. Choice of method to follow the extent of reaction with respect to time (e.g., by spectroscopic or chromatographic analysis).
4. Choice of method to determine numerically the values of the parameters, and hence to establish the form of the rate law.

For a simple system, it is only necessary to follow the extent of reaction by means of a suitable measurement. This may be the concentration of one species. Batch reactors are traditionally used (see e.g., [Mazz97a], [Grop06], [Silva06]). The measurement of the relevant concentration-time courses is often time-consuming and tedious. A standard operation mode of reversible reactions is fixed-bed reactor. The common limitation in the performance of this type of reaction is that no complete conversion can be achieved. For this reason, chromatographic reactors are used widely as research tools.

1.3 Chromatographic Reactors

A powerful concept to perform reversible reactions in an efficient way is based on applying chromatographic separation principles simultaneously with the chemical reactions. Such chromatographic reactors have attracted the attention of researchers already for more than 40 years [Borr05]. However, there are still not much industrial applications.

The principles of chromatographic reactors that combine a reversible chemical reaction with a chromatographic separation are illustrated as in Figure 1.1. In this figure, a reaction of the type

$$A \rightleftharpoons B + C \qquad\qquad (1.1)$$

is used as an example to explain the operating principles.

In the example considered it is assumed that the reactant A has intermediate adsorption behavior and the products B and C are the more strongly and weakly adsorbed components. Reactant A is injected periodically as a pulse into the column. During its propagation along the column, A reacts to B and C. Owing to the different adsorption behavior of A, B and C, all components propagate with different velocities and are separated from each other. This restricts the backward reaction between B and C. Therefore, the restriction of an equilibrium-limited reaction can be overcome to convert the reactant A totally [Borr05]. Species leaving the chromatographic reactor can be detected using a suitable detector and recorded as a signal versus time in the chromatogram.
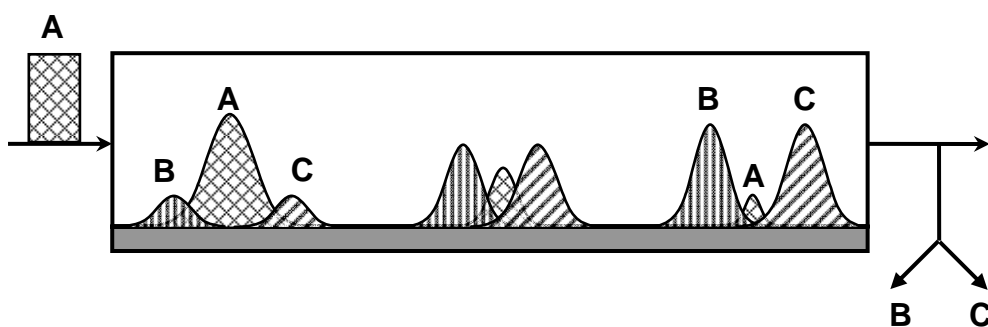
Figure 1.1. Principles of chromatographic reactors.

Figure 1.2 shows detector signals of a conventional UV-detector placed at the reactor outlet which were reported in the work of Falk *et al.* [Falk02]. The heterogeneously catalyzed hydrolysis of methyl formate ($HCOOCH_3$) to methanol (CH_3OH) and formic acid ($HCOOH$) was chosen as a model reaction. An acidic ion exchange resin was used as catalyst and adsorbent. It can be seen from Figure 1.2a that only a part of the ester is converted and there is not sufficient separation between the two products, whereas with a lower flow rate the ester can be converted completely and it is sufficient to separate the products (Figure 1.2b). The authors observed complex shapes of the profiles in Figure 1.2a revealing that it is not trivial task to select appropriate conditions to operate successfully such a reactor. For this end, the application of a suitable mathematical model appears to be mandatory.

Mathematical treatments of reaction chromatogram data are applied to quantify kinetic parameters, and hence to establish the actual form of the rate law. Examples of applications of chromatographic reactors for kinetic studies abound. Some of them can be seen in refs. [Bolm83], [Jeng92], [Mazz97b], and [Falk02].
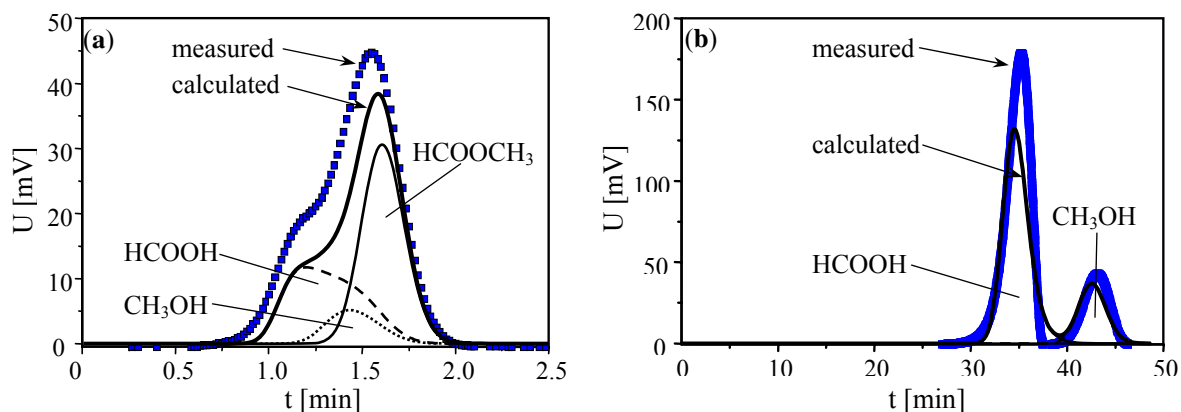
Figure 1.2. Comparisons of measured (symbols) and simulated (lines) detector signals. Influence of the flow rate for $V^{inj} = 20$ μL and $c_A^{inj} = 0.725$ mol/L: **a)** $\dot{V} = 2.5$ mL/min, **b)** $\dot{V} = 0.1$ mL/min [Falk02].

An alternative approach to the quantification of reaction rates that is rarely considered in this field is the application of calorimetry [Land91, Land94]. An accurate measurement of the time dependence of heat effects related to reactions allows one to quantify reaction rates [Hass00].

There is a relatively large number of studies available in the literature which report on the kinetics and chemical equilibrium of hydrolysis (e.g., [Weth74], [Cho80a], [Falk02]) and esterification (e.g., [Sard79], [Mazz97a], [Pöpk01], [Gelo03], [Sainio04], [Grob06]). In most cases, the same solid acting simultaneously as adsorbent and catalyst is used. A typical example of such solid is given by ion-exchange resins, such as those based on a microporous styrene-divinylbenzene copolymer functionalized by various amounts of sulfonic groups, which provide the acidity necessary for the catalytic function. In other cases, strongly mineral acids such as hydrochloric acid and sulfuric acid are used. However, comprehensive studies of these reactions are still lacking. This reveals that a thorough study of these reactions under catalysis of ion-exchange resins is necessary.

1.4 Aim and Outline

The aim of this work is to analyze experimentally the thermodynamics and chemical kinetics of four heterogeneously catalyzed ester hydrolysis reactions, and hence to enlarge the database related to these reactions.

For this, the reactions were studied in a reaction calorimeter. The aim includes: • the theoretical and experimental analysis of the phase equilibria of the multicomponent liquid mixtures in the absence and presence of a solid adsorbent/catalyst; • the theoretical and experimental study of the chemical reaction equilibria in the homogeneous and heterogeneous systems; • the experimental investigation of the chemical kinetics of the reactions catalyzed by a specific ion-exchange resin.

In order to achieve the aim of this work, the basics of thermodynamics governing chemical and phase equilibria, and of chemical kinetics are revised first in Chapter 2. This chapter explains theoretically the phase equilibrium behavior of multicomponent systems in the absence and presence of an ion-exchange resin. Mathematical equations for calculation of the liquid phase composition at equilibrium in the presence of an ion-exchange resin are presented as well in this chapter. Then expressions capable to describe the rates of homogeneously and heterogeneously catalyzed reactions are included. The concept of activity and activity coefficients used in the treatment of the non-ideal solutions is also introduced in this chapter.

The four model reactions, which are investigated during the work, are introduced subsequently in Chapter 3. This chapter includes also the description of the ion-exchange resin used.

Chapter 4 presents the calorimetric technique used and the models describing the reaction calorimeter. The equipments and experimental procedures used are described in Chapter 5.

In Chapter 6, the results obtained from the study are reported and discussed. This includes in particular the presentation of the determined reaction equilibrium data and the rate constants of the heterogeneously catalyzed reactions.

Finally, the summary and conclusions of the work are given in Chapter 7.

Theoretical Aspects

A substantial knowledge of thermodynamics governing chemical and phase equilibria, and of chemical kinetics is needed in order to understand chromatographic reactors. Concepts, principles and theories of thermodynamics that relate to chemical and phase equilibria, and chemical kinetics necessary for this work are shortly introduced in this chapter. General classic references are [Smith96], [Sand99], [Prau99], [O´con05], [Smith81], [Conn90], [Leven99] and [Miss99].

General equilibrium criteria for systems containing multicomponent mixtures are introduced in Section 2.1. These criteria are then used to establish the conditions of phase equilibrium for heterogeneous closed systems (Section 2.1.1), phase equilibria for systems containing a cross-linked elastic polymer phase in contact with a surrounding liquid phase (Section 2.1.2) and chemical reaction equilibria for reacting systems (Section 2.2). Adsorption isotherms as a special case of phase equilibria are discussed in Section 2.1.3. Section 2.2 also focuses on the calculation of equilibrium compositions for systems that contain a reacting liquid mixture and an ion-exchange resin. Reaction kinetics are discussed in Section 2.3. Finally, the activities of components in solution and the calculation of activity coefficients are introduced in Section 2.4.

2.1 Phase Equilibria

Phase compositions at equilibrium depend on several variables, such as temperature and pressure, and on the chemical nature and concentrations of the substances in the system. Phase equilibrium thermodynamics seeks to establish the relations among various state

properties (in particular temperature, pressure, and composition) that ultimately prevail when one or more phases reach the state of equilibrium wherein all tendency for further change has ceased [Prau99].

The equilibrium criteria for a closed multicomponent system are found to be as shown in Eq. (2.1), where S, G, A, and U stand respectively for the entropy, Gibbs free energy, Helmholtz free energy and internal energy of the system; M, T, p and V for the mass, temperature, pressure and volume of the system [Smith96, Sand99, O´con05]:

- S = maximum for equilibrium at constant M, U, and V
- G = minimum for equilibrium at constant M, T, and p (2.1)
- A = minimum for equilibrium at constant M, T, and V

For a non-reactive closed system, a combined statement of the first and second laws of thermodynamics is [Prau99]:

$$dU = TdS - pdV \qquad (2.2)$$

If the system is open, e.g., connected to another system, a change in composition must be taken into account as expressed in the following equation:

$$dU = TdS - pdV + \sum_{i=1}^{N_c} \mu_i dn_i \qquad (2.3)$$

or in another arrangement:

$$dS = \frac{1}{T} dU + \frac{p}{T} dV - \frac{1}{T} \sum_{i=1}^{N_c} \mu_i dn_i \qquad (2.4)$$

where μ_i is the chemical potential (equal to the partial molar Gibbs free energy) of component i, n_i is the mole number of component i and N_c is the number of components in the system.

2.1.1 Phase Equilibrium in a Two-Phase Closed System

Within a non-reactive closed system consisting of two phases, each of the individual phases is an open system because of the possible exchange with the other phase. Equation (2.4) may therefore be written for each phase:

$$dS^I = \frac{1}{T^I} dU^I + \frac{p^I}{T^I} dV^I - \frac{1}{T^I} \sum_{i=1}^{N_c} \mu_i^I dn_i^I \qquad (2.5a)$$

$$dS^{II} = \frac{1}{T^{II}} dU^{II} + \frac{p^{II}}{T^{II}} dV^{II} - \frac{1}{T^{II}} \sum_{i=1}^{N_c} \mu_i^{II} dn_i^{II} \qquad (2.5b)$$

where superscripts *I* and *II* identify the phases.

Considering a closed, adiabatic constant-volume system, the equilibrium criterion is $S =$ maximum subject to the constraints of constant *U*, *V*, and total number of moles of each components n_i. Thus, the following equation must hold at equilibrium:

$$dS = dS^I + dS^{II} = 0 \qquad (2.6)$$

Since the total internal energy, total volume, and the number of moles of each component are fixed, one can have

$$
\begin{aligned}
dU^{II} &= -dU^I \\
dV^{II} &= -dV^I \qquad\qquad\qquad\qquad i = 1,\dots, N_c \qquad (2.7)\\
dn_i^{II} &= -dn_i^I
\end{aligned}
$$

Substituting Eq. (2.7) into Eqs. (2.5a-b), Eq. (2.6) can be rewritten as follows:

$$dS = \left(\frac{1}{T^I} - \frac{1}{T^{II}} \right) dU^I + \left(\frac{p^I}{T^I} - \frac{p^{II}}{T^{II}} \right) dV^I - \sum_{i=1}^{N_c} \left(\frac{\mu_i^I}{T^I} - \frac{\mu_i^{II}}{T^{II}} \right) dn_i^I = 0 \qquad (2.8)$$

The conditions for equilibrium are that the differentials of the entropy with respect to all variations of the independent and unconstrained variables (here dU^I, dV^I and dn_i^I) are zero. Therefore, the following conditions must be met in order for *dS* to be zero:

1) $T^I = T^{II}$ $\qquad\qquad\qquad\qquad\qquad\qquad\qquad\qquad\qquad\qquad\qquad$ (2.9a)

2) $p^I = p^{II}$ $\qquad\qquad\qquad\qquad\qquad\qquad\qquad\qquad\qquad\qquad\qquad$ (2.9b)

3) $\mu_i^I = \mu_i^{II}$ $\qquad\qquad\qquad\qquad\qquad\qquad i = 1,\dots, N_c \qquad\qquad\qquad$ (2.9c)

In other words, for phase equilibrium to exist in a closed, non-reactive multicomponent system at constant energy and volume, the temperature, the pressure and the chemical potential of each component must be the same in each phase.

Alternatively, the basic relation connecting the Gibbs free energy to the temperature and pressure can be expressed as in equation (2.10) for any closed system, and as in equation (2.11) for any open system.

$$dG = Vdp - SdT \tag{2.10}$$

$$dG = Vdp - SdT + \sum_{i=1}^{N_c} \mu_i dn_i \tag{2.11}$$

Equation (2.11) can be written for each of the individual phases in a closed system consisting of two phases as below:

$$dG^I = V^I dp^I - S^I dT^I + \sum_{i=1}^{N_c} \mu_i^I dn_i^I \tag{2.12a}$$

$$dG^{II} = V^{II} dp^{II} - S^{II} dT^{II} + \sum_{i=1}^{N_c} \mu_i^{II} dn_i^{II} \tag{2.12b}$$

Considering a closed system at constant temperature and pressure, the conditions for phase equilibrium can be derived from the equilibrium criterion that G should be a minimum, and the differential of G for the system is therefore equal to zero.

$$dG = dG^I + dG^{II} = 0 \tag{2.13}$$

Substituting Eqs. (2.12a-b) into Eq. (2.13) yields

$$dG = Vdp - SdT + \sum_{i=1}^{N_c} \mu_i^I dn_i^I + \sum_{i=1}^{N_c} \mu_i^{II} dn_i^{II} = 0 \tag{2.14}$$

Since the temperature and pressure are constant, the changes dp and dT are equal to zero. However, in a closed system not undergoing chemical reaction, the number of moles of each component is constant. Thus, mass conversation of each species for the closed system requires that

$$dn_i^{II} = -dn_i^{I} \qquad\qquad i = 1,\ldots, N_c \qquad\qquad (2.15)$$

Substitution of Eq. (2.15) into Eq. (2.14) shows that at equilibrium

$$dG = \sum_{i=1}^{N_c} \left(\mu_i^{I} - \mu_i^{II} \right) dn_i^{I} = 0 \qquad\qquad\qquad (2.16)$$

Setting the derivative of the Gibbs free energy with respect to each of its independent variables (here the mole numbers n_i^{I}) equal to zero yields

$$\mu_i^{I} = \mu_i^{II} \qquad\qquad i = 1,\ldots, N_c \qquad\qquad (2.17)$$

Thus, it is again found that the equality of chemical potentials is a necessary condition for the existence of phase equilibrium for systems subject to a variety of constraints.

These analyses for equilibrium of two-phase systems can easily be generalized to multiphase systems. The result for a φ-phase system is

$$\mu_i^{I} = \mu_i^{II} = \cdots = \mu_i^{\varphi} \qquad\qquad i = 1,\ldots, N_c \qquad\qquad (2.18)$$

2.1.2 Phase Equilibrium in a Solvent–Polymer System

Ion exchange resins, which are defined as insoluble polymers containing charged groups or ions that can be exchanged for charged groups or ions present in a surrounding solution, have been widely used in physical and chemical processes [Willi99]. In particular, a resin based on a microporous styrene-divinylbenzene copolymer, which is functionalized by the sulphuric acid type (SO_3H) will be used as a catalyst in this work (see more details in Section 3.2). An understanding of the corresponding phase equilibria in such a polymer is important. The derivation of quantitative relations that describe phase equilibrium for a polymer in contact with a solvent mixture is introduced below. This has been extensively described in the article of Sainio *et al.*, 2004 [Sainio04] and in the published dissertation of T. Sainio, 2005 [Sainio05]. Main parts are revised below.

Consider a system wherein a cross-linked elastic polymer phase is in contact with a surrounding liquid phase. When a cross-linked elastic polymer comes into contact with a liquid, it can swell until an equilibrium is reached [Flory53]. Chemical species can partition between the polymer and surrounding liquid. In this work, only the distribution of

neutral liquid components, but not ionic species between a liquid phase and the polymer phase is discussed. The term "phase equilibrium" here does not refer to the equilibrium of phase transformation, but to the equilibrium distribution of chemical species between the two phases in contact. The system in this case is considered to consist of a homogeneous polymer solution, a homogeneous surrounding liquid phase, and an elastic structure. The polymer phase behaves like a bulk liquid phase encaged in an elastic structure where the role of the structure is similar to that of a semipermeable membrane in an osmotic equilibrium. The structure discussed here is elastic and therefore the energy of that structure depends on the volume of the polymer phase [Maur96].

As introduced in the previous section, a combined statement of the first and second laws of thermodynamics is expressed as in Eq. (2.2) for a reversible process in a closed system.

$$dU = TdS - pdV \qquad\qquad\qquad (2.2)$$

Any extensive state function of the system is the sum of contributions from all homogeneous phases. Denoting respectively the liquid phase surrounding the polymer, the polymer phase (or the "solid phase") and the elastic structure by L, S and el, one can write the following extensive state functions of the system:

$$dU = dU^L + dU^S + dU^{el} \qquad\qquad\qquad (2.19a)$$

$$dV = dV^L + dV^S + dV^{el} \qquad\qquad\qquad (2.19b)$$

$$dS = dS^L + dS^S + dS^{el} \qquad\qquad\qquad (2.19c)$$

In the classical theory of rubber elasticity, deformation of the elastic structure does not involve changes in the internal energy or volume of the elastic structure, but only changes in its configurational entropy ([Flory53], p. 451). Thus,

$$dU^{el} = 0 \qquad\qquad\qquad (2.20a)$$

$$dV^{el} = 0 \qquad\qquad\qquad (2.20b)$$

At fixed temperature, the elastic behavior of the structure is influenced only by the volume of the solid phase. It should be noted that pressure p in Eq. (2.2) is the external pressure which is equal to p^L. From Eqs. (2.19b) and (2.20b), one can then write:

$$pdV = p^L(dV^L + dV^S)$$ (2.21)

Introducing Eqs. (2.19), (2.20) and (2.21) into Eq. (2.2) leads to

$$dU^L + p^L dV^L - TdS^L + dU^S + p^L dV^S - TdS^S - TdS^{el} = 0$$ (2.22)

Since temperature T and external pressure p^L are constant, the differential of the Gibbs free energy for the liquid and solid phase can be expressed as

$$dG^L = dU^L + p^L dV^L - TdS^L$$ (2.23a)

$$dG^S = dU^S + p^S dV^S + V^S dp^S - TdS^S$$ (2.23b)

Thus, Eq. (2.22) can be rearranged to give

$$dG^L + dG^S + (p^L - p^S)dV^S - V^S dp^S - TdS^{el} = 0$$ (2.24)

At constant temperature T and external pressure p^L, Eq. (2.24) can be simplified to

$$d[G^L + G^S - V^S(p^S - p^L) - TS^{el}] = 0$$ (2.25)

The Gibbs free energy of the solid phase $G^S(T, p^S, n^S)$, wherein the independent variables are temperature T, pressure p^S and mole numbers n_1^S, n_2^S,... etc. denoted by n^S, can be replaced by $G^S(T, p^L, n^S)$ because of the constant external pressure p^L. For this end, one can derive the following relation [Eq. (2.26)] for a change of pressure from p^L to p^S in the solid phase at constant temperature and mole numbers, with an assumption that the solid phase is incompressible when T and p^L are constant.

$$G^S(T, p^S, n^S) = G^S(T, p^L, n^S) + V^S(p^S - p^L)$$ (2.26)

Substituting Eq. (2.26) into Eq. (2.25) yields (n^L is a vector of mole numbers n_1^L, n_2^L,...):

$$d[G^L(T, p^L, n^L) + G^S(T, p^L, n^S) - TS^{el}] = 0$$ (2.27)

It is told by Eq. (2.27) that at equilibrium, for a reversible change at constant temperature T, and external pressure p^L, the sum of the Gibbs free energy of the liquid phase, G^L, and

that of the solid phase, G^S, minus the product of temperature T and the entropy of the elastic structure, S^{el}, reaches a minimum value.

The effect of the elastic response of the polymer structure can be expressed in terms of more easily measured quantities than dS^{el}. The stress in a cross-linked polymer structure due to a deformation by an external force is obtained from the classical theory of rubber elasticity. The nominal stress of an unswollen cross-linked polymer structure (i.e., tensile force per unit area of unswollen undeformed sample) under uniaxial deformation is computed as in Eq. (2.28) [Flory53], where τ is the nominal stress, W is the work of deformation, $V^{S,o}$ is the volume of the unswollen undeformed sample, and α is the deformation factor. Exact and inexact differentials are denoted with d and δ, respectively.

$$\tau = \frac{1}{V^{S,o}}\frac{\delta W}{d\alpha} = -\frac{T^S}{V^{S,o}}\frac{dS^{el}}{d\alpha} \qquad (2.28)$$

The true stress that opposes further swelling of a swollen sphiercal cross-linked polymer network (i.e., tensile force per unit area of swollen sample) is calculated using Eq. (2.29). The true stress, which is denoted with π_{sw}, can be interpreted as an additional pressure exerted on the solid phase, and is termed as "swelling pressure" [Flory53]. As a result, the pressure of the solid phase is the sum of the pressure of the liquid phase and the swelling pressure [Eq. (2.30)].

$$\pi_{sw} = -\frac{T^S}{3\alpha^2 V^{S,o}}\frac{dS^{el}}{d\alpha} \qquad (2.29)$$

$$p^S = p^L + \pi_{sw} \qquad (2.30)$$

The factor $3\alpha^2$ in the dominator of Eq. (2.29) originates from the spherical geometry and the assumption of isotropic swelling. Since $3\alpha^2 d\alpha V^{S,o} = dV^S$, the change in the configurational entropy of the elastic structure can be expressed in terms of the swelling pressure and the volume of the solid phase as follows [Sainio04]:

$$dS^{el} = -\frac{\pi_{sw}dV^S}{T^S} \qquad (2.31)$$

Eq. (2.27) can now be rewritten to give

$$d\left[G^L(T,p^L,n^L) + G^S(T,p^L,n^S) + \pi_{ws}V^S\right] = 0 \qquad (2.32)$$

Applying the Gibbs-Duhem equation at constant temperature T, constant external pressure p^L results in

$$dG^L\left(T,p^L,n^L\right)=\sum_{i=1}^{N_c}\mu_i^L\left(T,p^L,n^L\right)dn_i^L \qquad (2.33a)$$

$$dG^S\left(T,p^L,n^S\right)=\sum_{i=1}^{N_c}\mu_i^S\left(T,p^L,n^S\right)dn_i^S \qquad (2.33b)$$

The total volume of the solid phase is the sum of the partial molar volumes, $V_{m,i}$, as expressed in Eq. (2.34).

$$V^S=\sum_{i=1}^{N_c}n_i^S V_{m,i} \qquad (2.34)$$

Since mass balances are

$$dn_i^L=-dn_i^S \qquad\qquad i=1,\dots,N_c \qquad (2.35)$$

substitution of Eqs. (2.33 – 2.35) into Eq. (2.32) gives

$$\sum_{i=1}^{N_c}\left[\mu_i^L(T,p^L,n^L)-\mu_i^S(T,p^L,n^S)-\pi_{sw}V_{m,i}\right]dn_i^L=0 \qquad (2.36)$$

Therefore, at constant temperature T and external pressure p^L, the criterion for phase equilibrium is

$$\mu_i^L\left(T,p^L,n^L\right)=\mu_i^S\left(T,p^L,n^S\right)+\pi_{sw}V_{m,i} \qquad\qquad i=1,\dots,N_c \qquad (2.37)$$

The relation of chemical potential μ_i in each phase with activity a_i (the activity a_i is defined and discussed later in Section 2.4) is given in Eq. (2.38), where μ_i^o is the chemical potential at the standard state.

$$\mu_i(T,p,n)=\mu_i^o(T,p)+RT\ln a_i(T,p,n) \qquad\qquad i=1,\dots,N_c \qquad (2.38)$$

With an assumption that the standard chemical potential of component i is the same in both phases, Eq. (2.37) can be expressed in terms of activities as below:

$$\ln a_i^L\left(T,p^L,n^L\right)=\ln a_i^S\left(T,p^L,n^S\right)+\pi_{sw}V_{m,i} \qquad i=1,\ldots,N_c \qquad (2.39)$$

As discussed earlier, the second term on the right-hand side of Eqs. (2.37) and (2.39) gives the influence of the increase of pressure from the liquid phase, p^L, to that of the solid phase, p^S.

A determination of the partitioning of component between a liquid and a solid phase at equilibrium is very important. In reality, it is difficult to experimentally determine the portion of a component in the solid phase. It can be alternatively determined from the measurable portion of the component in the liquid phase using an equilibrium function. At a given temperature this equilibrium function is called "adsorption isotherm". A brief introduction of adsorption isotherms is given in the following section.

2.1.3 Adsorption Equilibria

A simple and straightforward possibility to express the equilibrium between a liquid phase and a solid phase is to introduce adsorption isotherms. In the case of adsorption from liquid solutions, at a given concentration of a component in the liquid phase, some portion of the component is partitioning out of the liquid phase onto the solid phase, and some portion is desorbing and re-entering the liquid phase. As component concentrations in the liquid phase change, the relative amounts of component that are adsorbing and desorbing will change. The relationship between the loading of a component i on the solid phase (designated by q_i) and its concentration in the liquid phase (designated by c_i) at equilibrium is referred as the adsorption isotherm. Adsorption isotherms generally exhibit one of several characteristic shapes, depending on the sorption mechanism [Ruth84, Do98].

The thermodynamic approach to the study of equilibrium can be applied to adsorption equilibria as just to any other phase equilibrium. Hence one can use the equilibrium criterion that the chemical potential in the adsorbed phase is equal to the chemical potential in the liquid phase [Myers65, Radke72]:

$$\mu_i^S = \mu_i^L \qquad\qquad\qquad i=1,\ldots,N_c \qquad (2.40)$$

where S denotes the adsorbed phase ("solid" phase), and L denotes the liquid phase.

The theoretical approach to the investigation of liquid-solid equilibria is more complex and much less advanced than the study of gas-solid equilibria. Numerous models, which were

first developed to describe the adsorption behavior of components in gas-solid systems, have been extended to liquid-solid systems. A few should be mentioned here.

2.1.3.1 Linear Adsorption Isotherms

The simplest expression of equilibrium adsorption is the linear isotherm (see Fig. 2.1a), which is valid for the component that is present in the liquid phase at low concentrations. The linear relation between the fluid phase concentration, c_i, and its loading on the solid phase, q_i, is described by Henry's law:

$$q_i = K_i c_i \qquad\qquad i = 1,...,N_c \qquad\qquad (2.41)$$

Henry coefficient, K_i, is the adsorption constant, which is independent to other components.

2.1.3.2 Non-linear Adsorption Isotherms

At high liquid phase concentrations, the adsorption isotherm is no longer linear (see Fig. 2.1b). The most common model describing adsorption behavior in liquid-solid systems is the Langmuir isotherm:

$$q_i(c_i) = q_{s,i} \frac{b_i c_i}{1 + b_i c_i} \qquad\qquad i = 1,...,N_c \qquad\qquad (2.42)$$

where $q_{s,i}$ is the saturation capacity of the solid phase for component i, b_i is the isotherm coefficient of pure component i, which have to be determined experimentally. At low liquid phase concentration the term $1 + b_i c_i \approx 1$, so that the Langmuir isotherm for this case reduces to the linear form, or Henry's law form Eq. (2.41).

The Langmuir isotherm for pure-component adsorption can readily be extended to a multi-component system. In this case, the Langmuir isotherm accounts for the competitive interactions of the components with the solid phase. For a N_c-component system, the Langmuir isotherm holds

$$q_i(c_i) = q_{s,i} \frac{b_i c_i}{1 + \sum_{j=1}^{N_c} b_j c_j} \qquad\qquad i = 1,...,N_c \qquad\qquad (2.43)$$
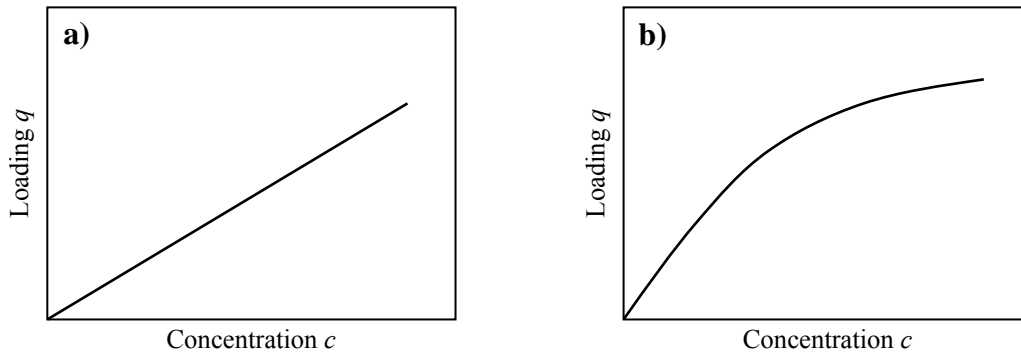
Figure 2.1. (a) Linear adsorption isotherm, and (b) Nonlinear adsorption isotherm

Eqs. (2.41–2.43) can be also expressed using activities a_i^L and a_i^S instead of c_i and q_i. More information regarding activity of a component in solution is given in Section 2.4.

2.1.3.3 Heat of Adsorption

The heat of adsorption provides a direct measure of the strength of the bonding between adsorbed molecules and the surface of the adsorbent. Physical adsorption from the gas phase is invariably exothermic [Ruth84]. This is generally true also for adsorption from the liquid phase, as may be shown by a simple thermodynamic argument. Since the adsorbed molecule has at most two degrees of translational freedom on the surface and since the rational freedom of the adsorbed species must always be less then that of the liquid phase molecule, the entropy change on adsorption ($\Delta S = S_{ads} - S_{liquid}$) is necessarily negative. In order for significant adsorption to occur spontaneously, the Gibbs free energy change on adsorption (ΔG) must also be negative. From $\Delta G = \Delta H - T\Delta S$ follows that ΔH is negative, and adsorption is exothermic. However, unlike adsorption from the gas phase, the argument is less cogent and exceptions are possible in the case of adsorption from the liquid phase.

One of the basic quantities in adsorption studies is the isosteric heat, which is the ratio of the infinitesimal change in the adsorbate enthalpy to the infinitesimal change in the amount of adsorbed [Do98]. The Clausius–Clapeyron equation relates the isosteric heat of adsorption to the temperature dependence of the adsorption isotherm as shown below [Smith96]:

$$\frac{\partial \ln p}{\partial T}\bigg|_q = \frac{\Delta H_{st}}{RT^2} \tag{2.44}$$

where ΔH_{st} is the isosteric heat of adsorption of a pure gas at an adsorbate loading of q and temperature T. The corresponding equilibrium gas phase pressure is p. The Clausius–Clapeyron equation in this form is true only for the case that the bulk gas phase is considered ideal and the adsorbed phase volume is neglected. However, it can generally be also applied for adsorption from the ideal liquid phase. In that case, p in Eq. (2.44) can be replaced by the equilibrium concentration in the liquid phase c (see, e.g., [Sato87]).

$$\frac{\partial \ln c}{\partial T}\bigg|_q = \frac{\Delta H_{st}}{RT^2} \tag{2.45}$$

The temperature dependence of the adsorption equilibrium constant, K, should follow a van't Hoff equation [Ruth84]:

$$\frac{d \ln K}{dT} = -\frac{\Delta H_{ads}}{RT^2} \tag{2.46}$$

where ΔH_{ads} is the heat of adsorption.

The assumptions of identical sites with no interactions between adsorbed molecules imply that the heat of adsorption is independent of coverage. It follows by differentiation of Eq. (2.41) that the isosteric heat of adsorption, ΔH_{st}, is the same as the heat of adsorption, ΔH_{ads}:

$$\frac{\partial \ln c}{\partial T}\bigg|_q = \frac{\Delta H_{st}}{RT^2} = -\frac{d \ln K}{dT} = \frac{\Delta H_{ads}}{RT^2} \tag{2.47}$$

The magnitude of the heat of adsorption can often be used to distinguish between physical adsorption and chemisorption. For chemisorption, ΔH_{st} magnitudes usually range from 60 to 170 kJ/mol. For physical adsorption, the values are typically smaller [Smith96].

2.2 Chemical Reaction Equilibria

In this section the equilibrium composition of reacting systems is considered. Equation 2.1 also provides a means of identifying the equilibrium state when chemical reactions occur. The criterion for equilibrium in a closed system at constant temperature T and pressure p is also that the Gibbs free energy of the system attains its minimum value. Hence it follows at the equilibrium state, that

$$dG|_{T,p} = 0 \tag{2.48}$$

Equation 2.11 gives the basic relation connecting the Gibbs free energy to the temperature, pressure and composition changes for a single phase system:

$$dG = Vdp - SdT + \sum_{i=1}^{N_c} \mu_i dn_i \tag{2.11}$$

2.2.1 Single Reactions

Consider the case of a single chemical reaction occurring in a single phase in a closed system at constant temperature and pressure. The mole number of component i, n_i, present at any time can be calculated from the initial mole number, n_i^o, according to the following mass balance:

$$n_i = n_i^o + \nu_i \xi \qquad\qquad i = 1,...,N_c \tag{2.49}$$

where ξ denotes the extent of reaction; and ν_i is the stoichiometric coefficient for component i (positive for products and negative for reactants). Taking the differential of Eq. (2.49) yields the relation between a differential change in the number of moles of a reacting component and a differential change of the extent of reaction:

$$dn_i = \nu_i d\xi \qquad\qquad i = 1,...,N_c \tag{2.50}$$

Substitution of Eq. (2.50) into Eq. (2.11) gives

$$dG = Vdp - SdT + \sum_{i=1}^{N_c} \nu_i \mu_i d\xi \tag{2.51}$$

At constant temperature and pressure, Eq. (2.51) becomes

$$dG\big|_{T,p} = \sum_{i=1}^{N_c} v_i \mu_i d\xi \tag{2.52}$$

Combination of Eqs. (2.48) and (2.52), the condition of chemical reaction equilibrium can be written

$$\sum_{i=1}^{N_c} v_i \mu_i = 0 \tag{2.53}$$

Equation 2.53 shows that, for a chemical reaction at constant temperature T and pressure p, the net chemical potential of the reactants (weighted by the stoichiometric coefficients) must be equal to the net chemical potential of the products at equilibrium.

The following equation shows the relation of the chemical potential of a component in solution to that of the component in its standard state, which is characterized by temperature T^o and pressure p^o.

$$\mu_i(p,T) = \mu_i^o(p^o,T^o) + RT \ln \frac{f_i}{f_i^o} \qquad\qquad i = 1,...,N_c \tag{2.54}$$

where f_i is the fugacity of component i in solution, f_i^o is the fugacity of component i in its standard state. The ratio f_i/f_i^o is called the activity a_i of component i in solution (see Section 2.4 for more details):

$$a_i \equiv \frac{f_i}{f_i^o} \qquad\qquad i = 1,...,N_c \tag{2.55}$$

Equation (2.54) then becomes

$$\mu_i = \mu_i^o + RT \ln a_i \qquad\qquad i = 1,...,N_c \tag{2.56}$$

Elimination of μ_i in Eq. (2.53) by Eq. (2.56) gives the following relation for the equilibrium state of a chemical reaction:

$$\sum_{i=1}^{N_c} v_i \left(\mu_i^o + RT \ln a_i \right) = 0 \qquad (2.57)$$

or

$$\sum_{i=1}^{N_c} v_i \mu_i^o + RT \sum_{i=1}^{N_c} \ln a_i^{\,v_i} = 0 \qquad (2.58)$$

The standard chemical potential μ_i^o of component i corresponds to the standard Gibbs free energy of its formation $\Delta G_{f,i}^o$. Thus,

$$\sum_{i=1}^{N_c} v_i \mu_i^o = \sum_{i=1}^{N_c} v_i \Delta G_{f,i}^o \left(T^o \right) \equiv \Delta G_r^o \left(T^o \right) \qquad (2.59)$$

with ΔG_r^o being the standard Gibbs free energy change of reaction. It is the different between the Gibbs free energies of formation of the products and reactants (weighted by their stoichiometric coefficients) when each is in its standard state as a pure substance at the system temperature and at a fixed pressure. Thus, the value of ΔG_r^o is fixed for a given reaction once the temperature is established, and is independent of the equilibrium pressure and composition [Smith96]. Extensive tabulations of values of the Gibbs free energies of formation for common compounds in the standard state, $\Delta G_{f,i}^o$, can be found in handbooks and in most thermodynamics texts. (see, e.g., [Stull69], [Reid87], [Barin89], [Perry99] and [CRC05]).

Combining Eqs. (2.58) and (2.59) gives

$$\Delta G_r^o \left(T^o \right) + RT \ln \sum_{i=1}^{N_c} \ln a_i^{\,v_i} = 0 \qquad (2.60)$$

or

$$\Delta G_r^o \left(T^o \right) + RT \ln \prod_{i=1}^{N_c} a_i^{\,v_i} = 0 \qquad (2.61)$$

The product in the second term on the left hand side of Eq. (2.61) is typically called the equilibrium constant K_a:

$$K_a = \prod_{i=1}^{N_c} a_i^{\,v_i} \qquad (2.62)$$

From Eqs. (2.61) and (2.62) one can derive

$$\Delta G_r^o\left(T^o\right) = -RT \ln K_a \tag{2.63}$$

or

$$K_a = \exp\left[-\frac{\Delta G_r^o\left(T^o\right)}{RT}\right] \tag{2.64}$$

According to the definition of the activity coefficient [see Eq. (2.116) in Section 2.4], Eq. (2.62) can be rewritten as

$$K_a = \prod_{i=1}^{N_c}\left(\gamma_i x_i\right)^{\nu_i} \tag{2.65}$$

In the case of ideal solution, all activities γ_i are unity, and the reaction equilibrium constant can be expressed also in terms of mole fractions, x_i, or concentrations, c_i, at equilibrium:

$$K_x = \prod_{i=1}^{N_c} x_i^{\nu_i} \tag{2.66}$$

$$K_c = \prod_{i=1}^{N_c} c_i^{\nu_i} \tag{2.67}$$

2.2.2 Multiple Reactions

For the case that there are several chemical reactions occurring in a single phase in a closed system at constant temperature and pressure, the mass balance of component i is

$$n_i = n_i^o + \sum_{j=1}^{N_R} \nu_{ij}\xi_j \qquad\qquad i = 1,\ldots, N_c \tag{2.68}$$

where N_R is the number of independent reactions j; ν_{ij} is the stoichiometric coefficient of component i for reaction j; and ξ_j is the extent of reaction j. Since the stoichiometric coefficients are constant, differentiation of Eq. (2.68) gives

$$dn_i = \sum_{j=1}^{N_R} \nu_{ij} d\xi_j \qquad\qquad i = 1,\ldots, N_c \tag{2.69}$$

Substituting Eq. (2.69) into Eq. (2.11) yields

$$dG = Vdp - SdT + \sum_{i=1}^{N_c}\sum_{j=1}^{N_R} v_{ij}\mu_i d\xi_j \tag{2.70}$$

At constant temperature and pressure, Eq. (2.70) becomes

$$dG\big|_{T,p} = \sum_{i=1}^{N_c}\sum_{j=1}^{N_R} v_{ij}\mu_i d\xi_j \tag{2.71}$$

The condition for chemical equilibrium in this multireaction system is that $dG = 0$ [Eq. (2.1)] for all variations consistent with stoichiometry at constant temperature, pressure and total mass. For the present case, this implies

$$\frac{\partial G}{\partial \xi_j}\bigg|_{T,p,\xi_{k\neq j}} = 0 \qquad\qquad j = 1,...,N_R \tag{2.72}$$

Thus

$$\frac{\partial G}{\partial \xi_j}\bigg|_{T,p,\xi_{k\neq j}} = 0 = \sum_{i=1}^{N_c} v_{ij}\mu_i \qquad\qquad j = 1,...,N_R \tag{2.73}$$

As discussed above for the case of a single reaction, a separate equilibrium constant is evaluated for each reaction in the present case. Eq. (2.62) then becomes

$$K_{a,j} = \prod_{i=1}^{N_c} a_i^{v_{ij}} \qquad\qquad j = 1,...,N_R \tag{2.74}$$

In the case of ideal solution, Eqs. (2.66) and (2.67) become

$$K_{x,j} = \prod_{i=1}^{N_c} x_i^{v_{ij}} \qquad\qquad j = 1,...,N_R \tag{2.75}$$

$$K_{c,j} = \prod_{i=1}^{N_c} c_i^{v_{ij}} \qquad\qquad j = 1,...,N_R \tag{2.76}$$

In the next section, a few aspects regarding the calculation of equilibrium compositions of systems containing an active multicomponent mixture and an ion-exchange resin are given.

2.2.3 Calculation of Equilibrium Compositions

Recent advances in equilibrium analysis permit the rapid calculation of the equilibrium composition of a complex reacting mixture [Smith82]. There are two basic approaches for computing chemical equilibria. In the first one, the equilibrium constants of chemical reactions and the mass balance equations are employed to determine equilibrium composition. The second approach is based on minimization of the Gibbs free energy with the mass balances of the elements as constraints. The first approach was used in this work. Several chemical reactions occurring simultaneously in a system containing a solvent mixture and an ion-exchange resin are considered.

As described in Section 2.2.2, the equilibrium state for multiple reactions occurring in a single phase system at constant temperature and pressure is identified by finding the state for which

$$\sum_{i=1}^{N_c} v_{ij}\mu_i = 0 \qquad\qquad j = 1,...,N_R \qquad\qquad (2.73)$$

subject to the mole balances

$$n_i = n_i^o + \sum_{j=1}^{N_R} v_{ij}\xi_j \qquad\qquad i = 1,...,N_c \qquad\qquad (2.68)$$

However, for multiple reactions occurring in a liquid–solid phase system, the corresponding mole balances can be formulated as follows:

$$n_i^L = n_i^o + \sum_{j=1}^{N_R} v_{ij}\xi_j - n_i^S \qquad\qquad i = 1,...,N_c \qquad\qquad (2.77)$$

where again superscripts L and S denote the liquid and solid phases, respectively; n_i^o is the total mole number of component i in the system, and n_i^S is the amount present in the solid phase.

Recalling Eq. (2.74), one can write the equilibrium constant expressions for each of N_R reactions in the liquid phase as follows:

$$K_{a,j}^L = \prod_{i=1}^{N_c} \left(a_i^L\right)^{\nu_{ij}} \qquad\qquad j = 1,...,N_R \qquad\qquad (2.78)$$

The mole number of component i in the solid phase, n_i^S, is a function of the liquid phase composition according to the adsorption isotherm (Section 2.1.3). The activity of component i in the liquid phase is also a function of the liquid phase composition. Therefore, with the mass balance shown in Eq. (2.77), the activity of component i in the liquid phase is a function of the N_R unknown extents of reaction ξ_j. Equation (2.78) together with Eq. (2.77) represents a nonlinear system of algebraic equations with the unknown ξ_j. The compositions of the liquid phase and the solid phase as well in the simultaneous phase and chemical equilibrium system can be computed by finding the roots ξ_j (e.g., Newton–Raphson method). In order to start iterative computations, initial approximations for the roots are needed. The method converges when the initial approximations are sufficiently close to the true roots, but may diverge when the initial approximations are far from the true roots. Thus, finding initial approximations sufficiently close to the true roots to achieve convergence is most important.

If the adsorption equilibrium functions are decoupled and linear, i.e.,

$$q_i = K_i c_i \qquad\qquad i = 1,...,N_c \qquad\qquad (2.79)$$

then the mole number of component i in the solid phase, n_i^S, can be computed as

$$n_i^S = K_i c_i V^S = K_i n_i^L \frac{V^S}{V^L} \qquad\qquad i = 1,...,N_c \qquad\qquad (2.80)$$

where V^L and V^S denote the volume of the surrounding liquid and solid phase, respectively.

Defining the volume fraction of the liquid phase (the liquid fraction) as

$$\varepsilon = \frac{V^{L,o}}{V^{L,o} + V^S} \qquad\qquad (2.81)$$

where $V^{L,o}$ is the total volume of the liquid including the volume of liquids in the solid phase, Eq. (2.80) can be rearranged with the assumption that the density of the liquid phase is constant:

$$n_i^S = K_i n_i^L \frac{1-\varepsilon}{\varepsilon} \frac{V^{L,o}}{V^L} \qquad\qquad i = 1,\ldots, N_c \qquad\qquad (2.82)$$

By substituting n_i^S from Eq. (2.82) into Eq. (2.77), one can write

$$n_i^L = n_i^o + \sum_{j=1}^{N_R} v_{ij}\xi_j - K_i n_i^L \frac{1-\varepsilon}{\varepsilon}\frac{V^{L,o}}{V^L} \qquad\qquad i = 1,\ldots, N_c \qquad\qquad (2.83)$$

or

$$n_i^L = \frac{n_i^o + \sum_{j=1}^{N_R} v_{ij}\xi_j}{1 + K_i \dfrac{1-\varepsilon}{\varepsilon}\dfrac{V^{L,o}}{V^L}} \qquad\qquad i = 1,\ldots, N_c \qquad\qquad (2.84)$$

The volume of the liquid phase V^L can be estimated as follows if ideal mixing is assumed, where $V_{m,i}$ are the molar volume of component i:

$$V^L = V^{L,o} - \sum_{i=1}^{N_c} n_i^S V_{m,i} \qquad\qquad i = 1,\ldots, N_c \qquad\qquad (2.85)$$

The sum on the right-hand side of Eq. (2.85) is the total volume of the components stored in the solid phase, which can be expressed in more details [last term of Eq. (2.86)] by substituting n_i^S from Eq. (2.82).

$$V^L = V^{L,o} - \frac{1-\varepsilon}{\varepsilon}\frac{V^{L,o}}{V^L}\sum_{i=1}^{N_c} K_i n_i^L V_{m,i} \qquad\qquad i = 1,\ldots, N_c \qquad\qquad (2.86)$$

Substituting n_i^L from Eq. (2.84) into Eqs. (2.78) and (2.86) yields a system of (N_R+1) nonlinear equations involving variables ξ_j and V^L which can be expressed as follows:

$$F_k\left(\xi_j, V^L\right) = 0 \qquad\qquad j = 1,\ldots, N_R;\ k = 1,\ldots, N_R+1 \quad (2.87)$$

If ε is set equal to 1 for a single phase liquid system, the nonlinear equations which need to be solved reduce to

$$F_j\left(\xi_j\right) = 0 \qquad\qquad\qquad j = 1,\ldots, N_R \qquad\qquad (2.88)$$

2.2.4 Heat of Reaction

Every chemical process is associated with some type of heat effect. The heat of reaction is defined as the amount of heat that must be added or removed during a chemical reaction in order to keep all of the substances present at the same temperature. If the pressure in the vessel containing the reacting system is kept at a constant value, the measured heat of reaction also represents the change in enthalpy, ΔH_r. Tabulation of all possible heat effects for all possible reactions is impossible. Therefore, the heat effects for reactions carried out in any conditions are calculated from data for reactions carried out at certain standard conditions.

The standard heat of reaction is defined as the enthalpy change that occurs by the chemical reaction under the standard conditions. This definition of a standard heat of reaction can be expressed mathematically by the following equation:

$$\Delta H_r^o = \sum_{i=1}^{N_c} v_i H_i^o \qquad\qquad\qquad (2.89)$$

where ΔH_r^o is the standard reaction enthalpy, and H_i^o is the enthalpy of component i in its standard state. The standard enthalpy of a chemical compound is equal to its heat of formation plus the standard enthalpies of its constituent elements. The standard enthalpy of elements is established to be zero. Thus, the standard enthalpy of each compound is its standard heat of formation, $H_i^o = \Delta H_{f,i}^o$, and Eq. (2.89) becomes

$$\Delta H_r^o = \sum_{i=1}^{N_c} v_i \Delta H_{f,i}^o \qquad\qquad\qquad (2.90)$$

Extensive tabulations of values of the enthalpies of formation for common compounds at the standard state, $\Delta H_{f,i}^o$, can be found in handbooks and in most thermodynamics texts. (see, e.g., [Stull69], [Reid87], [Barin89], [Perry99] and [CRC05]).

For standard reactions, all components are always at the standard pressure of 1 bar. Standard enthalpies are therefore functions of temperature only:

$$dH_i^o = c_{p_i}^o dT \qquad\qquad i = 1,...,N_c \qquad\qquad (2.91)$$

Since v_i is a constant, from Eq. (2.91) one can write

$$d\sum_{i=1}^{N_c} v_i H_i^o = \sum_{i=1}^{N_c} v_i c_{p_i}^o dT \qquad\qquad (2.92)$$

The term $\sum_{i=1}^{N_c} v_i H_i^o$ is the standard heat of reaction as defined by Eq. (2.89). Similarly, the standard heat capacity change of reaction can be defined as

$$\Delta c_p^o = \sum_{i=1}^{N_c} v_i c_{p_i}^o \qquad\qquad (2.93)$$

Using these definitions, Eq. (2.92) becomes

$$d\Delta H_r^o = \Delta c_p^o dT \qquad\qquad (2.94)$$

Equation (2.94) provides the temperature dependence of enthalpy of reaction. The integration of Eq. (2.94) from temperature T^o to T gives

$$\Delta H_r^o(T) = \Delta H_r^o(T^o) + \int_{T^o}^T \Delta C_p^o dT \qquad\qquad (2.95)$$

where $\Delta H_r^o(T)$ and $\Delta H_r^o(T^o)$ are heats of reaction at temperature T and at reference temperature T^o respectively.

2.2.5 Influence of Temperature on Reaction Equilibrium Constants

The standard Gibbs free energy of reaction is considered as a measure of the spontaneity of a reaction. In turn, this thermodynamic parameter measures a combination of changes in heat, work, and entropy that occur during a reaction. The Gibbs free energy of reaction is defined as

$$\Delta G_r^o = \Delta H_r^o - T\Delta S_r^o \qquad\qquad (2.96)$$

where ΔG_r^o and ΔS_r^o are the standard reaction enthalpy and entropy, respectively.

By rearranging Eq. (2.96) and using the relationship in Eq. (2.63), one can obtain

$$\ln K_a = -\frac{\Delta H_r^o}{RT} + \frac{\Delta S_r^o}{R} \qquad (2.97)$$

Thus, if one measures K_a as a function of temperature, a plot of $\ln K_a$ versus $1/T$ should yield a straight line with a slope of $-\Delta H/R$ and an intercept of $\Delta S/R$. This relationship can be expressed as a differential equation describing the temperature dependence of the equilibrium constant K_a:

$$\frac{d(\ln K_a)}{dT} = -\frac{\Delta H_r^o}{RT^2} \qquad (2.98)$$

As discussed earlier in Section 2.2.4, ΔH_r^o is also a function of temperature [Eq. (2.95)]. However, for small temperature differences, ΔH_r^o is assumed to be constant, and then

$$\ln K_a(T) = \ln K_a(T^o) - \frac{\Delta H_r^o}{R}\left(\frac{1}{T} - \frac{1}{T^o}\right) \qquad (2.99)$$

Eq. (2.98) is known as the van't Hoff equation, and by performing a van't Hoff analysis, the reaction enthalpy and entropy can be extracted.

2.3 Reaction Rates

Broad knowledge regarding the kinetics of chemical reactions can be found in the literature (for example [Smith81], [Conn90], [Leven99] and [Miss99]). In this section, a short empirical macroscopic description of the rates of chemical reactions is given. The description concentrates on the definition of reaction rates and on the development of a quantitative analysis of the dependence of the reaction rates on the reaction conditions, including concentration of involved components and temperature. In fact, most real reactors need catalysts to speed up reaction, i.e., to make reaction occur at lower temperatures or to attain a higher selectivity to a particular product. The catalysts can be homogeneous or heterogeneous. For the heterogeneous systems, chemical reactions can take place in all individual phases. Therefore, the overall rate can be dependent on the rates in all individual phases. In Section 2.3.1, the rates of chemical reactions in a homogeneous

single phase are introduced. Subsequently, a description of the reaction rates in a heterogeneous system is given (Section 2.3.2).

2.3.1 Homogeneous Systems

The reaction rate is defined either as the amount of product produced or the amount of reactant consumed per unit volume of the reaction phase per unit time (see, e.g., [Schm98]). For a N_R-reaction system in a homogeneous phase, the rate of transformation of component i, $r_i^{overall}$, in the system can be written as

$$r_i^{overall} = \sum_j^{N_R} v_{ij} r_j \qquad\qquad i = 1,...,N_c \qquad\qquad (2.100)$$

where v_{ij} is the stoichiometric coefficient of component i in reaction j, and r_j is the rate of reaction j.

The rate of a single reaction is typically defined as

$$r = \frac{1}{V_R v_i} \frac{dn_i}{dt} \qquad\qquad i = 1,...,N_c \qquad\qquad (2.101)$$

In the above equation, V_R is the single phase reaction volume; n_i is the number of moles of component i; and N_c is the number of components. The specific numbers of moles of component i in a batch reactor are simply the reactor volume V_R times the volumetric concentration c_i:

$$n_i = V_R c_i \qquad\qquad i = 1,...,N_c \qquad\qquad (2.102)$$

With this, Eq. (2.101) becomes

$$r = \frac{1}{V_R v_i} \frac{d(V_R c_i)}{dt} = \frac{1}{V_R v_i}\left(V_R \frac{dc_i}{dt} + c_i \frac{dV_R}{dt} \right) \qquad\qquad i = 1,...,N_c \qquad\qquad (2.103)$$

If volume is constant, then Eq. (2.103) reduces to

$$r = \frac{1}{v_i} \frac{dc_i}{dt} \qquad\qquad i = 1,...,N_c \qquad\qquad (2.104)$$

Postulating that the rate-controlling mechanism involves the collision or interaction of a single molecule of a reactant with a single molecule of the other reactants, then the number of collision of those molecules is proportional to the rate of reaction [Miss99]. However, in the case of ideal solution, at a given temperature the number of collisions is proportional to the concentration of reactants in the mixture. Thus, for an irreversible reaction the rate of reaction can be described as

$$r = k(T)\prod_{i}^{N_r}(c_i)^{m_i} \tag{2.105}$$

where N_r is the number of reactants; m_i is the order of the reaction with respect to the component i. The rate constant $k(T)$ is found empirically to be dependent on temperature as shown in the following Arrhenius equation [Miss99].

$$k(T) = k_o \exp\left(-\frac{E_A}{RT}\right) \tag{2.106}$$

where E_A is called the activation energy for the reaction and k_o is called the pre-exponential factor.

If the reaction is reversible, the rate can be written as a difference between the rate of the forward reaction r_f and the rate of the backward reaction r_b,

$$r = r_f - r_b = k_f(T)\prod_{i}^{N_c}(c_i)^{m_{f,i}} - k_b(T)\prod_{i}^{N_c}(c_i)^{m_{b,i}} \tag{2.107}$$

with

$$m_{f,i} = \frac{1}{2}\left(|v_i| - v_i\right)$$

$$m_{b,i} = \frac{1}{2}\left(|v_i| + v_i\right)$$

or

$$r = k_f(T)\left(\prod_{i}^{N_c}(c_i)^{m_{f,i}} - \frac{1}{K_c}\prod_{i}^{N_c}(c_i)^{m_{b,i}}\right) \tag{2.108}$$

where k_f and k_b are the rate constants of the forward and backward reactions, respectively. K_c is the concentration-based reaction equilibrium constant [Eq. (2.67)].

Alternatively, the reaction rate can be expressed in terms of activities as in Eq. (2.109) in order to take into account the non-idealities of the solution. K_a is the activity-based reaction equilibrium constant [Eq. (2.62)], and a_i is the activity of component i.

$$r = k_f(T)\left(\prod_i^{N_c}(a_i)^{m_{f,i}} - \frac{1}{K_a}\prod_i^{N_c}(a_i)^{m_{b,i}}\right)$$
(2.109)

2.3.2 Heterogeneous Systems

For heterogeneous systems, a study of the kinetics is more complex than dealing with homogeneous systems. Specifically, there are more factors to consider for heterogeneous system. For instance, for a solid-catalyzed reaction, there can be five basic steps in the sequence of mass transfer and reaction over a solid catalyst [Harri03]:

1. Diffusion of reactants to the external surface of the catalyst and into the pores
2. Adsorption of one or both reactants on active sites
3. Reaction on the surface between adsorbed species or between surface species and a reactant in the liquid phase
4. Desorption of the products
5. Diffusion of products out of the pores and into the external liquid

When the system is at steady state, all the steps in the sequence take place at the same rate. However, the overall rate is often controlled by one step, which is the slowest one. In many cases, this is the chemical reaction. In this work, the reaction in a system consisting of a solid catalyst and liquid reactants is considered.

For this case, the reaction can occur in both liquid and solid phases. The overall rate of reactions, $r^{overall}$, is the sum of the rates of the reaction taking place in the liquid phase, r^{hom}, (from now on, called homogeneous reaction) and the reaction taking place in the solid phase, r^{het}, (from now on, called heterogeneous reaction). The homogeneous reactions take place in the liquid phase with the volume fraction ε [Eq. (2.81)], the heterogeneous reactions take place in the solid phase with the volume fraction $(1-\varepsilon)$. At fixed temperature, r^{hom} depends on the component concentrations (c_1, c_2,… etc. denoted by $\bar{c}$), and r^{het} depends on the species loadings on the catalyst (q_1, q_2,… etc. denoted by $\bar{q}$). It follows for the overall rate that

$$r^{overall} = \varepsilon r^{hom}(\bar{c}) + (1-\varepsilon)r^{het}(\bar{c},\bar{q})$$
(2.110)

Application of the rate expression of reversible reactions derived above for homogeneous systems [Eq. (2.108)] can be extended to each phase in a heterogeneous system:

$$r^{\mathrm{hom}}\left(\overline{c}\right) = k_f^{\mathrm{hom}}\left(T\right)\left(\prod_i^{N_c}\left(c_i\right)^{m_{f,i}} - \frac{1}{K_c^{\mathrm{hom}}}\prod_i^{N_c}\left(c_i\right)^{m_{b,i}}\right) \tag{2.111}$$

and

$$r^{\mathrm{het}}\left(\overline{c},\overline{q}_{av}\right) = k_f^{\mathrm{het}}\left(T\right)\left(\prod_i^{N_c}\left(q_{av,i}\right)^{m_{f,i}} - \frac{1}{K_c^{\mathrm{het}}}\prod_i^{N_c}\left(q_{av,i}\right)^{m_{b,i}}\right) \tag{2.112}$$

with

$$m_{f,i} = \frac{1}{2}\left(\left|v_i^*\right| - v_i^*\right)$$

$$m_{b,i} = \frac{1}{2}\left(\left|v_i^*\right| + v_i^*\right) \quad *\text{) hom or het}$$

In the above equations, k_f^{hom} and k_f^{het} denote the rate constants, K_c^{hom} and K_c^{het} the equilibrium constants of the forward reactions in the liquid and solid phases, respectively. $q_{av,i}$ is the average loading of component i on the solid phase.

In principle, the loading of a component on the solid phase depends on its concentration in the liquid phase. Since, in fact, it is difficult to experimentally determine the loading of a component in the solid phase, models must be developed to predict the loadings as functions of the concentrations in the liquid phase. The rate expression of reactions in the solid phase can then be written in terms of the liquid concentration. The relationship between the loading of a component on the solid phase and its concentration in the liquid phase at equilibrium is referred as the adsorption isotherm. This has been discussed previously in Section 2.1.3.

In order to take into account the non-idealities of systems, the rate expressions should be written in terms of activities. For this end, the following equations (2.113) and (2.114) can be written, where a^L and a^S denote activities in the liquid and solid phase, respectively.

$$r^{\mathrm{hom}}\left(\overline{a}^L\right) = k_f^{\mathrm{hom}}\left(T\right)\left(\prod_i^{N_c}\left(a_i^L\right)^{m_{f,i}} - \frac{1}{K_a^{\mathrm{hom}}}\prod_i^{N_c}\left(a_i^L\right)^{m_{b,i}}\right) \tag{2.113}$$

$$r^{\mathrm{het}}\left(\overline{a}^S\right) = k_f^{\mathrm{het}}\left(T\right)\left(\prod_i^{N_c}\left(a_i^S\right)^{m_{f,i}} - \frac{1}{K_a^{\mathrm{het}}}\prod_i^{N_c}\left(a_i^S\right)^{m_{b,i}}\right) \tag{2.114}$$

2.4 Activity and Activity Coefficients

In the above sections, several times activity a_i the activity coefficients γ_i were introduced. Now a more detailed introduction about activity and discussion of how to calculate activity coefficients are presented. As basic references regarding activity and activity coefficients, [Prau99], [Sand99] and [Neve02] are recommended. The activity of component i in a mixture at some temperature, pressure, and composition is defined as the ratio of the fugacity of component i at these conditions to its fugacity in the standard state, that is a state at the same temperature as that of the mixture and at some specified condition of pressure and composition [Prau99]:

$$a_i(T,p,x) \equiv \frac{f_i(T,p,x)}{f_i^o(T,p^o,x^o)} \qquad\qquad i = 1,...,N_c \qquad\qquad (2.115)$$

where p^o and x^o are, respectively, an arbitrary but specified pressure and composition.

The activity coefficient γ_i is the ratio of the activity of component i to some convenient measure of the concentration of component $i,$ usually the mole fraction:

$$\gamma_i \equiv \frac{a_i}{x_i} \qquad\qquad i = 1,...,N_c \qquad\qquad (2.116)$$

The fugacity of component i in a liquid solution, $f_i,$ is defined in relation with the partial molar Gibbs free energy of component i by the equation:

$$g_i = \Gamma_i(T) + RT \ln f_i \qquad\qquad i = 1,...,N_c \qquad\qquad (2.117)$$

where g_i is the partial molar Gibbs free energy of component i; and $\Gamma_i(T)$, a function of temperature, is the integration constant at constant T. In the other context, the fugacity of component i in a liquid solution is most conveniently related to the mole fraction x_i by:

$$f_i = \gamma_i x_i f_i^o \qquad\qquad i = 1,...,N_c \qquad\qquad (2.118)$$

In an ideal solution at some constant temperature and pressure, the fugacity of component i is proportional to some suitable measure of its concentration, usually the mole fraction. It follows that

$$f_i = \mathfrak{R}_i x_i \qquad\qquad i = 1,...,N_c \qquad\qquad (2.119)$$

where $\mathfrak{R}_i$ is a proportionality constant dependent on temperature and pressure but independent of x_i.

Based on the definition of the fugacity [Eq. (2.117)], at constant temperature and pressure, for a component i in solution, the following relation can be written:

$$g_{i(\text{real})} - g_{i(\text{ideal})} = RT\Big[\ln f_{i(\text{real})} - \ln f_{i(\text{ideal})}\Big] \qquad i = 1,...,N_c \qquad (2.120)$$

By differentiation at constant T, p, and n_j ($j \neq i$) of the equation defining the excess Gibbs free energy, G^E,

$$G^E \equiv G_{(\text{real solution at } T, p \text{ and } x)} - G_{(\text{ideal solution at same } T, p \text{ and } x)} \qquad (2.121)$$

the partial molar excess Gibbs free energy is introduced:

$$g_i^E = g_{i(\text{real})} - g_{i(\text{ideal})} \qquad\qquad i = 1,...,N_c \qquad (2.122)$$

Combination of Eqs. (2.120) and (2.122) yields

$$g_i^E = RT \ln \frac{f_{i(\text{real})}}{f_{i(\text{ideal})}} \qquad\qquad i = 1,...,N_c \qquad (2.123)$$

Substituting Eq. (2.119) into Eq. (2.123) gives

$$g_i^E = RT \ln \frac{f_i}{\mathfrak{R}_i x_i} \qquad\qquad i = 1,...,N_c \qquad (2.124)$$

If the standard fugacity f_i^o is set equal to $\mathfrak{R}_i$, then one can have

$$a_i = \gamma_i x_i = \frac{f_i}{\mathfrak{R}_i} \qquad\qquad i = 1,...,N_c \qquad (2.125)$$

For an ideal solution f_i is equal to $\mathfrak{R}_i x_i$ [Eq. (2.119)] and therefore, $\gamma_i = 1$ and $a_i = x_i$. Substituting Eq. (2.125) into Eq. (2.124) yields

$$g_i^E = RT \ln \gamma_i \qquad\qquad i = 1,...,N_c \qquad (2.126)$$

Thus the molar excess Gibbs free energy of a solution can be expressed in relation with mole fractions and activity coefficients as follows:

$$g^E = RT \sum_{i=1}^{N_c} x_i \ln \gamma_i \qquad (2.127)$$

Many equations have been proposed for the relation between activity coefficients and mole fractions [Prau99]. UNIQUAC equation first given by Abrams and Prausnitz [Abram75] is one of the most reliable equations for many practical calculations. The UNIQUAC equation, which is used in this work, is introduced below.

Calculation of activity coefficients using UNIQUAC equation

The UNIQUAC equation for the excess Gibbs free energy g^E consists of two parts, a *combinatorial part* g^C that attempts to describe the dominant entropic contribution, and a *residual part* g^R that is due primarily to intermolecular forces that are responsible for the enthalpy of mixing. The combinatorial part is determined only by the composition and by the sizes and shapes of the molecules; it requires only pure-component data. The residual part, however, depends also on intermolecular forces; the two adjustable binary parameters, therefore, appear only in the residual part. The UNIQUAC equation is:

$$g^E = g^C + g^R \qquad (2.128)$$

For a multicomponent system holds:

$$g^C = \sum_{i=1}^{N_c} x_i \ln \frac{\Phi_i}{x_i} + \frac{z}{2} \sum_{i=1}^{N_c} q_i^u x_i \ln \frac{\theta_i}{\Phi_i} \qquad (2.129)$$

$$g^R = -\sum_{i=1}^{N_c} q_i^{u'} x_i \ln \left(\sum_{j=1}^{N_c} \theta_j' \tau_{ji} \right) \qquad (2.130)$$

where the coordination number z is set equal to 10 [Prau99]. Segment fraction, Φ, and area fractions, θ, and θ', are given by:

$$\Phi_i \equiv \frac{x_i r_i^u}{\sum_{j=1}^{N_c} x_j r_j^u} \qquad i = 1,...,N_c \qquad (2.131)$$

and

$$\theta_i \equiv \frac{x_i q_i^u}{\sum\limits_{j=1}^{N_c} x_j q_j^u} \qquad \theta_i' \equiv \frac{x_i q_i^{u'}}{\sum\limits_{j=1}^{N_c} x_j q_j^{u'}} \qquad\qquad i = 1,...,N_c \qquad\qquad (2.132)$$

The parameters r^u, q^u, and $q^{u'}$ are pure-component molecular-structure constants depending on molecular size and external surface areas. In the original formulation, $q^u = q^{u'}$. To obtain better agreement for systems containing water or lower alcohols, $q^{u'}$ values for water and alcohols were adjusted empirically by [Ander78] to give an optimum fit to a variety of systems containing these components. For alcohols, the surface of interaction $q^{u'}$ is smaller than the geometric external surface q^u, suggesting that intermolecular attraction is dominated by the OH group (hydrogen bonding). For fluids other than water and lower alcohols, $q^u = q^{u'}$.

Subscript i identifies again species, and j is a dummy index; all summations are over all species. Note that $\tau_{ji} \neq \tau_{ij}$; however, when $i = j$, then $\tau_{ii} = \tau_{jj} = 1$. The influence of temperature on g^E enters through the interaction parameters τ_{ji} of Eq. (2.130), which are temperature dependent:

$$\tau_{ij} = \exp\left(-\frac{a_{ij}^u}{T}\right) \quad \text{and} \quad \tau_{ji} = \exp\left(-\frac{a_{ji}^u}{T}\right) \qquad\qquad i, j = 1,...,N_c \qquad\qquad (2.133)$$

Parameters for the UNIQUAC equation are therefore values of a_{ij}^u and a_{ji}^u.

An expression for $\ln \gamma_i$ is found by application of Eq. (2.134):

$$\ln \gamma_i = \left[\frac{\partial\left(G^E / RT\right)}{\partial n_i}\right]_{T,P,j} \qquad\qquad i, j = 1,...,N_c \qquad\qquad (2.134)$$

to the UNIQUAC equation for g^E [Eqs. (2.128)-(2.130)]. The result is given by the following equations:

$$\ln \gamma_i = \ln \gamma_i^C + \ln \gamma_i^R \qquad\qquad i = 1,...,N_c \qquad\qquad (2.135)$$

$$\ln \gamma_i = \ln \frac{\Phi_i}{x_i} + \frac{z}{2} q_i^u \ln \frac{\theta_i}{\Phi_i} + l_i - \frac{\Phi_i}{x_i} \sum_{j=1}^{N_c} x_j l_j$$

$$- q_i^{u'} \ln \left(\sum_{j=1}^{N_c} \theta_j' \tau_{ji} \right) + q_i^{u'} - q_i^{u'} \sum_{j=1}^{N_c} \frac{\theta_j' \tau_{ij}}{\sum_{k=1}^{N_c} \theta_k' \tau_{kj}} \qquad\qquad i = 1,...,N_c \qquad\qquad (2.136)$$

where in addition to Eq. (2.136),

$$l_j = \frac{z}{2} \left(r_j^u - q_j^u \right) - \left(r_j^u - 1 \right) \qquad\qquad\qquad j = 1,...,N_c \qquad\qquad (2.137)$$

Again subscript i identifies species, and j and k are dummy indices.

An extensive collection of values for the parameters r_i^u, q_i^u, a_{ij}^u and a_{ji}^u allowing the prediction of activity coefficients with Eqs. (2.135–2.137) is given by Gmehling *et al.*, 2002 [Gmeh02].

Model Reactions, Catalysts and Adsorbents

In Chapter 2, main theoretical aspects of relevance for the present work have been discussed. This chapter introduces the model reactions investigated in this work including the catalysts used. This is followed by a section summarizing the experimental investigations carried out.

3.1 Model Reactions

3.1.1 Hydrolysis of Esters

In this work, the hydrolysis of the four carboxylate esters is studied, i.e., the hydrolysis of methyl formate, methyl acetate, ethyl formate and ethyl acetate to the corresponding carboxylic acids and alcohols. There are several specific analyses of some of these reactions in the literature (e. g., [Newl36], [Shah54], [Bell55], [Bala69], [Weth74], [Raja78], [Cho80a], [Cho80b], [Goto83], [Indu93], [Vilcu94], [Pöpk01], [Lode03] and [Yu04]).

Typically the hydrolysis of esters is slow at neutral pH, but faster at acidic or basic pH. Acids and bases can catalyze ester hydrolysis reactions. The four reactions can be described with the following stoichiometric equations:

$$CH_3\text{-}OOCH \quad + \; H_2O \quad \overset{H^+ \text{ or } OH^-}{\rightleftharpoons} \quad CH_3OH \; + \; HCOOH \qquad (3.1a)$$

$$CH_3\text{-}OOCCH_3 \; + \; H_2O \quad \overset{H^+ \text{ or } OH^-}{\rightleftharpoons} \quad CH_3OH \; + \; CH_3COOH \qquad (3.1b)$$

$$C_2H_5\text{-}OOCH \quad + \; H_2O \quad \overset{H^+ \text{ or } OH^-}{\rightleftharpoons} \quad C_2H_5OH \; + \; HCOOH \qquad (3.1c)$$

$$C_2H_5\text{-}OOCCH_3 \; + \; H_2O \quad \overset{H^+ \text{ or } OH^-}{\rightleftharpoons} \quad C_2H_5OH \; + \; CH_3COOH \qquad (3.1d)$$

In order to describe the four simpler reactions in a systematic manner, the following indicators are used in this work:

$$
\begin{aligned}
&CH_3\text{-} &&\equiv Al_1\text{-} &&\text{(the methyl group of alcohol 1)} \\
&C_2H_5\text{-} &&\equiv Al_2\text{-} &&\text{(the ethyl group of alcohol 2)} \\
&\text{-}OOCH &&\equiv Ac_1\text{-} &&\text{(the formate group of acid 1)} \\
&\text{-}OOCCH_3 &&\equiv Ac_2\text{-} &&\text{(the acetate group of acid 2)} \\
&CH_3\text{-}OOCH &&\equiv Es_{11} &&\text{(ester of alcohol 1 and acid 1)} \\
&CH_3\text{-}OOCCH_3 &&\equiv Es_{12} &&\text{(ester of alcohol 1 and acid 2)} \\
&C_2H_5\text{-}OOCH &&\equiv Es_{21} &&\text{(ester of alcohol 2 and acid 1)} \\
&C_2H_5\text{-}OOCCH_3 &&\equiv Es_{22} &&\text{(ester of alcohol 2 and acid 2)} \\
&H_2O &&\equiv W
\end{aligned}
\qquad (3.2)
$$
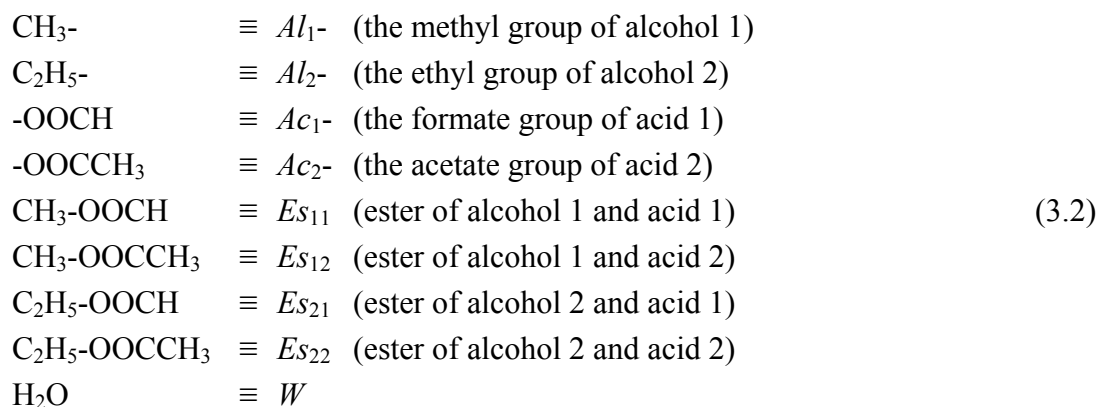
Using the above notations, the four hydrolysis reactions of the four esters can be described in a scheme as shown in Eq. (3.3):

$$Es_{ij} \quad + \; W \quad \overset{H^+ \text{ or } OH^-}{\rightleftharpoons} \quad Al_i \quad + \; Ac_j \qquad i, j = 1, 2 \qquad (3.3)$$

Below, in some cases, Es_{ij}, Al_i, and Ac_j are simply denoted by Es, Al, and Ac respectively.

Catalysts for the reactions can be a mineral acid (e.g., HCl, H_2SO_4, HNO_3) or a mineral base (e.g., NaOH, KOH) in the liquid form. The catalyst can also be an acidic or basic ion-exchange resin. For example, cation-exchange resins based on styrene divinylbenzene copolymers functionalized by sulphuric acid groups (SO_3H) have been frequently used (e.g., [Sard79], [Mazz79a-b], [Pöpk00], [Falk02], [Lode03] and [Sainio04]).

Long chain esters are usually weakly polar. Therefore, they dissolve badly in water. Among the four esters mentioned above, the best and worst solubility in water correspond to methyl formate and ethyl acetate, respectively (Table 3.1). Values of some selected physical parameters of the components relevant to the hydrolysis of the four esters are listed in Table 3.1.

The standard enthalpies and standard Gibbs free energies of formation of many compounds for the liquid and gas phase can be found in the literature (e.g., [Afee05], [Barin95], [CRC05], [Perry99] and [Stull69]). A summary of those values for the compounds involved to the reactions investigated is given in Tables 3.2 and 3.3.

Table 3.1. Selected physical parameters of the compounds in the investigated reactions system from [Merck05].

Compound	M_i [g/mol]	$\rho_{i,20^oC}$ [g/cm^3]	$t_{boiling,1013mbar}$ [^{o}C]	Solubility in water at 20 ^{o}C [g/L]	[mol/mol]
Es_{11}	60.05	0.968	31 - 33	300	0.090
Es_{12}	74.08	0.93	56 - 58	250	0.061
Es_{21}	74.08	0.92	54	105	0.026
Es_{22}	88.11	0.90	77	85.3	0.017
Al_1	32.04	0.79	64.5	∞	∞
Al_2	46.07	0.79	78.3	∞	∞
Ac_1	46.03	1.22	101	∞	∞
Ac_2	60.05	1.05	116 - 118	∞	∞
W	18.02	1.00	100	∞	∞

The standard Gibbs free energy of formation of methyl formate in the liquid phase can not be found directly in the literature. It can be calculated from the standard Gibbs free energy of formation of methyl formate in the gas phase and the partial vapor pressure ([Stull69], p. 134). The needed partial vapour pressure of methyl formate is computed using the Antoine equation and the coefficients which can be found in the literature (e.g., [Jaku92] and [Lange99]). The Antoine equation and the relevant coefficients are introduced in Appendix A. The calculated value of the standard Gibbs free energy of formation of methyl formate in the liquid phase is shown in Table 3.3.

Using Eqs. (2.90) and (2.59) and the values from [CRC05] and [Stull69] given in Tables 3.2 and 3.3, the standard reaction enthalpies and the standard Gibbs free energies of hydrolysis of the four esters in the liquid phase were respectively calculated and are shown

in Table 3.4. For ethyl formate, the enthalpy values of formation in the liquid phase found in two various sources are significantly different (see Table 3.2). Therefore, the standard reaction enthalpy of the hydrolysis of methyl formate calculated using the values from these two sources are also significantly different. Particularly, it will be -17.21 kJ/mol if the value from [Stull69] is used and +13.7 kJ/mol if the value from [Hine74] is used. In fact, the hydrolysis of ethyl formate is endothermal, thus the value from [Hine74] is more reliable and used in this work (Table 3.4).

Table 3.2. Standard enthalpies of formation of the compounds involved to the investigated reactions from several different sources.

| Compound | $\Delta H^o_{f,i}$, $T^o = 25\ ^oC$ [kJ/mol] | | | |
	[CRC05]	[Stull69]	[Perry99]	[Hine74]
Es_{11} (liquid)	-386.1	-378.49	-	-391.0
Es_{11} (gas)	-357.4	-350.02	-352.4	-362.0
Es_{12} (liquid)	-445.9	-441.71	-	-
Es_{12} (gas)	-413.3	-409.89	-411.9	-
Es_{21} (liquid)	-	-399.59	-	-430.5
Es_{21} (gas)	-	-371.54	-388.3	-398.0
Es_{22} (liquid)	-479.3	-479.35	-	-
Es_{22} (gas)	-443.6	-443.21	-444.5	-
Al_1 (liquid)	-239.2	-238.73	-	-
Al_1 (gas)	-201.0	-201.30	-200.94	-
Al_2 (liquid)	-277.6	-277.17	-	-
Al_2 (gas)	-234.8	-234.96	-234.95	-
Ac_1 (liquid)	-425.0	-425.04	-	-
Ac_1 (gas)	-378.7	-378.86	-378.6	-
Ac_2 (liquid)	-484.3	-484.41	-	-
Ac_2 (gas)	-432.2	-435.13	-432.8	-
W (liquid)	-285.8	-	-	-
W (gas)	-241.8	-242.0	-241.8	-

Table 3.3. Standard Gibbs free energies of formation of the compounds involved to the investigated reactions from several different sources.

Compound	$\Delta G^o_{f,i}$, $T^o = 25\ ^oC$ [kJ/mol]			
	[CRC05]	[Stull69]	[Perry99]	Calculated
Es_{11} (liquid)	-	-	-	-297.6
Es_{11} (gas)	-	-297.39	-295.0	
Es_{12} (liquid)	-	-	-	-325.55
Es_{12} (gas)	-	-	-324.2	
Es_{21} (liquid)	-	-	-	-304.32
Es_{21} (gas)	-	-	-303.1	
Es_{22} (liquid)	-	-332.93	-	
Es_{22} (gas)	-	-327.62	-328.0	
Al_1 (liquid)	-166.6	-166.34	-	
Al_1 (gas)	-162.3	-162.62	-162.32	
Al_2 (liquid)	-174.8	-174.25	-	
Al_2 (gas)	-167.9	-168.39	-167.85	
Ac_1 (liquid)	-361.4	-361.70	-	
Ac_1 (gas)	-	-351.23	-351.0	
Ac_2 (liquid)	-389.9	-389.62	-	
Ac_2 (gas)	-374.2	-376.94	-374.6	
W (liquid)	-237.1	-	-	
W (gas)	-228.6	-228.77	-228.6	

Table 3.4. Standard enthalpies ΔH^o_r and standard Gibbs free energies ΔG^o_r of hydrolysis of the four esters in the liquid phase from different sources. $T^o = 25\ ^oC$.

Reactant	ΔH^o_r [kJ/mol]		ΔG^o_r [kJ/mol]
	Eq. (2.90)	Literature	Eq. (2.59)
Es_{11}	+7.7	+16.3 [Reut89]	+6.66
Es_{12}	+8.2	+6.51 [Song98][*]	+6.68
Es_{21}	+13.7	-	+5.47
Es_{22}	+3.2	+5.83 [Yu04][*]	+6.16

*) Esterification reactions investigated.

UNIQUAC Parameters

In Section 2.4 the UNIQUAC model, which is used in this work to calculate the activity coefficients in the liquid phase, has been introduced. The values of pure-component and interaction parameters used in the UNIQUAC model for the relevant components were found in the literature [Gmeh02] and are listed Tables 3.5 and 3.6.

Table 3.5. Values of UNIQUAC pure-component parameters [Gmeh02], Eqs. (2.135–2.137).

No.	Component	r_i^u	q_i^u
1	Es_{11}	2.1298	2.0360
2	Es_{12}	2.8042	2.5760
3	Es_{21}	2.8042	2.5760
4	Es_{22}	3.4786	3.1160
5	Al_1	1.4311	1.4320
6	Al_2	2.1055	1.9720
7	Ac_1	1.5280	1.5320
8	Ac_2	2.2024	2.0720
9	W	0.9200	1.4000

Table 3.6. Values of UNIQUAC binary parameters a_{ij}^u, a_{ji}^u [Gmeh02], Eqs. (2.135–2.137).

	Es_{11}	Es_{12}	Es_{21}	Es_{22}	Al_1	Al_2	Ac_1	Ac_2	W
Es_{11}	0	463.95	*	*	623.26	417.42	-209.63	*	*
Es_{12}	-358.35	0	-63.254	-102.45	611.23	267.02	578.81	806.84	830.79
Es_{21}	*	65.512	0	404.36	726.58	429.69	*	*	*
Es_{22}	*	261.17	-302.49	0	770.30	436.04	*	1078.5	1267.7
Al_1	-2.0107	-70.982	-102.97	-138.98	0	-202.14	*	321.78	-328.41
Al_2	103.95	-79.292	-20.769	-98.562	258.69	0	*	294.46	103.68
Ac_1	268.97	-378.72	*	*	*	*	0	-478.56	-91.788
Ac_2	*	-467.12	*	-476.49	-323.04	-293.99	689.57	0	588.45
W	*	47.502	*	-277.55	506.20	112.69	-282.69	-308.74	0

*) Missing data.

Acid – Base Equilibrium

As discussed above, acids and bases can accelerate the hydrolysis of esters. Thus, the H^+ ion dissociated from acids and alcohols which are the products of the hydrolysis process should be considered. The catalysis of this kind of H^+ on the hydrolysis process is known as autocatalysis. Table 3.7 lists the dissociation (ionization) constants of formic acid, acetic acid, methanol, ethanol and water. All data apply to dilute aqueous solutions and are presented as values of pK_{Ac}, which is defined as the negative of the logarithm of the equilibrium constant K_{Ac} for the following dissociation reactions:

$$HCOOH \rightleftharpoons HCOO^- + H^+ \tag{3.5}$$

$$CH_3COOH \rightleftharpoons CH_3COO^- + H^+ \tag{3.6}$$

$$CH_3OH \rightleftharpoons CH_3O^- + H^+ \tag{3.7}$$

$$C_2H_5OH \rightleftharpoons C_2H_5O^- + H^+ \tag{3.8}$$

$$H_2O \rightleftharpoons OH^- + H^+ \tag{3.9}$$
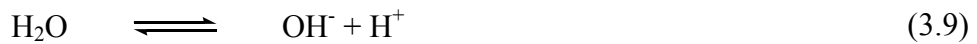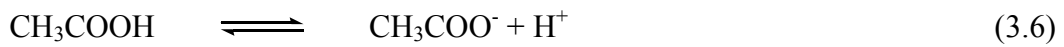
Table 3.7. Dissociation constants (pK_{ac} values) of several investigated compounds [Eqs. (3.5–3.9)] at 25 ^oC from [CRC05].

Compound	Temperature [^oC]	pK_{Ac} [-]
Ac_1	25	3.75
Ac_2	25	4.75
Al_1	25	15.5
Al_2	25	15.5
W	25	14.0

The pK_{Ac} values in Table 3.7 show that formic acid and acetic acid are weak acids. Formic acid is the strongest unsubstituted fatty acid. Its acidity is about ten times lager than that of acetic acid. The acidic strengths of methanol and ethanol are almost the same and extremely small.

3.1.2 Chemical Reaction Equilibria

Applying Eqs. (2.67) and (2.62) presented earlier, the equilibrium constants of hydrolysis of the four esters in the liquid phase can be expressed as shown below Eqs. (3.10) and (3.11) for the ideal and non-ideal liquid mixture, respectively. In these expressions, Es_{ij}, Al_i, and Ac_j are simply expressed as Es, Al, and Ac.

$$K_c = \frac{c_{Al}c_{Ac}}{c_{Es}c_W} \tag{3.10}$$

or

$$K_a = \frac{a_{Al}a_{Ac}}{a_{Es}a_W} \tag{3.11}$$

If the concentration of the ester is small, then during the reaction the concentration of water will be reasonably constant near that of pure water (55 mol/L). The rate of reaction can then be expressed in terms of volumetric concentrations as follows:

$$r = k^{mod}c_{Es}\left(1 - \frac{c_{Al}c_{Ac}}{K_c^{mod}}\right) \tag{3.12}$$

Therefore, on can introduce a modified equilibrium constant sometimes used in the literature:

$$K_c^{mod} = \frac{c_{Al}c_{Ac}}{c_{Es}} = K_c c_W \tag{3.13}$$

If the standard Gibbs free energies of reaction are known, the reaction equilibrium constants at 25 ^{o}C can be computed as shown earlier in Eq. (2.64).

With the values of the standard Gibbs free energies of reaction ΔG_r^o shown in Table 3.4, the thermodynamic reaction equilibrium constants of the four ester hydrolysis reactions in the liquid phase at the standard temperature (25 ^{o}C) were calculated using Eq. (2.64). The reaction equilibrium constants at different temperatures were estimated using the integrated form of the van't Hoff equation [Eq. (2.99)]. The obtained results are shown in Table 3.8.

Beside the calculation from the thermodynamic data, the reaction equilibrium constants can also be experimentally determined. The chemical equilibria of hydrolysis or synthesis of the four esters have been studied and reported in the literature (e.g., [Schu39], [Weth74], [Falk99], [Du99], [Hiwa04] and [Stoye06]).

The chemical equilibrium of the methyl formate hydrolysis was experimentally analysed in the work of Schultz [Schu39]. It was found that the reaction equilibrium constant for the methyl formate hydrolysis depends on the water/ester ratio. With a water/methyl formate molar ratio of 1, the reaction equilibrium constant is 0.14, but with a molar ratio of 15, it is 0.24.

Table 3.8. Reaction equilibrium constants of hydrolysis of the four esters in the liquid phase at the standard temperature (25 ^{o}C) calculated from the values of the standard Gibbs free energies of reaction ΔG_r^o [Eq. (2.64)], and at other temperatures estimated using the integrated form of the van't Hoff equation [Eq. (2.99)].

Reactant	K_a [Eq. (2.64)]			
	25 ^{o}C	35 ^{o}C	45 ^{o}C	55 ^{o}C
Es_{11}	0.068	0.075	0.083	0.090
Es_{12}	0.067	0.074	0.083	0.090
Es_{21}	0.110	0.132	0.156	0.182
Es_{22}	0.083	0.086	0.090	0.093

In the work of Wetherold [Weth74], the chemical equilibrium of the methyl formate hydrolysis with various concentrations of hydrochloric acid at the temperature range of 22 to 24 ^{o}C was experimentally investigated. In his work, the values of the reaction equilibrium constant of the methyl formate hydrolysis were given as values of K_c^{mod} [Eq. (3.13)]. To be able to compare to the other values given by other works, those values from [Weth74] were converted to K_c and are listed in Table 3.9.

Table 3.9. Equilibrium constants K_c and K_c^{mod} of the methyl formate hydrolysis from [Weth74].

c_{HCl}	K_c [Eq. (3.10)]	K_c^{mod} [Eq. (3.13)]
[mol/L]	[-]	[mol/L]
0.054	0.169	9.29
0.54	0.152	8.36
1.06	0.123	6.75

Falk *et al.* (1999) also estimated the reaction equilibrium constant of the methyl formate hydrolysis at 25 ^{o}C from the equilibrium composition. A value of $K_c = 0.12$ was obtained in relatively good agreement with the value given by Wetherold *et al.* (1974).

For the methyl acetate hydrolysis, the equilibrium constant, K_c, value range of $0.12 - 0.14$ was estimated by Du *et al.* (1999). In the other work, Hiwale *et al.* (2004) found the value of K_c between 0.14 and 0.2.

Stoye (2006) showed the reaction equilibrium constant of the ethyl acetate esterification at 40 ^{o}C to be 2.51. It can be converted to the equilibrium constant of the reverse reaction,

ethyl acetate hydrolysis, as defined $K_{\text{hydrolysis}} = 1/K_{\text{esterification}}$. Thus, the equilibrium constant of ethyl acetate hydrolysis K_c at 40 $^{\circ}$C is 0.40.

The data available in the literature are still not fully satisfying. It is one of purposes of this work to enlarge the regarding data set.

3.2 Catalysts and Adsorbents

As discussed earlier, the hydrolysis of esters is slow at neutral pH, but accelerated at acidic pH. Therefore, acids can catalyze the ester hydrolysis reaction. The catalyst of the reaction can be a mineral acid (e.g., HCl, H_2SO_4, and HNO_3) in the liquid form. Liquid acids are rather rarely used in practice, since the separation of acids from the mixture after the reaction is costly. An alternative that can be efficiently utilized is the application of heterogeneous catalysis by an acid in the solid form. This is a cation-exchange resin. Typical representatives of this resin group are commercially available cation-exchange resins that are offered by, for example, Dow Chemical Company (Dowex), Bayer (Lewatit), Rohm and Haas (Amberlyst), Degussa (Deloxan). These resins have been often used by many researchers as a catalysts and adsorbents (e.g., [Mazz79a-b], [Pöpk00], [Falk02], [Lode03] and [Sainio04]).

In this work, two batches of the strongly acidic cation-exchange resin Dowex 50W-X8 (Dow Chemical Company) were mainly used. This resin is based on a microporous styrene-divinylbenzene copolymer functionalized by the sulphuric acid type (SO_3H). It acts as both adsorbent and catalyst. The difference between the two batches was essentially the range of particle sizes. The catalyst with the smaller particle size (Cat1) was already used extensively in other investigations [Falk99, Falk02]. The second (Cat2) was purchased prior to the study discussed here. Several physical and chemical properties of the catalysts are listed in Table 3.10.

In addition, in some experiments a mineral acid – hydrochloric acid – was also used as a homogeneous catalyst.

Table 3.10. Physical and chemical properties of the two catalysts.

Catalyst characteristic	Cat1	Cat2
Particle size, μm	32-45	38-75
Type	Dowex 50W-X8	
Cross-link density, wt-%	8.0	
Active group	sulfonic acid	
Matrix	styrene-divinylbenzene	
Ionic form	H^+	
Bulk density, kg/m^3	800	
Feature	"old" (already 5 years in use)	Newly acquired

3.3 Summary and Outline of Experimental Program

There are existing data in the literature regarding the four hydrolysis reactions considered. However, there are several inconsistencies and important data are missing. With the experimental investigations performed during this work, new data should be acquired to enlarge the database related to these hydrolysis reactions. Toward that end, in particular kinetic parameters of the four hydrolysis reactions in the liquid and solid phases should be estimated. The phase equilibria of the relevant components in the liquid–resin system, and the chemical equilibria of the hydrolysis of the four esters should also be examined.

In order to achieve these goals, experimental studies performed in a reaction calorimeter are proposed. From these calorimetric experiments, the heat flows due to reaction and, therefore, the reaction rates and enthalpies can be determined. In parallel, several other set ups as a conventional batch reactor and a equilibration equipment should also be used to collect more data necessary. A description of the equipments used and the experimental procedures is given in Chapter 5. Before, because calorimetry is used intensively, in the coming chapter basics of calorimetric techniques are introduced (Chapter 4).

Calorimetric Techniques

In order to achieve the goals of the work, several experimental methods were applied. In particular, thermodynamic and kinetic data were collected by performing experiments in a reaction calorimeter. This chapter gives a basic description of the calorimetric techniques. The particular reaction calorimeter and other equipments used in this work together with procedures to collect the data are explained in the next chapter. This chapter also introduces the models describing the reaction calorimeter applied in this study.

4.1 Reaction Calorimetry

Reaction calorimetry is a suitable tool for the purpose of kinetic and thermodynamic screening in early stages of process development. A review on the principles and the development of different types of reaction calorimeters is presented by [Beck68], [Karl87a], [Land96] and [Regen97]. A comprehensive overview on different calorimetric principles and their application in research and commercial devices is given by [Pastré00]. A rather general overview about calorimetry is given by [Hemm84] and [Günth06].

A unique technique for the simultaneous determination of kinetic and thermodynamic parameters is calorimetry [LeBl96]. Calorimetry, in the broadest sense, means the quantitative measurement of energy exchanged in the form of heat during a reaction of any type. By contrast, thermal analysis is concerned only with the measurement and recording of temperature-induced changes or temperature differences. Since almost chemical reactions and many physical changes (e.g., deformation, phase transformations) are associated with the uptake or release of heat, the quantitative investigation of heat

exchange is a relatively simple and universal method for characterizing particular processes both in an overall sense and with respect to time [Günth06].

Nevertheless, only in recent decades has calorimetry emerged from the laboratories of a few thermodynamicists and specialists to become a widespread, convenient analytical method. The development of commercial calorimeters since the 1950s has led to rapid dissemination and application of the method even beyond the bounds of universities.

Reaction calorimetry was widely applied to investigate thermodynamic and kinetic parameters of chemical reactions [Beck68], [Regen83], [Land94], [LeBl96], [Semp98], [Pastré00], [Pastré01], [Ball00], [Ball02], [Ubrich99], [Dyer02], and [Stapp02]. However, for complex reaction systems the heat signal of chemical reactions itself is not enough to open a way to kinetic parameters. Then other analytical techniques are required.

4.1.1 Methods of Calorimetry

As noted above, heat that is released or consumed by a process cannot be measured directly. Unlike material quantities such as amount of substance, which can be determined with a balance, or the volume of a liquid, which can be established with a liter measure, the quantity of heat must be measured indirectly through its effect on a substance whose temperature either raises or lowers. The fundamental equation required to analyze experiments is the relationship between heat exchanged and a corresponding temperature change:

$$\Delta Q = c_p(T) \Delta T \tag{4.1}$$

where ΔQ is the exchanged heat, ΔT is the observed temperature change, and $c_p(T)$ is an overall heat capacity.

For temperature changes that are not too large, the heat effect is directly proportional. However, if the temperature change exceeds a few Kelvin, knowledge of the temperature function of the particular heat capacity in question is required in order to quantify the heat effect on the basis of a measured temperature difference.

The relationship given above is directly applied in the standard calorimetric methods for determining the heats of certain processes: A) either temperature is held constant by appropriate compensation for the heat effect, and the required compensation power is

measured, or B) a temperature change is measured and used to calculate the corresponding value for the exchanged heat [Günth06].

A) Compensation for Thermal Effects

In the first method of heat measurement, temperature changes in the calorimeter contents are avoided by supplying or withdrawing heat in the amount (but opposite in sign) associated with the process under investigation. Electrical energy is used to provide this compensation, either by introduction in the form of Joule heating or dissipation through the Peltier effect [Nilss82]. A combination approach is also possible, with an appropriate constant level of cooling and simultaneous controlled electrical heating. The required amount of compensation power can be provided with a high degree of precision.

The method of compensation is advantageous, since it permits measurements to be carried out under quasi-isothermal conditions, thereby avoiding heat loss from the calorimeter to the surroundings by heat transport processes. Furthermore, there is no need for calibrated temperature measurements.

B) Measurement of a Temperature Difference

In this alternative method of heat measurement, which is indirect, a measured temperature difference is used to calculate the amount of heat exchanged. A distinction can be made between temporal and spatial temperature-difference measurements. In *temporal* temperature-difference measurement, the temperature of the calorimeter content is measured before and after a process, and a corresponding heat is calculated on the basis of equation (4.1). In the *spatial* method, a temperature difference between two points within the calorimeter (or between the calorimeter content and the surroundings) is the quantity of interest. In this case, the basis for interpretation is from Fourier's law of heat conduction:

$$\dot{Q} = U_W(T) A_W \Delta T \tag{4.2}$$

where $\dot{Q}$ is the heat flow rate, $U_W(T)$ is the coefficient of thermal conductivity, A_W is the cross-section area, and ΔT is again the temperature difference.

This expression shows that the heat flow rate through a heat-conducting material is proportional to the corresponding temperature difference. If the temperature difference is recorded as a function of time, then for a given thermal conductivity one acquires a

measure of the corresponding heat flow rate, which can be integrated to give a total amount of heat related to the process observed. The technique itself is very simple, but the result will be correct only if the measured temperature difference accurately reflects the total heat flow rate and no heat is lost through undetected "heat leaks".

4.1.2 Basic Reaction Calorimeter Types

Differing with respect to measuring principle, mode of operation, and general construction, there are different calorimetric techniques, such as DSC (Differential Scanning Calorimetry), Micro Calorimetry, Bomb Calorimetry, Solution Calorimetry, ARC (Accelerating Rate Calorimetry), and Reaction Calorimetry [Hemm84]. As in reaction calorimetry the system is typically investigated under conditions that are similar to the normal production reactor, it is the appropriate technique for the purpose of reaction optimization. This section will not discuss thermal analysis devices such as DSC (Differential Scanning Calorimeter) or other micro calorimetric devices, but will focus on reaction calorimeter.

Most of the existing reaction calorimeters use a double-jacketed vessel as a reactor. A liquid used as heat transfer agent is pumped through the double jacket of the reactor in a closed circulation system. This keeps the temperature of the reactor contents, T_r, at the set temperature (see Figure 2.2). Such devices can be classified according to their measurement and control principles into three categories: I) Heat-Flow, II) Power-Compensation, and III) Heat-Balance reaction calorimeters [Land96]. They are briefly described in the following subsections.

I) Heat-Flow Reaction Calorimeter

The temperature of the reactor contents (T_r) is controlled by varying the temperature of the heat exchange liquid (T_j). The heat flow through the reactor wall ($\dot{Q}$) is determined by measuring the difference between the temperature of the reactor contents and the jacket temperature. In order to convert this temperature signal into a heat-flow signal, a heat-transfer coefficient has to be determined using a calibration heater. To allow a fast control of the T_r, the flow rate of the heat exchange liquid through the jacket should be high. Most of the commercially used reaction calorimeters are based on the Heat-Flow principle, such as the RC1 from Mettler Toledo used in this work (see Section 5.1.1). A detailed calculation of the complete heat-flow balance is given in Section 4.1.4.

II) Power-Compensation Reaction Calorimeter

The temperature of the reactor contents (T_r) is controlled by varying the power of a compensation heater inserted directly into the reactor contents. As with an electrical heater, cooling is not possible, the compensation heater always maintains a constant temperature difference between the reactor jacket and the reactor contents. Thus "cooling" is achieved by reducing the power of the compensation heater. The heat flow from the reactor contents through the wall to the jacket is typically not determined because the reaction power is directly visible in the power consumption of the compensation heater. The jacket temperature (T_j) is kept constant by an external cryostat. The Power-Compensation principle was first implemented by Andersen ([Ander66] and [Ander69]) and was further developed by [Köhl72], [Hent79] and [Schild81]. [Poll01] and [Pastré01] reported a small scale Power-Compensation calorimeter. A commercial Power-Compensation calorimeter is the AutoMate [Simm00] and the Simular (combined with Heat Flow [Singh97]) from [HEL].

III) Heat-Balance Reaction Calorimeter

The temperature of the reactor contents (T_r) is controlled by varying the temperature of the heat exchange liquid (T_j). The heat flow through the reactor wall ($\dot{Q}$) is determined by measuring the difference between the jacket inlet ($T_{j,\ IN}$) and outlet temperature ($T_{j,\ OUT}$) and the mass flow of the heat exchange liquid. Together with the heat capacity of the heat exchange liquid, the heat-flow signal is directly determined without calibration. The Heat-Balance principle was first implemented by [Meek68]. Commercial versions are the RM200 from [Chemis], SysCalo 2000 Series from [Systag] and the ZM-1 from [Zeton].

4.1.3 Operation Modes

Depending on how calorimeters are operated, different operation modes can be distinguished: isothermal, isoperibolic, adiabatic and temperature programmed. As shown in Table 4.1 and previous discussion (Section 4.1.1), the isothermal operation mode is supposed to be the easiest in application because no heat accumulation by the reactor contents has to be considered. Therefore, no temperature-dependent heat capacities such as a function of T_r of the reaction mixture as well as of the reactor inserts (e.g., stirrer, sensors, baffles …) are required. However, in reality due to the non-idealities of the control circuits of the calorimeters and the principles of heat flow, the reaction temperature cannot be controlled strictly isothermal. Because most chemical and physical changes taking place

during a reaction step depend on the temperature, the evaluation of the measured data will
be simpler if isothermal conditions are fulfilled [Karl87a, Schle97].

Table 4.1 Different modes of operation of a reaction calorimeter.

Operation mode	Principle
Isothermal	Constant T_r by varying T_j or using an electric compensation heater
Isoperibolic	Constant jacket temperature T_j
Adiabatic	Continuous readjustment of T_j to be equal to T_r
Temperature programmed	Linear heating to a final temperature

In the present work, calorimetric measurements were carried out under isothermal
conditions.

4.1.4 Contributions to Heat Balance

For the following discussions, ideal isothermal controlling of the reaction temperature T_r
will be assumed. Therefore, in Figure 4.2 no heat accumulation terms of the reaction
mixture and the reactor inserts are indicated. However, this assumption does not hold for
all applications of calorimetry.

The task of a reaction calorimeter is to measure the total heat production or consumption
$\dot{Q}_{tot}$ during a chemical reaction. Generally, a heat effect due to any kind of physical
process occurring in the vessel is included. For the isothermal condition, the total heat $\dot{Q}_{tot}$
is the heat flow through the reactor wall $\dot{Q}_{wall}$. This total heat flow $\dot{Q}_{tot} \equiv \dot{Q}_{wall}$ can be
expressed for steady state conditions as follows:

$$\dot{Q}_{tot} \equiv \dot{Q}_{wall} = \dot{Q}_{chem} + \dot{Q}_{mix} + \dot{Q}_{phase} + \dot{Q}_{stir} - \dot{Q}_{dos} - \dot{Q}_{loss} + \dot{Q}_{c} + ... \tag{4.3}$$

where $\dot{Q}_{chem}$ is the heat flow due to chemical reactions, $\dot{Q}_{mix}$ is the heat flow occurring due
to non ideal mixing of different fluids, $\dot{Q}_{phase}$ is the heat flow due to possible phase change
processes, $\dot{Q}_{stir}$ is the heat flow resulting related to energy input by the stirrer, $\dot{Q}_{dos}$ is the
heat flow caused by the dosing of reactants, $\dot{Q}_{loss}$ is the heat flow lost to the surroundings,
and $\dot{Q}_{c}$ is the heat flow from the calibration heater. Further possible influences which can

also contribute the effect to the total heat flow (e.g., radiation, friction,…) are not considered. For a single reaction, the most relevant reaction heat flow can be expressed as follows:

$$\dot{Q}_{chem} = V_R r \Delta H_r \tag{4.4}$$

where V_R is the volume of the reaction mixture, r is the reaction rate, and ΔH_r is the reaction enthalpy.

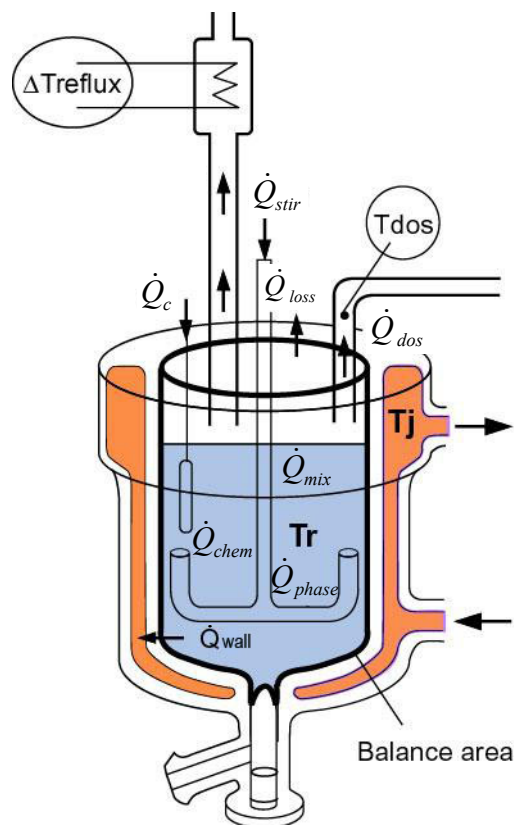**Figure 4.2.** Main heat flows that have to be considered in a reaction calorimeter running at isothermal conditions.

The heat evolved by the stirrer $\dot{Q}_{stir}$ can be described by [Zogg93]:

$$\dot{Q}_{stir} = Ne \rho_r n_S^3 d_R^5 \tag{4.5}$$

where Ne is the Newton number, ρ_r is the density of the reaction mixture, n_S is the reversions per second of the stirrer, and d_R is the diameter of the stirrer.

The heat flow caused by the dosing of reactants $\dot{Q}_{dos}$ can be expressed as:

$$\dot{Q}_{dos} = \dot{F}c_{p,dos}(T_r - T_{dos})$$ (4.6)

where $\dot{F}$ is the dosing rate, $c_{p,dos}$ and T_{dos} are the specific heat capacity and the temperature of the liquid dosed, respectively.

The heat flow through the calorimeter wall $\dot{Q}_{wall}$ depends on the wall temperature T_W. Figure 4.3 shows the steady-state temperature profile when heat flows from the reactor contents through the reactor wall into the cooling liquid. Generally, the temperature of the reactor contents T_r and the cooling liquid T_j are assumed to be homogeneous except to a thin film layer close to the reactor wall (without convection). Thus, the heat transfer can be separated into three different steps: 1) the reactor-side heat transfer, described by the heat-transfer coefficient h_r; 2) the heat conduction through the reactor wall, described by the thickness of the wall L and the heat conduction coefficient λ_W; and 3) the jacket-side heat transfer, described by the heat-transfer coefficient h_j. The heat flow on the reactor side $\dot{Q}_{wall,r}$ (Figure 4.3) can be expressed as follows:

$$\dot{Q}_{wall,r}(t) = A_W \lambda_W \left. \frac{\partial T_W}{\partial l} \right|_L = A_W h_r [T_r(t) - T_W(L,t)]$$ (4.7)

where A_W is the total heat transfer area, l is the position inside the wall, and T_W is the temperature of the reactor wall. The heat flow $\dot{Q}_{wall,j}$ on the jacket side (Figure 4.3) can be expressed as follows:

$$\dot{Q}_{wall,j}(t) = A_W \lambda_W \left. \frac{\partial T_W}{\partial l} \right|_0 = A_W h_j [T_r(t) - T_W(0,t)]$$ (4.8)

At steady state, when the temperature profile and all the heat flows do not change in time, the heat flow entering the reactor wall must be equal to the heat flow leaving the wall, and then there is no heat accumulation inside the wall. The steady-state heat flow $\dot{Q}_{wall}$ can then be expressed as follows:

$$\dot{Q}_{wall} = \dot{Q}_{wall,r} = \dot{Q}_{wall,j}$$ (4.9)
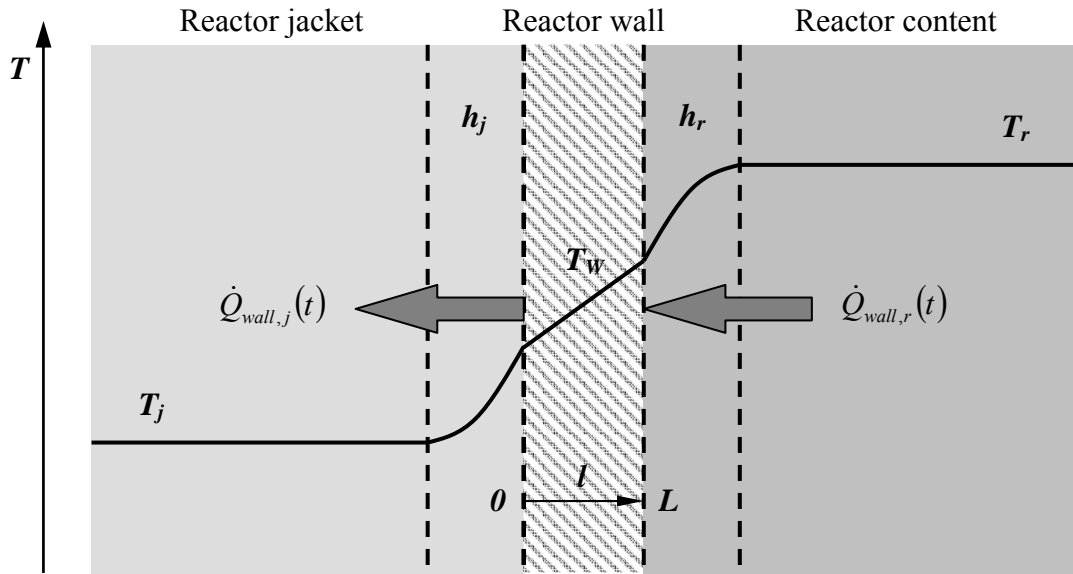
Figure 4.3. Steady-state temperature profile when heat flows from the reactor content through the reactor wall into the cooling liquid of the jacket.

At steady-state conditions, the temperature profile inside a homogeneous reactor wall is linear because only heat conduction is taking place (Figure 4.3). Thus, the following conditions are further fulfilled:

$$\left.\frac{\partial T_W}{\partial l}\right|_0 = \left.\frac{\partial T_W}{\partial l}\right|_L = const \text{ and } \left.\frac{\partial T_W}{\partial l}\right|_0 L = T_W(L) - T_W(0) \tag{4.10}$$

Combination of Eqs. (4.7) to (4.10) gives the steady-state heat flow through the reactor wall as follows:

$$\dot{Q}_{wall} = U_W A_W \left(T_r - T_j\right) \tag{4.11}$$

where U_W is the overall heat transfer coefficient. It comprises three main heat-transfer resistances in the following expression:

$$\frac{1}{U_W} = \frac{1}{h_r} + \frac{L}{\lambda_W} + \frac{1}{h_j} \tag{4.12}$$

The two steady-state heat-transfer coefficients h_r and h_j depend on physical properties of the reaction mixture and the cooling liquid, respectively.

Thus, U_W generally varies during the measurement of a chemical reaction because of two main reasons:

- h_r varies because the physical properties of the reaction mixture change during a reaction (e.g., viscosity increase during a polymerization reaction).

- depending on the calorimetric system chosen, h_j may vary because the jacket temperature T_j varies during the measurement of a reaction and consequently the physical properties of the cooling liquid.

Not only U_W but the total heat-transfer area A_W in Eq. (4.11) can also change during a reaction measurement because of dosing, density changes or due to reactions not conserving the mole number. Conventionally, these two parameters have to be calibrated by means of a calibration heater (see Figure 4.2) before and after a reaction experiment. Such a calibration is not possible during the reaction as $\dot{Q}_c$ has to be zero. Therefore, a change of U_W or A_W caused by the chemical reaction will cause an error in the measured $\dot{Q}_{tot}$.

4.2 Modeling of Case Study

In this work, a reaction calorimeter containing a suspension of a solid catalyst was used to observe thermal effects occurring during ester hydrolysis. To describe the development of concentration profiles and heat flows due to reaction in the reaction calorimeter, a more detailed mathematical model is useful. Standard models are based on classical conservation equation [West84, Tomi98]. Since the proton (H^+) dissociated from the acid that is a product of the hydrolysis process can catalyze the reaction in the liquid phase, the homogeneously catalyzed reaction should also be considered. The model summarized below is based on further assumptions: (i) There is no temperature gradient inside the catalyst particle. (ii) The loading profiles of the relatively small catalyst particles can be described using an average value. (iii) Intraparticle transport is quantified using a corresponding linear driving force expression. With these assumptions, the following mass and energy balance equations can be formulated.

4.2.1 Mass Balances

Assuming perfect mixing, the mass balance for component i in the liquid phase can be written as follows:

$$\varepsilon \frac{dc_i}{dt} = \varepsilon v_i r^{\text{hom}}(\overline{c}) + (1-\varepsilon)\beta_i \left[q_{av,i} - q_i^*(\overline{c})\right] \qquad\qquad i = 1,...,N_c \qquad (4.13)$$

In the above equation, c_i and $q_{av,i}$ are the liquid phase concentration and the average loading on the solid phase, respectively, of component i; $q_i^*(\overline{c})$ is the loading of component i on the solid phase at equilibrium with all liquid phase concentrations; r^{hom} is the rate of the reaction taking place in the homogeneous liquid phase as defined previously in Section 2.3 [Eq. (2.111)]; ε is the volume fraction of the liquid phase (or porosity); V_R is the reactor volume; β_i is an intraparticle mass-transfer coefficient of component i; v_i is the stoichiometric coefficient of component i and N_c is the number of components involved.

Similarly, the mass balance for component i in the solid phase can be written as follows:

$$(1-\varepsilon)\frac{dq_{av,i}(c_i)}{dt} = (1-\varepsilon)v_i r^{\text{het}}(\overline{c},\overline{q}_{av}) - (1-\varepsilon)\beta_i \left[q_{av,i} - q_i^*(\overline{c})\right] \quad i = 1,...,N_c \qquad (4.14)$$

where r^{het} is the rate of the reaction taking place in the solid phase as defined previously in Section 2.3 [Eq. (2.112)].

Initial conditions $t = 0$ are

$$c_i(t=0) = c_i^o \text{ and } q_{av,i}(t=0) = q_i^*\left(c_i^o\right) \qquad\qquad i = 1,...,N_c \qquad (4.15)$$

For small particles as used in this work, it can be assumed that the intraparticle mass-transfer is rapid (the β_i parameters are large). Then, this heterogeneous two-phase model can be transformed into a simpler pseudo-homogeneous model. Then, Eqs. (4.13) and (4.14) can be lumped together to give

$$\varepsilon \frac{dc_i}{dt} + (1-\varepsilon)\frac{dq_{av,i}(\overline{c})}{dt} = \varepsilon v_i r^{\text{hom}}(\overline{c}) + (1-\varepsilon)v_i r^{\text{het}}(\overline{c}) \qquad\qquad i = 1,...,N_c \qquad (4.16)$$

If, in addition, all of the functions $q_i(\overline{c})$ are linear and decoupled [$q_i = K_i c_i$, Eq. (2.41)], the following simple system of ordinary equations describes the mass balances:

$$\frac{dc_i}{dt} = \left(1 + \frac{1-\varepsilon}{\varepsilon} K_i\right)^{-1} \left[\nu_i r^{hom}(\overline{c}) + \frac{1-\varepsilon}{\varepsilon} \nu_i r^{het}(\overline{c})\right] \qquad i = 1,...,N_c \qquad (4.17)$$

4.2.2 Energy Balances

4.2.2.1 Liquid Phase Energy Balance

Obviously, the key to analyze calorimetric experiments is the energy balance, which contains the rates of heat evolution or consumption due to reaction. In the previous Section 4.1.4, the energy balance was already discussed for a homogeneous reaction mixture operated in a semi-batch and isothermal mode [Eq. (4.3)]. For a batch and isothermal operation of a heterogeneous reaction mixture (particularly, liquid-solid system) the energy balance for the completely mixed liquid phase in the reaction calorimeter can be written as Eq. (4.18). An assumption of negligible heat losses, heat flows due to phase change and mixing processes and heat generated by the stirrer ($\dot{Q}_{loss} = \dot{Q}_{phase} = \dot{Q}_{mix} = \dot{Q}_{stir} = 0$) is taken.

$$\dot{Q}_{wall} = \dot{Q}_{chem}^{hom} + \dot{Q}_{transfer} \qquad (4.18)$$

where $\dot{Q}_{chem}^{hom}$ and $\dot{Q}_{transfer}$ are energy terms corresponding to the homogeneously catalyzed reaction and the heat transfer between the liquid phase and the solid phase, respectively.

Thus, $\dot{Q}_{chem}^{hom}$ can be calculated from Eq. (4.18) if $\dot{Q}_{transfer}$ and $\dot{Q}_{wall}$ can be measured with sufficient accuracy. The various terms in the Eq. (4.18) are described below.

Heat of homogeneously catalyzed reaction

$$\dot{Q}_{chem}^{hom} = \varepsilon V_R r^{hom}(\overline{c}) \Delta H_r^{hom} \qquad (4.19)$$

where ΔH_r^{hom} represents the enthalpy of a given homogeneous reaction.

Heat exchange to the coolant

It is assumed the heat exchange between the catalyst particles and the coolant is negligible. Heat exchange between the reaction mixture and the coolant is again described by

$$\dot{Q}_{wall} = U_W A_W (T_j - T^L) \tag{4.20}$$

where T_j is the temperature of the coolant (or the jacket temperature), T^L is the liquid phase temperature, U_W is the overall heat exchange coefficient to the reactor wall, and A_W is the heat exchange area between the reaction mixture and the reactor wall.

Heat transfer between the liquid phase and the solid phase

$$\dot{Q}_{transfer} = \varepsilon V_R \beta_h (T^L - T^S) \tag{4.21}$$

where T^S is the temperature of the solid phase, and β_h is the heat transfer coefficient through the liquid film surrounding a catalyst particle.

4.2.2.2 Solid Phase Energy Balance (adsorbed phase + catalyst)

Under steady state conditions holds

$$\dot{Q}_{transfer} = \dot{Q}_{chem}^{het} \tag{4.22}$$

The heat flow due to the heterogeneously catalyzed reaction is

$$\dot{Q}_{chem}^{het} = (1 - \varepsilon) V_R r^{het} (\bar{c}, \bar{q}_{av}) \Delta H_r^{het} \tag{4.23}$$

where ΔH_r^{het} represents the enthalpy of the heterogeneous reaction.

Substituting for $\dot{Q}_{transfer}$ from Eq. (4.22) into Eq. (4.18) gives

$$\dot{Q}_{wall} = \dot{Q}_{chem}^{hom} + \dot{Q}_{chem}^{het} = \left| \dot{Q}_{chem}^{total} \right| \tag{4.24}$$

Thus, the measurable time dependence of the heat flow over the calorimeter wall, $\dot{Q}_{wall}$, is directly and linearly related to the rates of reactions. $\dot{Q}_{wall}$ is positive here for endothermal reactions and negative for exothermal reactions. The simplified energy balance of a batch

calorimeter operated under isothermal conditions which is used in this work can be written as

$$\dot{Q}_{wall} = \left|\dot{Q}_{chem}^{total}\right| = \varepsilon V_R r^{hom}(\overline{c}) \Delta H_r^{hom} + (1-\varepsilon) V_R r^{het}(\overline{c}, \overline{q}_{av}(\overline{c})) \Delta H_r^{het} \tag{4.25}$$

The rates of reaction have been already defined and discussed in a general way in the previous Section 2.3. More detailed expressions for the hydrolysis reactions are described later in Section 6.4.3.

Experimental Section

The equipments used and the experiments are described in Section 5.1 of this chapter. The equipments include the reaction calorimeter for measuring the reaction heat flows, the equilibration equipment for determination of the reaction equilibrium constants, and the gas chromatography system for analysis of the reaction mixtures. Section 5.2 summarizes experimental procedures applied.

5.1 Experimental Equipments

5.1.1 Reaction Calorimeter

As discussed earlier in Section 4.1, reaction calorimetry is a suitable tool for the simultaneous determination of kinetic and thermodynamic parameters. Most of the commercially used reaction calorimeters are based on the heat-flow principle. In this work, the commercially available METTLER TOLEDO RC1 Reaction Calorimeter was used to quantify heat effects related to the course of the reactions. It was based on the heat-flow principle. The calorimeter was equipped with a RD10 dosing controller. WinRC^{NT} software was applied to control the RC1 calorimeter and the RD10 dosing controller by the PC.

Various types of reactors can be attached to the RC1. In this work, a double-jacketed glass reactor (AP01) was used. The AP01 reactor allowed for the analysis of volumes between 0.5 and 2.0 L. The thermostat controlled the temperature of the reactor. The silicon oil used as heat transfer agent was pumped through the double jacket of the reactor in a closed

circulation system. This kept the temperature of the reactor contents T_r at the set temperature. Both the jacket temperature, T_j, and the temperature of the reactor contents, T_r, could be measured precisely. This allowed for the calculation of the heat flow through the reactor wall. In this study, the isothermal mode was applied to perform experiments, i.e., T_r was kept constant. Figure 5.1 shows the operating principle of the RC1 in T_r mode and a view of the AP01 reactor. In this case, the T_r was always controlled by means that deviations of T_r from the set value (through heat of reaction) were compensated by appropriate correction of the jacket temperature, i.e., the heat generated or consumed by reactions was dissipated.

The stirrer speed could be varied between 30 and 850 rpm. However, it depends on stirrer type and viscosity of the reaction mass. The acquisition of the data was carried out every 2 seconds.
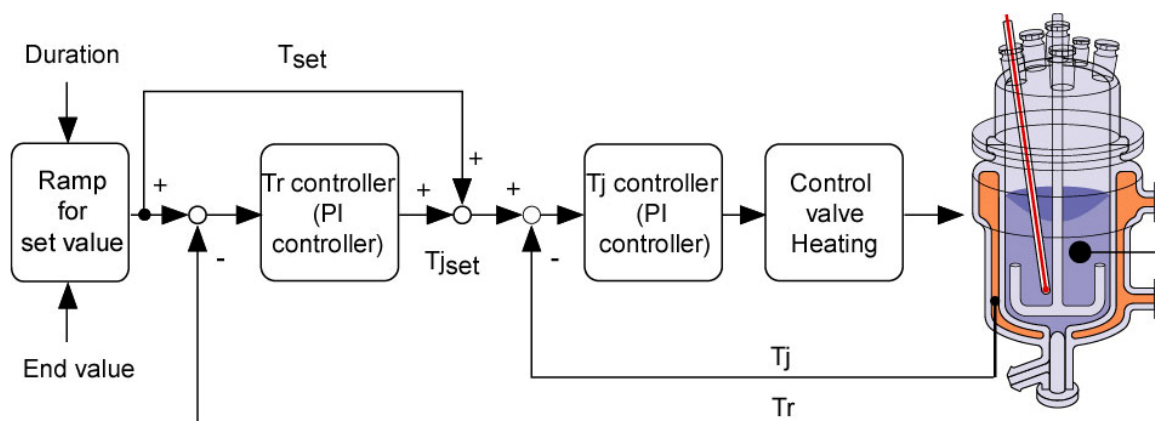
Figure 5.1. Operating principle of the RC1 in isothermal mode (T_r = constant) and a view of the AP01 reactor.

5.1.2 Equilibration Equipment

The experiments to determine reaction equilibrium constants were carried out in a conventional batch reactor. The reactor is a 100-mL glass flask, which is placed in a constant temperature shaking water bath. The temperature is controlled by thermostat from 20 to 90 ^{o}C with the sensitivity of $\pm$ 0.1 ^{o}C. Shaking speed range is 40 to 140 cycles per minute.

Additional experiments to determine reaction kinetics by the conventional method were also conducted in the same batch reactor.

5.1.3 Gas Chromatography

In the present work, reaction mixtures need to be quantitatively determined for estimation of reaction equilibrium constants and reaction extents as well. The technique of gas chromatography is adequate to analyze mixtures of volatile substances such as those involved in the investigated reactions. For this end, the 6890 series gas chromatography (GC) system manufactured by Agilent Technologies was used in this work. The GC system was equipped with a highly polar stationary-phase capillary column (DB-FFAP, Agilent) and a thermal conductivity detector (TCD). Helium was used as the carrier gas. Several typical characteristics of the capillary column are listed in Table 5.1. The ChemStation for GC was used for on-line data acquisition and data evaluation.

Table 5.1. Typical characteristics of the GC capillary column.

Characteristic	DB-FFAP capillary column
Stationary phase	Nitroterephthalic acid modified polyethylene glycol
Polarity	High
Length, m	60.0
Inner diameter, mm	0.25
Film thickness, μm	0.5
Temperature limits, ^{o}C	40 - 250

GC operating conditions for the analysis were as follows:
- GC inlet: split mode, split ratio of 1:100, setting temperature of 150 ^{o}C;
- Carrier gas flow rate: ramp mode, initial flow rate of 1 mL/min in 7 min, acceleration of 5.0 mL/min^2 to 4.0 mL/min then held for 3.4 min;
- Oven temperature: ramp mode, initial temperature of 120 ^{o}C in 7 min, acceleration of 50 ^{o}C/min to 150 ^{o}C then held for 3.4 min;
- Detector temperature: 210 ^{o}C;
- Total run time is 11 min.

Calibration

The determination of the amount of a certain component in the sample injected in gas chromatography requires the measurement of the peak area and a knowledge of the response factor of this component. Therefore, the calibration measurements were carried out to determine the response factors of the involved components. As used in this work, the

response factor, f, is defined as the proportionality coefficient between the peak area, A_i, and the concentration of the corresponding component, c_i. Thus,

$$c_i = f A_i \qquad\qquad\qquad\qquad\qquad (5.1)$$

Varied known concentration mixtures of each component with water were made by weighing in a volumetric flask. To be careful and avoid possible losses due to evaporation (and further, to avoid chemical reactions taking place in a reactive mixture in later analyses of samples), the calibration mixtures were cooled to 1 $^{\circ}$C. The sample was injected into the GC with the injection volume of 2 μL. For each sample, the injection was done 5 times. Calibration curves that present the relationships between concentration of the component and the corresponding peak area were determined (see Appendix B). Because the response factors of a thermal conductivity detector is rather stable in a long-term use [Guio88], the infrequent check (once every six months) of the response factors for selected components was done.

Accuracy and Precision

Quantitative analysis by GC is based on the determination of the parameters of the chromatograph related to the amount of the corresponding component of the injected sample. All sources of errors in the determination of these parameters as well as sources of fluctuations in the quantitative relationship between the amount of the compound and its peak size will contribute to the analytical error [Guio88].

The errors of measurements are essentially related to the influence of the parameters of the data acquisition system: (1) the frequency of data acquisition, (2) the time constant of the detector and the amplifier, (3) the threshold for peak detection and (4) the value of the signal to the noise ratio. The influence of these parameters can be studied conveniently by computer simulation. However, suitable experiments can be used to verify the validity of the conclusions achieved. The studies of this issue were more or less described in the literature (e. g., in [Gill67], [Bocek69], [Kaiser69], [King69], [Goed71], [Grant71], [Goed73a], [Goed73b] and [Goed7c]).

The reproducibility of injections with a syringe much depends on the syringe capacity and on the fraction of the total capacity which is injected. Bocek *et al.* [Bocek69] estimated with syringes the absolute standard deviation of the sample volume delivered to be around 0.04 μL for sample volumes between 1 and 10 μL. King and Dupre [King69] gave a similar result that is a repeatability of 5% at the 95% confidence level in the range 0.1 to 3 μL (i.e., a standard deviation around 0.002 to 0.06 μL). In this work, a 2 μL injection was

always used. Thus, the relative standard deviation of the sample volume injected can be assumed to be around 2%.

The measurement of the peak area contributes partially to the error of the GC analysis. Peak areas can be measured by different methods of integration. The errors introduced by different methods of integration could be different. For the method of integration from the data acquired with a computer, the repeatability of the measurements and the bias depend on the frequency of data acquisition, on the peak detection threshold and on the signal to the noise ratio. The influence of these different factors has been studied in detail, experimentally and by computer simulation, by Doedert and Guiochon [Goed71, Goed73a-c]. The repeatability of peak areas measured by computers has been estimated to be 0.5%.

In addition, the stability of the gas chromatograph and especially of the detector is a critical factor in achieving repeatable measurements [Guio71]. The response factor is a function of the value of a number of parameters which together determine the detector response. These parameters are kept more or less stable, depending on the quality of the instrument used and on the care with which it is maintained and set up by the analyst [Guio88]. For the thermal conductivity detector, the stability of the detector parameters has been studied and described in the literature (e.g., in [Jecko67], [Goed69] and [Clarke71]). They have shown that it is possible to achieve quantitative results with an excellent precision by using carefully built equipment, incorporating excellent control of all parameters, including the outlet pressure. They achieve the analysis of air and blast furnace gases with relative standard deviations for every component to be less than 1%.

From a combination of the methods and results described in the literature, Guiochon and Guillemin [Guio88] concluded that the repeatability of gas chromatographic measurements is normally between 1 and 2%.

5.2 Experimental Procedures

5.2.1 Characterization of the Catalysts

In addition to the information given by the manufacturers (Table 3.10), more information about the catalysts was obtained by characterization experiments. The goals of these experiments are to determine the swelling ratio of the catalysts in liquids, to measure acidity characteristics and the density of the catalysts.

The dry resins swell when they come into contact with liquids until an equilibrium is reached [Flory53]. The swelling ratio, i.e., the volume ratio of the swollen resin at equilibrium (V_{Re}^{eq}) to the dry resin (V_{Re}^{o}), depends on the nature of the liquid. In this work, the swelling ratios of the resins were estimated at 25 $^{\mathrm{o}}$C for all single components involved in the investigated reactions (Es_{ij}, Ac_i, Al_j and W). To this end, the resin was kept in contact with each of the liquid components until no further volume change could be detected. This was usually achieved after only a few minutes. Nevertheless, the final volume of the swollen resin was measured the next day after the resin had been separated from the liquid phase by centrifugation.

To compare the acidities of Cat1 and Cat2, the amounts of sulfonic acid groups per unit mass of the resins were quantified by titrating approximately 0.15 g of each of the catalysts with sodium hydroxide solution (0.1 N).

The density of the catalysts was measured in a 5-cm^3 pycnometer by using helium as the medium.

5.2.2 Calorimetric Experiments Using Catalyst Suspensions

5.2.2.1 Preliminary Experiments

Measurements of Heat Mixing Effects
In preliminary experiments, a semibatch mode was applied to estimate the extent of heat effects due to the mixing of water and esters in distinction from the heat effects caused by the chemical reactions. To this end, water and the catalyst were initially charged into the reactor at ambient conditions, and a temperature ramp was then applied to set the desired initial temperature. Approximately 15 min later, a certain amount of ester was added to the reactor using a dosing pump at a constant flow rate for about 3 – 5 min. A constant stirring rate of 200 rpm was employed throughout these experiments. A summary of the experiments is given in Table 5.2.

Table 5.2. Summary of preliminary calorimetric experiments to estimate the extent of heat effects due to the mixing of water and esters.

Run	Temperature [$^{\circ}$C]	Catalyst	First fill, W [g]	Dose, Es [g]	Dosing time [min]
A1-2	25	46.2 g of Cat1	1000	$Es_{11} = 200$	4
A3-4	25	0	1000	$Es_{11} = 200$	4
A5-6	25	0	1000	$Es_{11} = 200$	4
A7-8	25	0	1000	$Es_{11} = 100$	4
A9-10	25	0	1000	$Es_{11} = 75$	4

Measurements of Volume Mixing Effects

For ideal mixing processes, the mixture volume can be calculated as the sum of the individual volumes. However, this can not be applied in the case of non-ideal mixing processes because of mixing effects. To investigate properly the kinetics of hydrolysis of the four esters using calorimetric experiments, the initial volume of reactants mixture should be precisely measured. As discussed above, the calorimetric experiments were performed by means that one of the reactants (water) and the catalyst were first filled into the reactor, and then the second reactant (ester) was added after a certain time. Due to the manner of performance and the large reactor scale, it was difficult to determine directly the volume mixing effects in the reactor. Aside from the calorimetric experiments, extra experiments to estimate volume mixing effects of a single ester in water at 25 $^{\circ}$C were carried out.

Water and the ester were kept at 25 $^{\circ}$C by the thermostat. 100 mL of water was first filled in a 150-mL glass flask, and then a desired amount of ester was added to the flask. The flask was closed, well shaken, and then placed in the thermostat at 25 $^{\circ}$C for an hour. The added amount of ester was varied between about 2 mL and the saturation value. The volume of the mixture was then measured by 100-ml and 10-mL graduated measuring cylinders, which the graduations are in 1.0 and 0.1 mL steps, respectively.

5.2.2.2 Reaction Enthalpies and Rates of Reactions

When a reactant is dosed in the semibatch mode, a heat flow due to mixing and reaction is induced. Splitting this overall flow into its individual contributions is complicated. Thus, in the main part of this study, batch reactions were considered to analyze the effect of the reaction separately. For these reactions, an initial sample was taken approximately 5 min after the ester dosing was finished (long enough to ensure that mixing was complete) and analyzed off-line. This time was used as the starting time of a batch run. A second sample

was taken when the reaction was completely finished, i.e., when the heat flow was zero. The samples were analyzed by GC (see Section 5.1.3). In this way, batch hydrolysis reactions were conducted in the calorimeter at various temperatures and starting concentrations using suspensions of both catalysts. Batch esterification reactions of formic acid and acetic acid with methanol were also performed in the same ways. A summary of the experiments is given in Table 5.3.

Table 5.3. Summary of calorimetric experiments to estimate heat effects due to chemical reactions performed in the batch mode.

Run	Reactant	T_r	Catalyst	Initial concentration	First fill, W	Liquid fraction, ε
		[^{o}C]		[mol/L]	[L]	[-]
Hydrolysis of esters						
B1-4	Es_{11}	15	Cat1	2.17 – 3.64	~1.0	0.96
B5-8	Es_{11}	20	Cat1	2.10 – 3.17	~1.0	0.96
B9-14	Es_{11}	25	Cat1, Cat2	0.67 – 3.31	~1.0	0.96, 0.92
B15-20	Es_{12}	25–30	Cat1, Cat2	~2.8	~1.0	0.96, 0.92
B21-22	Es_{21}	25	Cat1, Cat2	~1.5	~1.0	0.96, 0.92
B23-24	Es_{22}	25	Cat1, Cat2	~0.6	~1.0	0.96, 0.92
Esterification of acids with alcohols						
B25-26	Ac_1, Al_1	25	Cat2	$Ac_1 : Al_1 = 1 : 1$	~1.0	0.92
B27-28	Ac_2, Al_1	25	Cat2	$Ac_2 : Al_1 = 1 : 1$	~1.0	0.92

5.2.3 Measurement of Reaction Equilibrium Constants

5.2.3.1 Hydrolysis of Esters

Binary Ester–Water Mixtures (homogeneous)
The experiments to analyze chemical equilibria of hydrolysis of the four esters were conducted in the simple equilibration equipment (Section 5.1.2). The initial mixtures included an ester and water with small amounts of hydrochloric acid as homogeneous catalyst. The initial concentration of esters was varied within the solubility range. In order to analyze the influence of temperature on the reaction equilibrium constants, the equilibration experiments were carried out at varied temperatures of 25, 35, 45 and 55 ^{o}C. The experiments were conducted by means that place the desired amount of reactants and catalyst in a 100-mL glass flask, which was then sealed and placed in the shaking water bath at a given temperature for a period of time. To check whether the chemical equilibrium was reached, samples were taken and analyzed by the GC (see Section 5.1.3)

at different times. The chemical equilibrium was realized when the reaction extent was constant within the analytical error. To stop any reaction taking place in the sample vials, the samples were cooled down to 1 °C immediately after sampling. The running time was varied from experiment to experiment depending on the reaction and temperature. It was observed and summarized in Table 5.4 together with the operating conditions. The experiments with the lower ester to water ratio were carried out at 25 °C only. The obtained results are presented and discussed in Section 6.3.

Table 5.4. Summary of equilibration experiments for hydrolysis of reactive binary ester–water mixtures catalyzed by homogeneous hydrochloric acid.

Run	Reactant	Initial Es/W ratio	c_{HCl}	V_R	Experiment duration[*]			
		[mol/mol]	[mol/L]	[L]	25 °C	35 °C	45 °C	55 °C
C1-5	Es_{11}	0.093, 0.018	0.025	0.1	3 days	2 days	1 day	1 day
C6-10	Es_{12}	0.066, 0.019	0.025	0.1	3 weeks	2 weeks	1 week	1 week
C11-15	Es_{21}	0.030, 0.009	0.025	0.1	1 weeks	5 days	3 days	2 days
C16-20	Es_{22}	0.012, 0.009	0.025	0.1	4 weeks	3 weeks	10 days	1 week

*) Sufficient to guarantee equilibrium conditions

Ternary Ester–Ester–Water Mixtures (homogeneous)

To observe if the equilibrium of an ester hydrolysis can be influenced by the presence of other esters in the initial mixtures, the determination of equilibrium constants of reactive mixtures consisting of more than one ester and water was carried out at 25 °C. The catalyst used for these experiments was also hydrochloric acid. Due to resolution limitations of the available GC capillary column (see Section 5.1.3 for more details) in elution of components whose retention times are too close, only equilibration experiments of reactive ternary ester–ester–water mixtures were systematically carried out. The experiments were performed in the same manner as described above for reactive binary ester–water mixtures. The initial concentration of ester was almost 0.5 mol/L. A summary of the experiments is given in Table 5.5.

Binary Ester–Water Mixtures (heterogeneous)

From the characterization of the catalysts (Section 5.2.1), the obtained swelling ratio data for single components can give some indications of the phase equilibrium behavior of a single component in presence of an ion-exchange resin catalyst. With a mixture of components, the behavior may be different.

Table 5.5. Summary of equilibration experiments for hydrolysis of reactive ternary ester–ester–water mixtures catalyzed by homogeneous hydrochloric acid.

Run	Temperature	c_{HCl}	V_R	Initial composition [mol/L]				
	[°C]	[mol/L]	[L]	Es_{11}	Es_{12}	Es_{21}	Es_{22}	W
D1	25	0.025	0.1	0.5113	0.4984	0	0	51.79
D2	25	0.025	0.1	0.5118	0	0.4989	0	51.74
D3	25	0.025	0.1	0.5093	0	0	0.4989	51.26
D4	25	0.025	0.1	0	0.5039	0.5016	0	51.27
D5	25	0.025	0.1	0	0.5051	0	0.5040	50.84
D6	25	0.025	0.1	0	0	0.5004	0.5047	50.62

In the case of a reactive system in presence of an ion-exchange resin catalyst, the mole fractions of the products – contrary to a homogeneously catalyzed reaction – may not be equal. Simultaneous chemical and phase equilibrium experiments with varied liquid fractions at 25 °C were carried out. The ion-exchange resin catalyst used for this series of experiments was Cat2 (see Section 3.2). The reactants and dry catalyst were placed in a sealed 100 mL flask, which was kept in a shaking-thermostated bath at 25 °C for two days. The liquid fraction was varied between 0.8 and 1.0. Since it is difficult to determine experimentally the solvent composition in the solid phase, only the liquid phase composition was determined. Liquid samples of the final mixture were taken and analyzed by the GC (see Section 5.1.3). A summary of the experiments is given in Table 5.6.

Table 5.6. Summary of simultaneous chemical and phase equilibrium experiments with varied phase ratios at 25 °C, under the catalyst Cat2.

Run	Phase ratio, ε	Liquid volume	Initial composition [mol/L]				
		[L]	Es_{11}	Es_{12}	Es_{21}	Es_{22}	W
E1	0.8 – 1.0	0.1	3.945	0	0	0	42.64
E2	0.8 – 1.0	0.1	0	2.866	0	0	43.72
E3	0.8 – 1.0	0.1	0	0	1.497	0	49.10
E4	0.8 – 1.0	0.1	0	0	0	0.616	52.29

5.2.3.2 Esterification of Acids with Alcohols (homogeneous)

In principle, the equilibrium constant of ester hydrolysis should be equal to the inverse of the equilibrium constant of the reverse reaction – the esterification of acids with alcohols. Thus, another way to verify the equilibrium constant of ester hydrolysis is to measure the

equilibrium constant of the corresponding esterification. The equilibration experiments for the esterification were performed with the same manner and equipment as done for the ester hydrolysis. The catalyst used in this series of experiments was hydrochloric acid with the concentration of 0.025 mol/L. The reaction temperature was 25 °C. In the first runs, the experiments were carried out in the dilute region where water was present in the initial mixture and in excess. The initial compositions were prepared so that the equilibrium compositions are similar to those of the corresponding ester hydrolysis. In the second and third runs, the acids to alcohols ratio of 1:3 and 3:1 was respectively chosen. A summary of the experiments is given in Table 5.7.

Table 5.7. Summary of equilibration experiments for esterification of acids with alcohols catalyzed by homogeneous hydrochloric acid at 25 °C.

Run	Product	Initial Ac/Al ratio [mol/mol]	Initial Ac/W ratio [mol/mol]	c_{HCl} [mol/L]	V_R [L]
F1-3	Es_{11}	1:1, 1:3, 3:1	0.101, 0.180, 0.513	0.025	0.1
F4-6	Es_{12}	1:1, 1:3, 3:1	0.070, 0.096, 0.356	0.025	0.1
F7-9	Es_{21}	1:1, 1:3, 3:1	0.031, 0.138, 0.322	0.025	0.1
F10-13	Es_{22}	1:1, 1:3, 3:1	0.021, 0.030, 0,090	0.025	0.1

5.2.4 Reaction Kinetic Experiments in Batch Reactors

The batch experiments for complementary determination of kinetics of the ester hydrolyses were performed in a glass flask thermostated and shaken by the water bath (see Section 5.1.2). Water was heated together with the catalyst to the desired reaction temperature. Ester was heated in separate vessels. When the liquids reached the desired reaction temperature, ester was added to the reactor. Samples were taken during the experiment to determine the concentration profiles of involved components. GC (see Section 5.1.3) was used to analyze the samples. Both homogeneous and heterogeneous catalysts were used. The concentration of homogeneous catalyst (HCl) was always 0.025 mol/L. A summary of the experiments is given in Table 5.8.

Table 5.8. Summary of kinetic experiments for hydrolysis of esters performed in conventional batch reactors at 25 $^\circ$C.

Run	Reactant	Catalyst	Liquid volume [L]	Initial concentration [mol/L]
G1-2	Es_{11}	HCl (0.025 mol/L)	0.1	3.91
G3-4	Es_{11}	Cat1 ($\varepsilon = 0.96$)	0.1	4.01
G5-6	Es_{11}	Cat2 ($\varepsilon = 0.92$)	0.1	4.06
G7-8	Es_{21}	HCl (0.025 mol/L)	0.1	2.45
G9-10	Es_{21}	Cat2 ($\varepsilon = 0.92$)	0.1	2.48
G11-12	Es_{12}	HCl (0.025 mol/L)	0.1	1.20
G13-14	Es_{12}	Cat2 ($\varepsilon = 0.92$)	0.1	1.22
G15-16	Es_{22}	HCl (0.025 mol/L)	0.1	0.86
G17-18	Es_{22}	Cat2 ($\varepsilon = 0.92$)	0.1	0.87

5.2.5 Chromatographic Reactor Measurements

The chromatographic reactor experiments were carried out in collaboration work [Vu03] to determine distribution equilibrium constants of the relevant components, and to record elution profiles for the four ester hydrolysis reactions. The experimental setup was equipped with two standard HPLC columns, which were packed with the two catalysts Cat1 and Cat2. Water was continuously pumped into the columns and thus acted, in addition to being a reactant, as the mobile phase for elution. Elution profiles were recorded with a refractive index detector (RI, Knauer K-2300) and a UV-vis detector (Hitachi L-7420).

The total porosities (or liquid phase fractions), ε, of the two columns were estimated from the retention times of the nonretained component Dextran Blue at 25 $^\circ$C, t_o, the corresponding volumetric flow rates, $\dot{V}$, and the volume of the column, V_{col}, according to:

$$\varepsilon = \frac{\dot{V} t_o}{V_{col}} \tag{5.2}$$

To determine the equilibrium constants, K_i, pulse experiments were carried out in an excess of water at 25 $^\circ$C, and 30 $^\circ$C. In order to examine whether the isotherms are linear, i.e., whether the retention times do not depend on concentration, the amounts injected were varied. For the reactive esters, the flow rate was also varied in order to change the

conversion and, thereby, to distinguish correctly between the peaks of the unconverted esters and the products peaks.

To measure elution profiles for the four ester hydrolysis reactions, the feed concentration of the four esters were varied. The injection volumes were typically 100 µL. In each experiment, the flow rate and the temperature were kept constant. The recorded elution profiles could be also used to validate the reaction rate constants.

Results and Discussion

All the experimental results obtained in this work are presented and discussed in this chapter. The information about the catalysts obtained from the characterization measurements are given first in Section 6.1. This is followed by the section about distribution equilibrium constants (Section 6.2). Chemical reaction equilibria are treated in Section 6.3. The main results obtained related to the use of calorimetric measurements in order to determine reaction rates are discussed in Section 6.4. In Section 6.5, the results obtained from the reaction kinetic estimation using batch experiments are shown. Finally in Section 6.7, the model and the parameters found are validated.

6.1 Catalyst Characterization

In addition to the information given by the manufacturers, more information about the catalysts was obtained by characterization experiments. The experiments were carried out as described in Section 5.2.1.

The **swelling ratio**, i.e., the volume ratio of the swollen resin at equilibrium (V_{Re}^{eq}) to the dry resin (V_{Re}^{o}), obtained for the relevant single components is listed in Table 6.1.

From the data in Table 6.1, it can be concluded that water has a significantly higher affinity toward the resin than the other components. This is due to the strong polarity inside the resin created by the sulfonic acid groups, which attract water most strongly, followed by the alcohols, acids, and esters.

Table 6.1. Swelling ratios of the resins in different components.

Component	Swelling ratio[a]	
	Cat1	Cat2
W	3.08	2.89
Al_2	2.56	2.38
Al_1	2.42	2.27
Ac_1	2.22	2.06
Ac_2	1.78	1.79
Es_{12}	1.79	1.67
Es_{22}	1.78	1.67
Es_{11}	1.49	1.42
Es_{21}	1.37	1.38

[a] Swelling ratio $= V_{Re}^{eq} / V_{Re}^{o}$ (see Section 5.2.1)

It can be also seen from the data that the swelling ratios of the two catalysts are similar. Cat1 seems to swell slightly more than Cat2 (Table 6.1). It should be also noted that the swelling rates of the resins were found to be rather high. It took only seconds to minutes for the resins to reach their equilibrium volumes.

The corresponding **sulfonic acid group concentrations** of Cat1 and Cat2 were found by titration to be 3.9×10^{-3} and 4.8×10^{-3} equiv/g.

The **density** of Cat1 and Cat2 were measured by the pycnometer to be 1.50 and 1.45 g/cm^3, respectively.

6.2 Distribution Equilibrium Constants

The results of the determination of distribution equilibrium constants have been published earlier [Mai04]. The experiments to determine the distribution equilibrium constants of the relevant components were carried out as described in Section 5.2.5.

The equilibrium constants can be calculated using Eq. (6.1), where ε is the total porosity [see Section 5.2.5, Eq. (5.2)] of the column, and t_{R_i} are the retention times.

$$K_i = \left(\frac{\varepsilon}{1-\varepsilon} \right) \left(\frac{t_{R_i}}{t_o} - 1 \right) \qquad\qquad (6.1)$$

In order to examine whether the isotherms are linear, i.e., whether the retention times do not depend on concentration, the amounts injected were varied. For the reactive esters, the flow rate was also varied in order to change the conversion and, thereby, to distinguish correctly between the peaks of the unconverted esters and the products peaks.

In Figure 6.1, typical elution profiles for various injection concentrations of Ac_1, Ac_2, Al_1, and Al_2 with Cat1 are shown. For each component, rather symmetrical peaks were observed at specific retention times. This indicates that the linear equilibrium model [Eq. (2.41)] is adequate. Because of the occurrence of the hydrolysis reactions, it was found to be difficult to get a single peak for the esters (especially for Es_{11}). For this reason, the pure esters had to be injected into the columns with an appropriate injection volume at a sufficiently high flow rate so that a significant amount was not converted. Table 6.2 summarizes the determined equilibrium constants for Cat1 and Cat2 calculated using Eq. (6.1). The elution order of the components in water is Ac_1, Ac_2, Al_1, Al_2, Es_{11}, Es_{12}, Es_{21}, and Es_{22}. Most of the equilibrium constant values (except those of the alcohols) are slightly smaller for Cat2 than for Cat1 (Table 6.2). Because of differences in the surface characteristics between the two catalyst batches, there are also differences in the elution orders. For the alcohols, acids, and esters, the elution orders correspond to the order of molecular weights. In a previous study performed with the same batch of Cat1 some years ago [Falk02], a smaller column was used to determine constants describing the distribution equilibria for Es_{11}, Ac_1, and Al_1. The obtained values were found to be slightly larger than the values found in this study. The old values are also included in Table 6.2 for comparison.

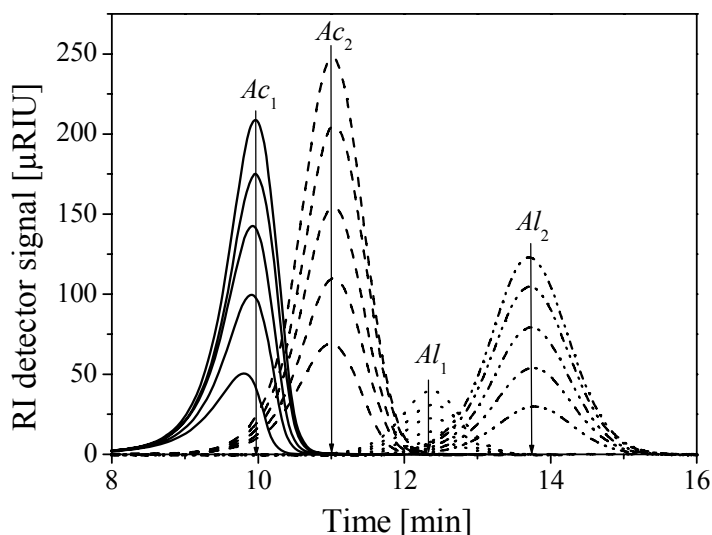
Figure 6.1. Elution profiles for various injection concentrations (0.1-0.5 mol/L) of Ac_1 (solid), Ac_2 (dashed), Al_1 (dotted), and Al_2 (dashed-dotted) (Cat1, flow rate = 0.75 mL/min, injection volume = 100 µL, temperature = 25 °C).

Table 6.2. Distribution equilibrium constants K_i at 25 $^{\circ}$C

Component	Cat1	Cat2
Ac_1	0.432 (0.476)[a]	0.380
Ac_2	0.520	0.476 (0.462)[b]
Al_1	0.628 (0.693)[a]	0.673 (0.663)[b]
Al_2	0.736	0.781
Es_{11}	0.850 (0.913)[a]	~0.65[c]
Es_{21}	0.995	0.819
Es_{12}	1.085	1.009 (0.910)[b]
Es_{22}	1.327	1.219

[a][Falk02],   [b]At 30 $^{\circ}$C,

[c]Uncertain value due to difficulties in identifying the corresponding peak.

Data for other temperatures were presented recently [Vu06]. These data allow to estimate the adsorption enthalpies of components ΔH_{ads} [Eq. (2.46)].

6.3 Chemical Reaction Equilibria

6.3.1 Reaction Equilibrium Constants

6.3.1.1 Reactive Binary Ester–Water Mixtures (homogeneous)

In order to obtain reliable knowledge about the chemical equilibrium, independent experiments were carried out as described in Section 5.2.3. The chemical equilibrium of the hydrolysis of each ester using homogeneous catalyst at 25 $^{\circ}$C was investigated. The initial compositions were prepared so that the ester concentrations were close to their solubility in water. The reaction equilibrium constants based on volumetric concentrations, K_c [Eq. (3.10)], were determined from the final compositions of batch experiments. Alternatively, the reaction equilibrium constants can be expressed from activities as K_a [Eq. (3.11)], in order to take into account the non-idealities of the solution. The activity coefficients were calculated by applying the UNIQUAC model as described in Section 2.4. The values of pure-component and binary parameters used in the UNIQUAC model for the relevant components were already listed in Tables 3.5 and 3.6 (Chapter 3).

The obtained reaction equilibrium constants for the ester hydrolysis at 25 $^{\circ}$C are listed in Table 6.3. From the values shown in Table 6.3, it can be seen that the hydrolysis of methyl

acetate is least favored, and the hydrolysis of ethyl formate is most favored. In the past, Wetherold *et al.* investigated experimentally the chemical equilibrium of methyl formate hydrolysis with various concentrations of hydrochloric acid in the temperature range between 22 and 24 °C [Weth74]. The values of the reaction equilibrium constant from [Weth74] are listed earlier in Table 3.9. It can be seen that the value for the reaction equilibrium constant of the methyl formate hydrolysis obtained by this work ($K_c = 0.22$) is in relatively good agreement with the value given by Wetherold *et al.* (1974). For the methyl acetate hydrolysis, the reaction equilibrium constant obtained ($K_c = 0.14$) is in very good agreement with the values given by Du *et al.* (1999) and Hiwale *et al.* (2004), which are in the ranges of $0.12 - 0.14$ and $0.14 - 0.2$, respectively.

To verify the reaction equilibrium constants obtained in the first series of experiments, additional equilibration experiments at the same temperature (25 °C) but with different initial compositions were carried out. Particularly, more dilute mixtures were chosen. The applied initial ratios of ester to water and the obtained values of the reaction equilibrium constants are also shown in Table 6.3. From the data in Tables 6.3, it can be seen that if the ester to water ratio deceases, the reaction equilibrium constants increase slightly. However, this increment of the reaction equilibrium constant is relatively insignificant and could be within the error of the method.

Table 6.3. Reaction equilibrium constants of the ester hydrolysis catalyzed by homogeneous catalyst (0.025 mol/L HCl) at 25 °C.

Reactant	Initial Es/W ratio	K_c	K_a
	[mol/mol]	[-]	[-]
Es_{11}	0.093	0.22	0.12
Es_{12}	0.066	0.14	0.03
Es_{21}	0.030	0.38	0.43
Es_{22}	0.012	0.33	0.38
Es_{11}	0.018	0.23	0.14
Es_{12}	0.019	0.15	0.04
Es_{21}	0.009	0.40	0.48
Es_{22}	0.009	0.33	0.40

In principle, the reaction equilibrium constant of an ester hydrolysis should be equal to the inverse of the equilibrium constant of the reverse reaction, i.e., the esterification of acids with alcohols. Several equilibration experiments for the esterification of acids with alcohols at the same temperature and with the same catalyst concentration were carried out. The initial compositions were varied as described in Section 5.2.3.2. Subsequently, the

results obtained from the different runs with different initial compositions are listed in Table 6.4. In order to be able to compare to the values for the hydrolysis reaction given in Tables 6.3, the reaction equilibrium constant values for the esterification ($K_{c(ester)}$ and $K_{a(ester)}$) were inverted. From these data, it was found that the reaction equilibrium constants of ester hydrolysis (K_c) are indeed very similar to the inverse of the reaction equilibrium constants of the corresponding esterifications of acids with alcohols ($1/K_{c(ester)}$). It can be further concluded that in the dilute regions considered, where the concentrations of the ester are lower than their solubility in water, the initial composition does not influence the obtained values for the equilibrium constants of the hydrolysis/esterification reactions.

Table 6.4. Reaction equilibrium constants of the esterification of acids with alcohols catalyzed by homogeneous catalyst (0.025 mol/L HCl) at 25 ^{o}C, with different initial ratio of acids to alcohols.

The initial mole ratio of acids to alcohols = 1:1					
Product	Initial $Ac(Al)/W$ ratio [mol/mol]	$K_{c(ester)}$ [-]	$1/K_{c(ester)}$ [-]	$K_{a(ester)}$ [-]	$1/K_{a(ester)}$ [-]
Es_{11}	0.101	4.37	0.23 (0.22)*	7.84	0.13
Es_{12}	0.070	7.30	0.14 (0.14)*	35.4	0.03
Es_{21}	0.031	2.58	0.39 (0.38)*	2.34	0.43
Es_{22}	0.012	2.93	0.34 (0.33)*	2.51	0.40
The initial mole ratio of acids to alcohols = 1:3					
Product	Initial Ac/W ratio [mol/mol]	$K_{c(ester)}$ [-]	$1/K_{c(ester)}$ [-]	$K_{a(ester)}$ [-]	$1/K_{a(ester)}$ [-]
Es_{11}	0.180	4.59	0.22 (0.22)*	11.5	0.09
Es_{12}	0.096	6.76	0.15 (0.14)*	51.1	0.02
Es_{21}	0.138	2.60	0.38 (0.38)*	4.38	0.23
Es_{22}	0.030	2.96	0.34 (0.33)*	3.62	0.28
The initial mole ratio of acids to alcohols = 3:1					
Product	Initial Ac/W ratio [mol/mol]	$K_{c(ester)}$ [-]	$1/K_{c(ester)}$ [-]	$K_{a(ester)}$ [-]	$1/K_{a(ester)}$ [-]
Es_{11}	0.513	4.67	0.21 (0.22)*	6.79	0.15
Es_{12}	0.356	7.33	0.14 (0.14)*	35.7	0.03
Es_{21}	0.322	2.66	0.38 (0.38)*	2.53	0.40
Es_{22}	0.090	2.99	0.33 (0.33)*	3.17	0.32

*) Reaction equilibrium constants of the ester hydrolysis reactions (Table 6.3).

6.3.1.2 Reactive Ternary Ester–Ester–Water Mixtures (homogeneous)

Studies of reactive ternary ester–ester–water mixtures were not reported up to now. In the case that more than one ester is present in a mixture with water, aside from the hydrolysis of each ester, the transesterification reactions can also take place. Transesterifications take place only if alkoxy group of the ester is different to that of the alcohol present in the mixture. For this end, the determination of chemical equilibrium constants of several reactive ternary ester–ester–water mixtures was carried out experimentally to observe if the equilibria of the ester hydrolysis reactions change. The experiments were performed in the manner as described in Section 5.2.3.1. The initial compositions for the experiments were prepared as presented earlier in Table 5.5. By gas chromatography not all concentrations could be determined due to peak overlap. Based on the knowledge of the stoichiometry, key components and reactions were chosen. The concentrations of the key components were determined by the GC. The concentrations of the other components were calculated from the determined concentrations using the material balances of the elements involved.

The equilibrium compositions of the mixtures and the equilibrium constants of the ester hydrolysis reactions obtained from the experiments are listed in Table 6.5. From the results shown, it can be seen that the reaction equilibrium constants of the hydrolysis determined from the ternary ester–ester–water mixtures are almost similar to that determined from the binary ester–water mixtures (Table 6.3). It was observed in runs D3 and D4 that, although the transesterifications take place and new esters are hence formed, the values of the equilibrium constants of the hydrolysis reactions are almost similar to the simpler case without transesterification (Table 6.3).

Table 6.5. Reactive ternary ester–ester–water mixtures: equilibrium composition of the mixtures and equilibrium constant of ester hydrolysis. Temperature: 25 °C, catalyst: 0.025 mol/L HCl.

Run[*]	Equilibrium composition [mol/L]									Measured K_c of hydrolysis of			
	Es_{11}	Es_{12}	Es_{21}	Es_{22}	Al_1	Al_2	Ac_1	Ac_2	W	Es_{11}	Es_{12}	Es_{21}	Es_{22}
D1	0.0361	0.0494	0	0	0.924	0	0.475	0.449	50.87	0.24	0.16	-	-
D2	0.0399	0	0.0215	0	0.472	0.477	0.949	0	50.79	0.22	-	0.41	-
D3	0.0192	0.0308	0.0111	0.0131	0.459	0.475	0.479	0.455	50.33	0.23	0.13	0.41	0.33
D4	0.0185	0.0266	0.0120	0.0143	0.459	0.475	0.471	0.463	50.33	0.23	0.16	0.37	0.31
D5	0	0.0504	0	0.0290	0.455	0.475	0	0.930	49.91	-	0.17	-	0.30
D6	0	0	0.0222	0.0312	0	0.952	0.478	0.474	49.67	-	-	0.41	0.29
Binary[**]										0.22	0.14	0.38	0.33

[*] Initial mixtures: Run D1: Es_{11}–Es_{12}–W; Run D2: Es_{11}–Es_{21}–W; Run D3: Es_{11}–Es_{22}–W; Run D4: Es_{12}–Es_{21}–W; Run D5: Es_{12}–Es_{22}–W; Run D6: Es_{21}–Es_{22}–W.

[**] Average values obtained from the binary ester–water mixtures (Table 6.3).

6.3.2 Influence of Temperature on Reaction Equilibrium Constants

In addition to 25 ^{o}C, equilibration experiments to evaluate the influence of temperature on chemical equilibria of hydrolysis of the four esters using homogeneous catalyst were also carried out at varied temperatures of 35, 45 and 55 ^{o}C (see Section 5.2.3 and Table 5.4). K_c and K_a were computed from the measured data using Eqs. (3.10) and (3.11), respectively. In addition, based on values of the standard reaction Gibbs energies (Table 3.4) the equilibrium constants of the four ester hydrolysis reactions in the liquid phase at the standard temperature (25 ^{o}C) can be estimated using Eq. (2.64). The reaction equilibrium constants at different temperatures were estimated using the integrated form of the van't Hoff equation [Eq. (2.99)] (see Table 3.8). The measured equilibrium compositions of the four hydrolysis reactions, corresponding calculated activity coefficients, and the determined equilibrium constants are shown in Table 6.6.

In Figure 6.2 are shown the results as plots of the natural logarithm of the equilibrium constants K_c and K_a versus the inverse of the absolute temperature. The slope of the linear regression of the data is related to the standard enthalpy of reaction ΔH_r^o (by the integrated form of the van't Hoff equation [Eq. (2.99)]), if a constant enthalpy of reaction is assumed, which is reasonable due to the relatively small temperature interval investigated. This allows one to compare the experimentally obtained results against the estimation based on thermodynamic data from the literature. The resulting values of ΔH_r^o from different sources for the four ester hydrolysis reactions are reported in Table 6.7. The dashed-dotted lines in Figure 6.2 show the temperature dependence of the equilibrium constants estimated from the standard Gibbs energies of formation. The solid and dashed lines show respectively the best fits of lnK_a and lnK_c resulting from the experimental data.

The similar slopes of the solid lines and dashed lines in Figure 6.2 indicate an agreement of the standard reaction enthalpies calculated from measured K_a and K_c. In Figure 6.2a, the dashed-dotted line has a similar slope as the other lines. This shows that the standard enthalpy values of methyl formate hydrolysis calculated from the experimental and literature data are in relatively good agreement. For the other three ester hydrolysis reactions, the standard enthalpy values calculated from the experimental and literature data are not in such good agreement (Figs. 6.2b-d).

Table 6.6. Hydrolysis of esters catalyzed by a homogeneous catalyst (0.025 mol/L HCl): influence of temperature on the equilibrium composition and constant.

| Hydrolysis of esters	Initial Es/W [mol/mol]	T_r [$^{\circ}$C]	Equilibrium concentration [mol/L]				K_c [-]
			Es	W	Ac	Al	
Es_{11}	0.093	25	1.0556	39.393	2.9158	3.1458	0.22
		35	0.9691	39.75	3.0024	3.2324	0.25
		45	0.9272	39.265	3.0443	3.2743	0.27
		55	0.8800	39.217	3.0915	3.3215	0.30
Es_{12}	0.066	25	0.7370	41.333	2.1047	2.1047	0.14
		35	0.6584	41.255	2.1834	2.1834	0.17
		45	0.5994	41.1958	2.2424	2.2424	0.20
		55	0.5727	41.169	2.2691	2.2691	0.22
Es_{21}	0.030	25	0.1162	47.1686	1.4514	1.4514	0.38
		35	0.1074	47.1598	1.4602	1.4602	0.42
		45	0.1042	47.157	1.4634	1.4634	0.44
		55	0.1022	47.154	1.4654	1.4654	0.45
Es_{22}	0.012	25	0.0264	51.215	0.6672	0.6672	0.33
		35	0.0238	51.213	0.6698	0.6698	0.37
		45	0.0217	51.211	0.6719	0.6719	0.40
		55	0.0198	51.209	0.6738	0.6738	0.45
Hydrolysis of esters	Initial Es/W [mol/mol]	T_r [$^{\circ}$C]	Activity coefficient [-]				K_a [-]
			Es	W	Ac	Al	
Es_{11}	0.093	25	1.9738	1.0115	0.6409	1.7241	0.12
		35	1.9691	1.0118	0.6596	1.7262	0.14
		45	1.9577	1.0124	0.6771	1.7251	0.16
		55	1.9490	1.0128	0.694	1.7254	0.18
Es_{12}	0.066	25	11.336	1.029	1.7402	1.3829	0.03
		35	11.004	1.0288	1.778	1.3987	0.038
		45	10.701	1.0285	1.8116	1.4142	0.047
		55	10.430	1.0281	1.8415	1.4306	0.054
Es_{21}	0.030	25	2.3633	1.0042	0.6518	3.9876	0.42
		35	2.3594	1.0043	0.6722	3.9062	0.47
		45	2.3556	1.0043	0.6919	3.8326	0.49
		55	2.352	1.0043	0.7109	3.7649	0.50
Es_{22}	0.012	25	9.8097	1.0019	2.6759	4.2637	0.38
		35	10.017	1.0019	2.7052	4.1810	0.41
		45	10.198	1.0019	2.7309	4.1049	0.44
		55	10.354	1.0018	2.7534	4.0345	0.48
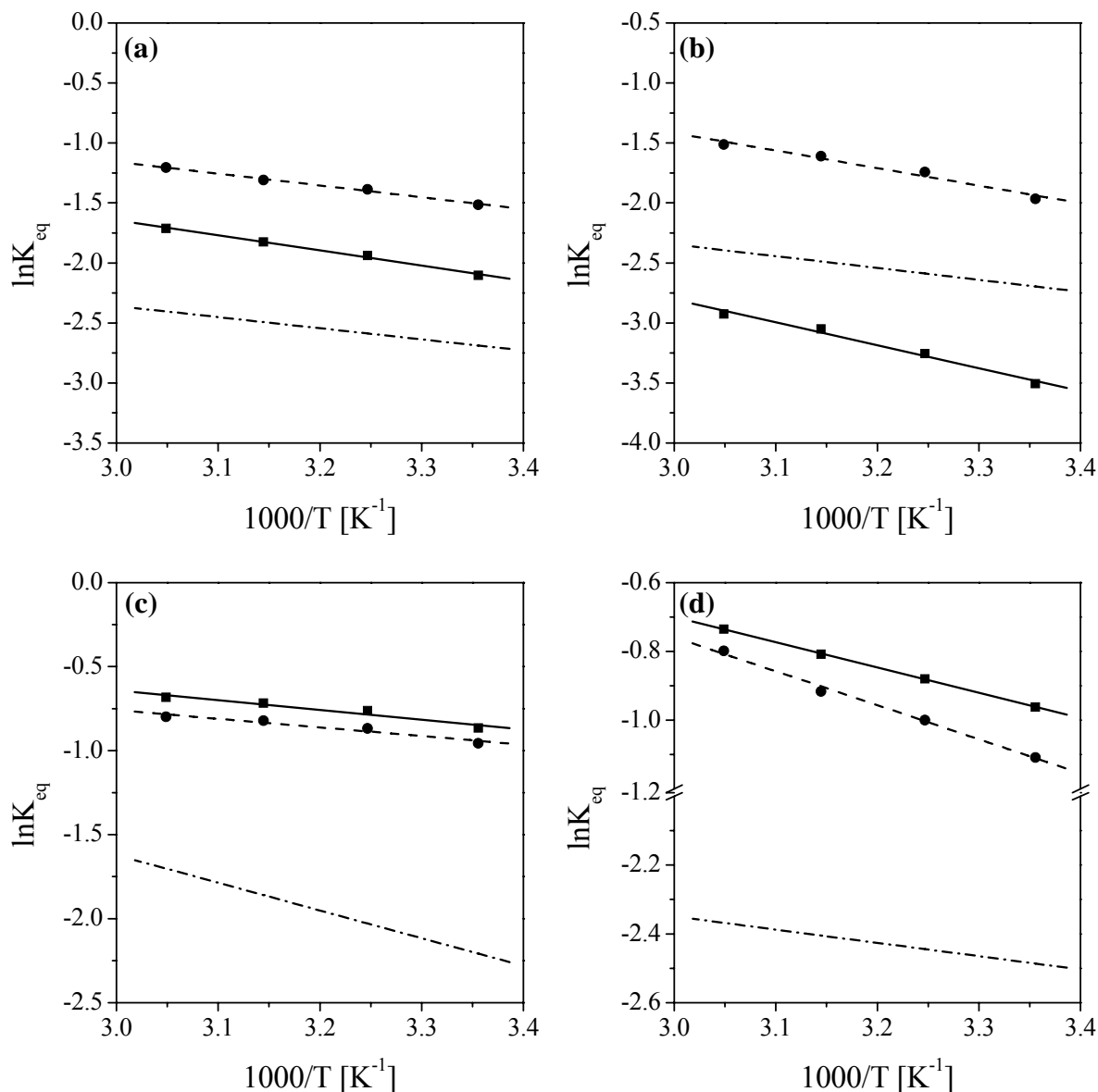
Figure 6.2. Temperature dependency of the equilibrium constants of ester hydrolysis: **a)** methyl formate, **b)** methyl acetate, **c)** ethyl formate, and **d)** ethyl acetate. Dashed-dotted lines: estimation based on Eq. (2.64) and thermodynamic data; (●) and dashed lines: K_c (Eq. 3.10) and the best fits; (■) and solid lines: K_a (Eq. 3.11) and the best fits.

Table 6.7. Standard reaction enthalpies of hydrolysis of the four esters obtained from different sources.

Source	ΔH_r^o of hydrolysis [kJ/mol]			
	Es_{11}	Es_{12}	Es_{21}	Es_{22}
From heats of formation (Eq. 2.90)	+7.70	+8.20	+13.7	+3.20
From determined K_c (Fig. 6.2)	+8.19	+12.2	+4.28	+8.23
From determined K_a (Fig. 6.2)	+10.5	+15.9	+4.84	+6.12
From literature (Table 3.4)	+16.3	+6.51	-	+5.82

6.3.3 Influence of Solid Catalyst on Equilibrium Compositions

The obtained data of swelling ratios and distribution equilibrium constants for single components presented above (Sections 6.1 and 6.2) give information about the phase equilibrium behavior of single components in presence of an ion-exchange resin catalyst. However, with a mixture of components, the behavior may be different. In the context of the present work, it is not the aim to examine the complex phase equilibrium behavior of the multicomponent systems of interest in details, but just to determine the influence of the solid catalyst on the liquid phase equilibrium composition of reactive systems. The amount of solid catalyst present in the system is quantified by the "solid fraction" $(1-\varepsilon)$, where ε is the "liquid fraction" (or porosity in chromatographic reactors, Eq. 5.2) defined already by Eq. (2.81). The influence of the liquid fraction on the liquid phase equilibrium composition in a batch reactor was studied for the hydrolysis reactions of the four esters catalyzed by Cat2 at 25 $^{\circ}$C. The experiments with the varied liquid fractions were carried out as described in Section 5.2.3.1. A summary of the experiment conditions is given in Table 5.6. Since it is difficult to determine experimentally the solvent composition in the solid phase, only the liquid phase composition was determined in this study. The solvent compositions in the solid phase and the liquid phase can be also calculated by using Eqs. (2.82) and (2.84) after solving the system of nonlinear equations defined in Eq. (2.87). In this model, linear adsorption isotherms which are valid for components that are present in the liquid phase at low concentrations, was assumed [Eq. (2.41)]. The distribution equilibrium constants (K_i) were taken from pulse experiment data for the single component systems in an excess of water as presented in Section 6.2.

The liquid phase compositions measured at equilibrium are shown in Table 6.8. In Figure 6.3 are shown the measured and calculated compositions of the liquid phase at equilibrium as functions of the liquid fraction. The symbols show the experimentally measured data and the lines show the calculated ones. The liquid phase compositions at equilibrium were calculated using Eq. (2.84) after solving the system of nonlinear equations defined in Eq. (2.87) (see Section 2.2.3). As can be seen in Figure 6.3, the experimental and calculated data are in relatively good agreement. This indicates also that the linear equilibrium adsorption model [Eq. (2.41)] is adequate. The figures also show that the selective adsorption of components on the catalyst has an effect on the liquid phase composition in a batch reactor. For instance, due to the different adsorption abilities of alcohols and acids on the catalyst, the lower the liquid fraction, the bigger the liquid-phase mole fraction difference between alcohols and acids.

Table 6.8. Hydrolysis of esters catalyzed by Cat2 at 25 $^{\circ}$C in a batch reactor: influence of liquid fraction on the equilibrium composition of the liquid phase. The initial ester concentrations were close to the solubility.

| Hydrolysis of esters	Liquid fraction, ε [vol/vol]	Measured liquid-phase equilibrium mole fraction			
		Es	W	Ac	Al
Es_{11}	0.81	0.0262	0.838	0.0614	0.0747
	0.85	0.0247	0.842	0.0600	0.0735
	0.88	0.0238	0.842	0.0617	0.0725
	0.91	0.0222	0.845	0.0629	0.0698
	0.93	0.0215	0.848	0.0627	0.0681
	0.95	0.0214	0.849	0.0636	0.0655
	0.97	0.0217	0.850	0.0634	0.0651
	1.00	0.0219	0.852	0.0628	0.0628
Es_{12}	0.81	0.0166	0.883	0.0458	0.0549
	0.85	0.0156	0.887	0.0440	0.0526
	0.88	0.0156	0.890	0.0430	0.0514
	0.91	0.0163	0.886	0.0468	0.0505
	0.93	0.0152	0.888	0.0474	0.0491
	0.95	0.0145	0.890	0.0467	0.0485
	0.97	0.0153	0.890	0.0465	0.0486
	1.00	0.0157	0.893	0.0458	0.0458
Es_{21}	0.81	0.00231	0.936	0.0277	0.0343
	0.85	0.00201	0.940	0.0252	0.0321
	0.88	0.00190	0.940	0.0263	0.0320
	0.91	0.00173	0.941	0.0269	0.0306
	0.93	0.00187	0.941	0.0271	0.0302
	0.95	0.00173	0.940	0.0279	0.0301
	0.97	0.00169	0.941	0.0275	0.0295
	0.98	0.00185	0.941	0.0284	0.0288
	1.00	0.00183	0.943	0.0277	0.0277
Es_{22}	0.81	0.000360	0.974	0.0116	0.0136
	0.85	0.000342	0.975	0.0110	0.0131
	0.88	0.000331	0.975	0.0112	0.0130
	0.91	0.000351	0.976	0.0112	0.0124
	0.93	0.000372	0.976	0.0115	0.0121
	0.95	0.000301	0.976	0.0114	0.0121
	0.97	0.000370	0.976	0.0117	0.0118
	1.00	0.000355	0.977	0.0113	0.0113
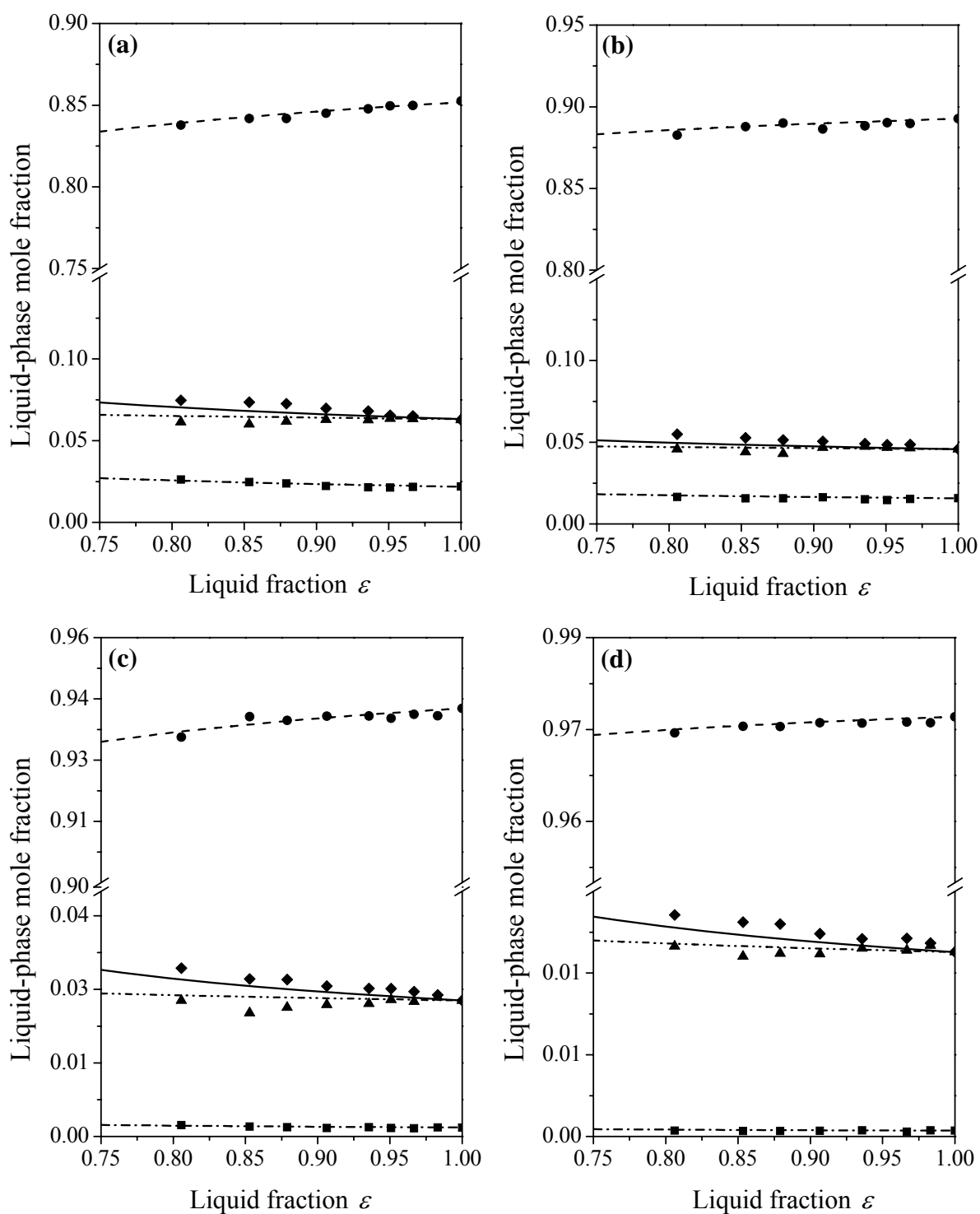
Figure 6.3. Influence of the liquid fraction ε (Eq. 2.81) on the liquid-phase equilibrium composition of the hydrolysis of: **a)** methyl formate, **b)** methyl acetate, **c)** ethyl formate, and **d)** ethyl acetate under the catalyst Cat2 at 25 $^{\circ}$C. Symbols: experimental data; lines: calculated using Eq. (2.84) with K_i values given in Table 6.2. ($\blacksquare$ and $--$) = esters, ($\bullet$ and $--$) = water, ($\blacktriangle$ and $-\cdot\cdot-$) = alcohols, and ($\blacklozenge$ and $—$) = acids.

As discussed above, it is difficult to determine experimentally the solvent composition in the solid phase. Therefore, the experimental determination of the extent of reaction is difficult to find in a batch reactor due to the solvent uptake by the solid catalyst. Only results found by solving the system of nonlinear equations defined in Eq. (2.87) are shown in this work. The behavior of the calculated fractional extent of reaction, which is defined as the ratio of the equilibrium extent to the initial mole number of ester (ξ / n_{Es}^{o}), is shown in Figure 6.4 as a function of the liquid fraction. The calculated results shown in Figure 6.4 have not been verified experimentally. However, the model appears to be trustworthy since it is capable of reproducing correctly the influence of the liquid fraction on the liquid phase compositions (see in Figure 6.3).

Figure 6.4 shows that the fractional extent of reaction in a batch reactor increases with increasing liquid fraction. This seems to be contrary to the results given by Sainio *et al.* (2004), which stated that the fractional extent of reaction increases with decreasing liquid fraction. However, they studied the esterification of acetic acid with ethanol by using Amberlyst 15 and two other resins as catalysts. In the both works, the ester mole fraction decreases with increasing liquid fraction due to the selective adsorption capacities of the catalysts (see Table 6.8 and Figure 6.3). This results in an increase in the fractional extent of reaction with increasing liquid fraction for the hydrolysis and in a decrease for the esterification.
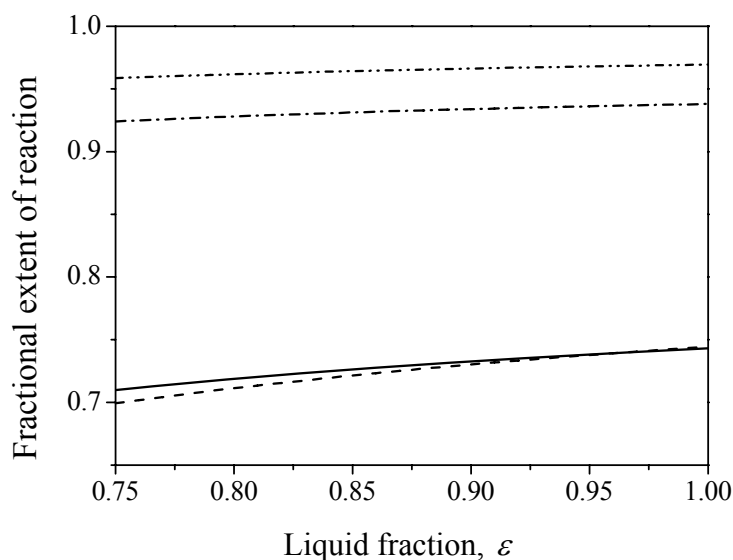

Figure 6.4. Influence of the liquid fraction on fractional extent of the hydrolysis of: (—) methyl formate, (– –) methyl acetate, (– –) ethyl formate, and (–··–) ethyl acetate under the catalyst Cat2 at 25 °C.

6.4 Calorimetric Measurements

As discussed in the introductory chapter, the application of calorimetry is an alternative attractive approach to the quantification of reaction rates. An accurate measurement of the time dependence of heat effects related to reactions allows one to quantify reaction rates. For this end, the experimental measurements of the time dependence of heat effects related to the hydrolysis reactions were performed using the calorimeter as described in Section 5.2.2. The experimental results are first qualitatively analyzed in the following Section 6.4.1. The more detailed interpretation of the measured reaction heat flows and the determination of the reaction kinetic parameters based on simulation of the heat flows are described afterwards in Section 6.4.2. As has been discussed earlier in Section 5.2.2.1, the volume of reactants mixtures should be precisely measured to analyze properly the kinetics of hydrolysis of the four esters using calorimetric experiments. Aside from the calorimetric experiments, extra experiments to estimate volume mixing effects of a single ester in water were carried out. The obtained results are also presented together with the measured heal mixing effects in Section 6.4.1.

6.4.1 Thermal and Volume Effects Due to Mixing

6.4.1.1 Thermal Effects Due to Mixing

In an attempt to estimate the extent of heat effects due to the mixing of water and esters in distinction from the heat effects caused by the chemical reactions, the heat effects of mixing processes were measured in semi-batch mode. The measured integral heats of mixing are expressed in Table 6.9. It is apparent that these mixing processes are exothermal.

Table 6.9. Measured integral heats of mixing, ΔH_{mix}, of water and various esters at 25 ^{o}C.

Ester	Ester/Water [g/g]	ΔH_{mix}* [kJ]
Es_{11}	200/1000	-0.48
Es_{12}	200/1000	-9.01
Es_{21}	100/1000	-1.85
Es_{22}	75/1000	-5.69

*) Integration performed over the whole curve

In Figure 6.5, typical mixing heat flows measured during the mixing of the individual esters and water performed in semi-batch mode at 25 °C are shown. It can be seen that the contribution of the mixing effect is significant for almost cases. Especially, in the case of mixing of methyl formate and water the transient of the heat flow is complicated.
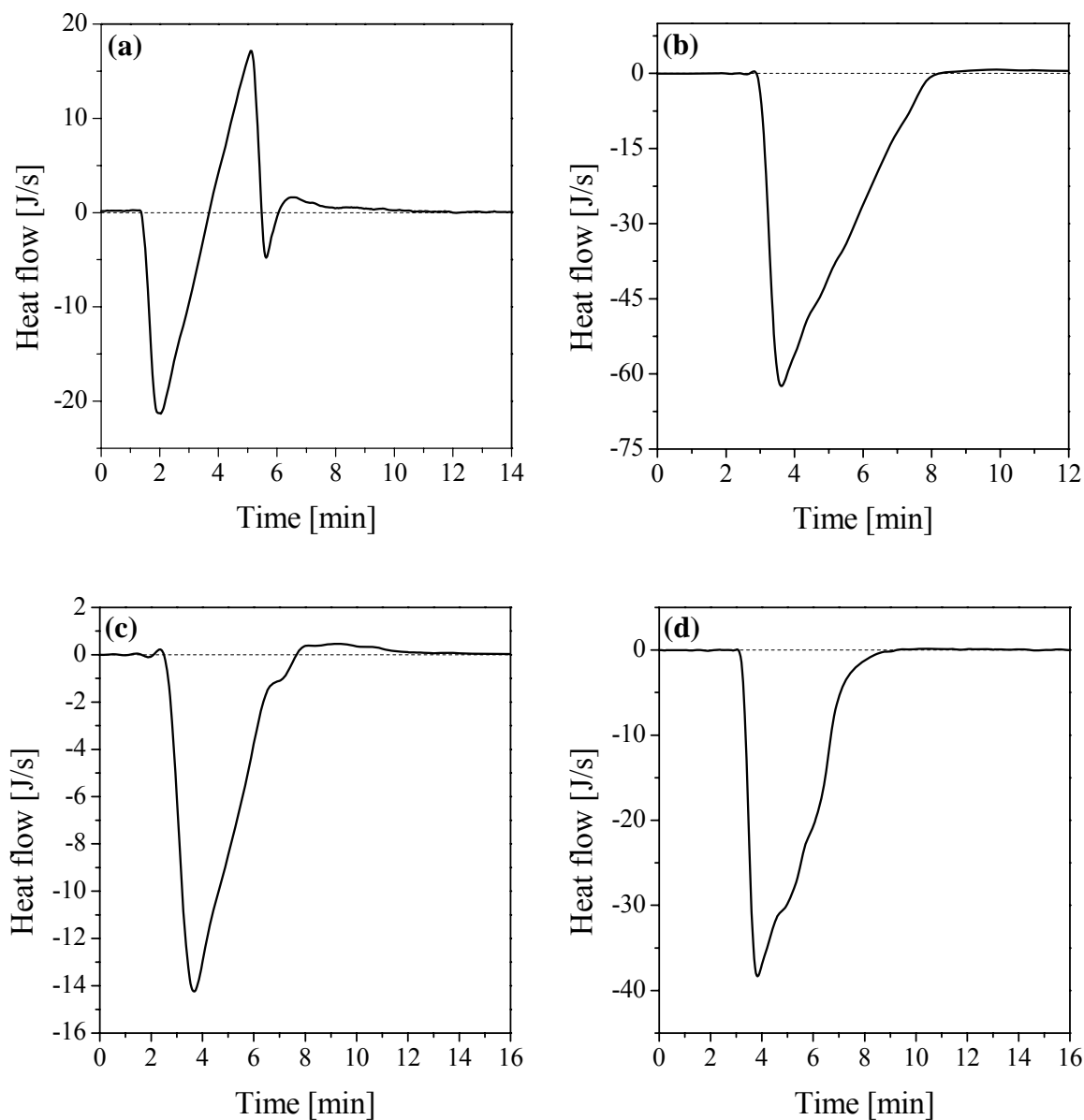

Figure 6.5. Measured heat flows for the mixing of water and (**a**) methyl formate, (**b**) methyl acetate, (**c**) ethyl formate, and (**d**) ethyl acetate performed in semi-batch mode at 25 °C.

Figure 6.6 shows a typical heat flow measured during the methyl formate hydrolysis using Cat1 in semi-batch mode. The complex part in the first few minutes of the profile is due to the joint effects of mixing and initial reaction. It is thus difficult to subtract the mixing heat effect from the joint effects of mixing and reaction. As seen in Figure 6.6, after starting dosing about 10 min, the heat flow is caused exclusively by chemical reaction. This can also be seen in Figure 6.5a, which shows that about 10 min after starting dosing the heat flow is about equal to zero in case of no reaction. Therefore, all subsequent experiments were analyzed only as batch runs after the mixing effects were "gone" and an initial sample had been taken (Figure 6.6).
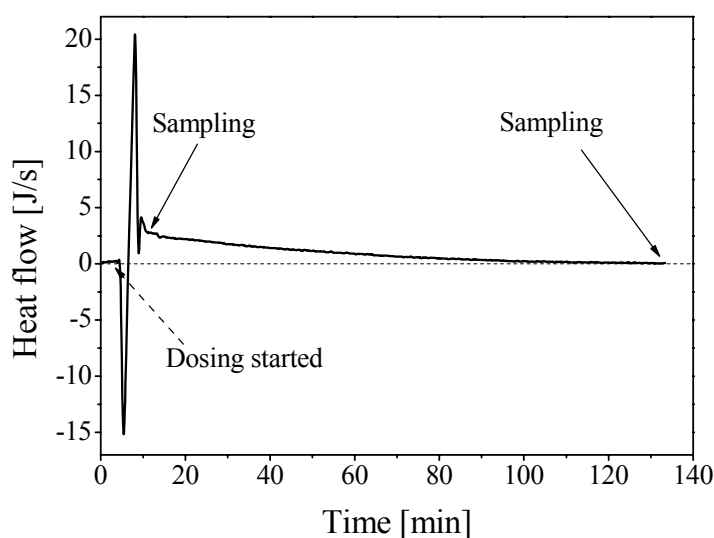

Figure 6.6. Heat flow for the hydrolysis of methyl formate performed in semibatch mode (Cat1, $T = 25\ ^{\circ}C$).

6.4.1.2 Volume Effects Due to Mixing

Aside from the calorimetric experiments, extra experiments to estimate volume mixing effects of a single ester in water at 25 $^{\circ}C$ were carried out as described in Section 5.2.2.1. Consequently, the initial volume of reactants mixture in the reaction calorimeter can be properly determined. The volume reduction was always observed in the four cases. Following figure (Fig. 6.7) and table (Table 6.10) present the obtained results. From the obtained data, it can be seen that the volume reduction due to mixing with water of ethyl formate is higher than what of the other esters. Methyl formate and ethyl acetate have similar and moderate effects, while methyl acetate has a lowest effect on the mixture volume.
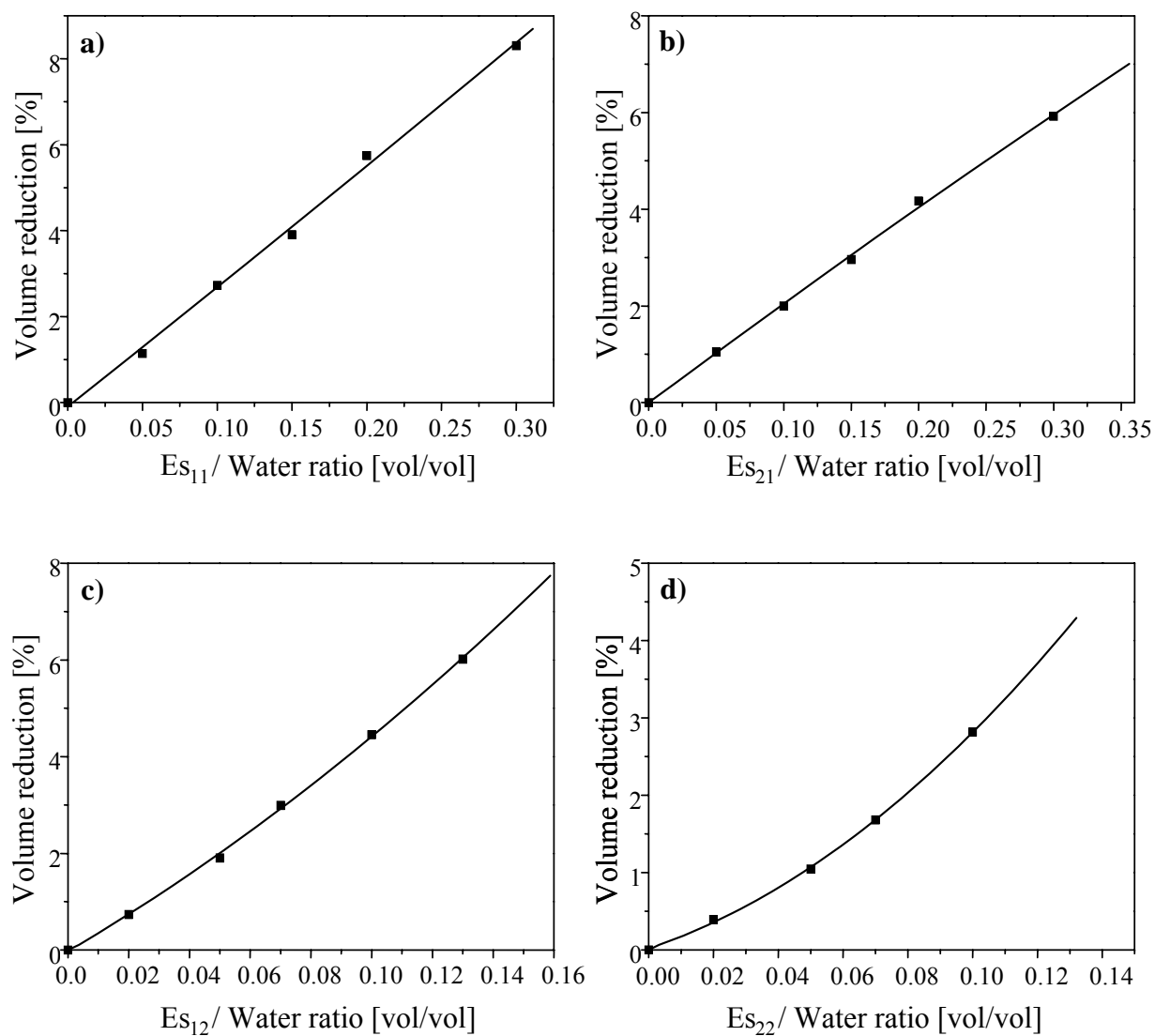
Figure 6.7. Volume reductions due to mixing of water and the four esters: **(a)** methyl formate, **(b)** methyl acetate, **(c)** ethyl formate, and **(d)** ethyl acetate.

Table 6.10. Volume reductions due to mixing of esters and water at 25 $^{\circ}$C.

Mixture	Es_{11} [mL]	Water [mL]	Measured mixture volume [mL]	Volume reduction [%]
1	0	100	100.0	0
2	5	100	103.8	1.14
3	10	100	107.0	2.73
4	15	100	110.5	3.91
5	20	100	113.1	5.75
6	30	100	119.2	8.31
	Es_{21} [mL]	Water [mL]	Measured mixture volume [mL]	Volume reduction [%]
7	0	100	100.0	0
8	5	100	103.9	1.05
9	10	100	107.8	2.0
10	15	100	111.6	2.96
11	20	100	115.0	4.17
12	30	100	122.3	5.92
	Es_{12} [mL]	Water [mL]	Measured mixture volume [mL]	Volume reduction [%]
13	0	100	100.0	0
14	2	100	101.3	0.69
15	5	100	103.0	1.90
16	7	100	103.8	2.99
17	10	100	105.1	4.45
18	13	100	106.2	6.02
	Es_{22} [mL]	Water [mL]	Measured mixture volume [mL]	Volume reduction [%]
19	0	100	100.0	0
20	2	100	101.6	0.39
21	5	100	103.9	1.05
22	7	100	105.2	1.68
23	10	100	106.9	2.82

6.4.2 Measured Reaction Heat Flows

Batch hydrolysis reactions of the four esters were conducted systematically at various feed concentrations and temperatures with Cat1 and Cat2. From the experimental results, a severe limitation of the applicability of the available reaction calorimeter was found. For the hydrolysis reactions of ethyl formate and ethyl acetate, the reaction calorimeter could not precisely detect the behavior of the heat flow. This is due to several joint effects: relatively low reaction enthalpies, low reaction rates, and limited sensitivity of the reaction calorimeter. The difference in reaction kinetics between hydrolysis reactions of methyl formate and methyl acetate could be detected properly, as shown in Figure 6.8a. However, the behavior of the heat flow for the methyl formate hydrolysis (Figure 6.8b) is quite good compared to that for the methyl acetate hydrolysis (Figure 6.8d). In agreement with the values shown in Table 3.4, it is apparent that these hydrolysis reactions are endothermal. It is further evident that the heat consumed by methyl formate hydrolysis is significantly higher than that consumed by the hydrolysis of methyl acetate for the same feed concentration, temperature, and catalyst.

Figure 6.8b shows the heat flows for the hydrolysis of methyl formate at 25 $^{\circ}$C with Cat1 and different feed concentrations. It is obvious that the higher the initial ester concentration, the higher the heat consumed by the reaction.

In preliminary experiments, it is found that the reaction calorimeter could also not precisely detect the behavior of the heat flow for the hydrolysis of methyl acetate catalyzed by Cat1. Thus, the hydrolysis of methyl acetate was studied with Cat2. Figures 6.8c and d compare the heat flows obtained at different temperatures for the hydrolysis of methyl formate and methyl acetate, respectively. From these figures, the accelerating typical effect of temperature on the reaction kinetics can be clearly observed. However, as can be also seen, there is considerable noise in the measurements for the methyl acetate hydrolysis, indicating that the sensitivity limit of the calorimeter is reached.
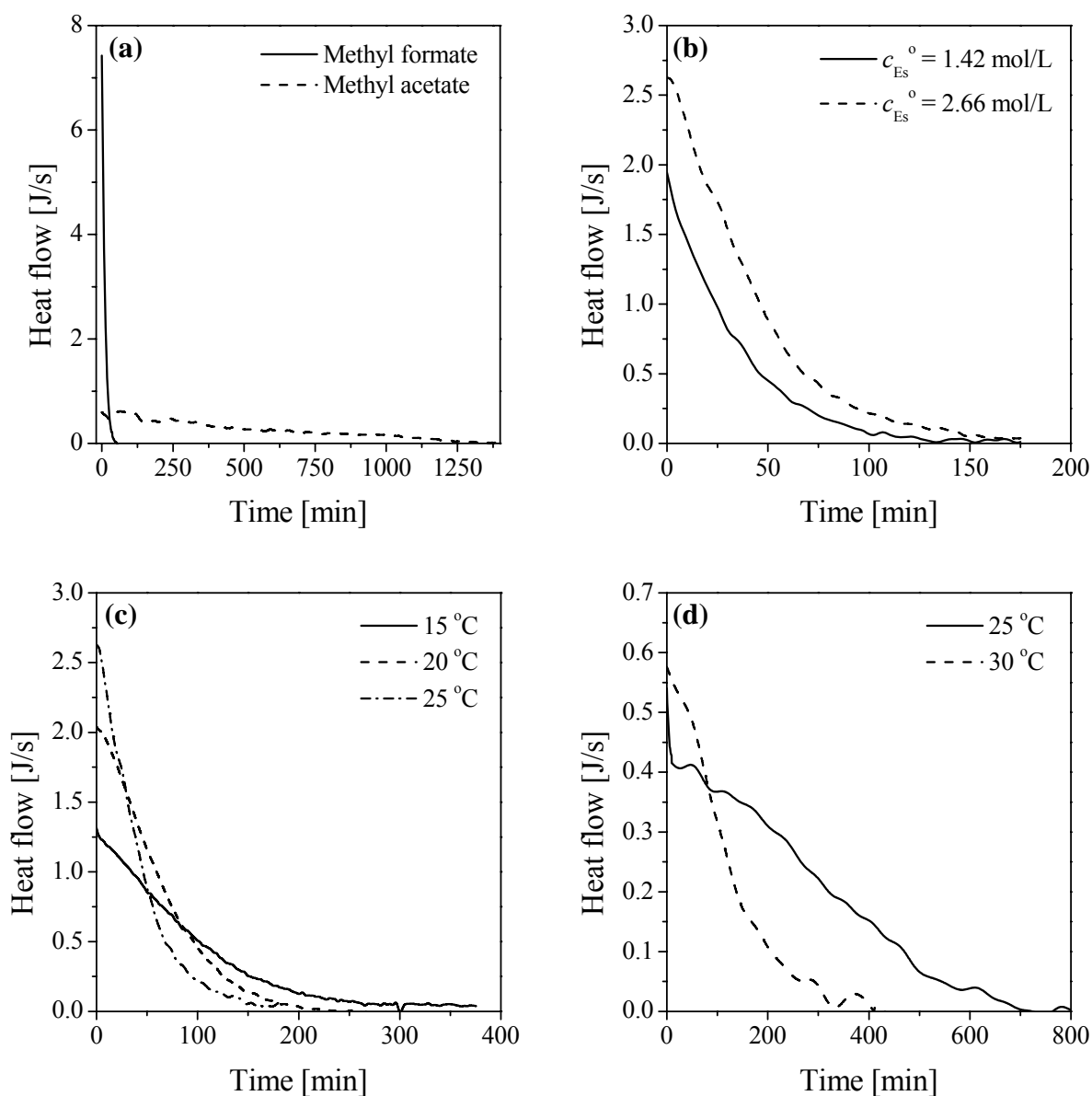
Figure 6.8. Measured heat flows of ester hydrolysis reactions: (**a**) methyl formate (solid) and methyl acetate (dashed), Cat2, $T = 25\ ^{\circ}$C; (**b**) methyl formate, Cat1, $T = 25\ ^{\circ}$C, $c^{o}_{Es_{11}} =$ 1.42 mol/L (solid) and $c^{o}_{Es_{11}} = 2.66$ mol/L (dashed); (**c**) methyl formate, Cat1, $T = 15\ ^{\circ}$C (solid), $T = 20\ ^{\circ}$C (dashed) and $T = 25\ ^{\circ}$C (dashed-dotted); (**d**) methyl acetate, Cat2, $T = 25\ ^{\circ}$C (solid) and $T = 30\ ^{\circ}$C (dashed).

6.4.3 Simulation of Heat Flows and Estimation of Reaction Rate Constants

In order to analyze in more details the measured heat flows and to determine reaction kinetic parameters, the model described in Section 4.2 was applied [Eq. (4.25)]. Ideal and non-ideal behaviors of both liquid and solid phases were alternatively considered. As mentioned earlier, only the behavior of the heat flow for the hydrolysis reactions of methyl formate and methyl acetate could be precisely detected with the available reaction calorimeter. Therefore, the quantitative analysis of the measured heat flows in this section was applied only for these two hydrolysis reactions.

6.4.3.1 Ideal Solution Behavior

Reaction rate constants of the two hydrolysis reactions studied in the calorimeter were quantified by applying the heterogeneous model [Eqs. (4.13) and (4.14)] and the pseudohomogeneous model [Eq. (4.16)] in combination with the energy balance [Eq. (4.25)]. Assuming ideal solution behavior, the concentration-based rate expression for reversible reactions was utilized for both homogeneous and heterogeneous reactions [Eqs. (2.111) and (2.112)]. However, the concentration of the catalyzing hydrogen proton in the liquid phase was additionally taken into account in the rate law expression for the homogeneous hydrolysis reaction. Using the notations [Eq. (3.2)] and the stoichiometric equation [Eq. (3.3)] described in Section 3.1, the rate equation (2.111) can be rewritten for the homogeneous hydrolysis reactions as follows, where the notation k_f^{hom} is simplified to k^{hom}:

$$r^{\text{hom}}\left(\overline{c}\right) = k^{\text{hom}} c_{H^+} \left(c_{Es} c_W - \frac{c_{Ac} c_{Al}}{K_c^{\text{hom}}} \right) \tag{6.2}$$

Protons H^+ are created by the dissociation of eventually externally added acids and the carboxylic acids, which exist in the reaction system. The concentration c_{H^+} is thus calculated with Eq. (6.3), where $c_{H^+}^{ext}$ and $c_{H^+}^{sys}$ are the H^+ concentrations contributed by the externally added acids and the acids which is part of the reaction system:

$$c_{H^+} = c_{H^+}^{ext} + c_{H^+}^{sys} \tag{6.3}$$

In the calorimetric experiments, only solid acidic ion-exchange resins (Cat1 and Cat2) were used as catalysts. The concentration c_{H^+} is, therefore, equal to $c_{H^+}^{sys}$. For the two reaction systems studied, the existing acids are formic acid and acetic acid. For established dissociation equilibria the concentration $c_{H^+}^{sys,eq}$ depends on the dissociation constants K_{Ac} of acids as described below:

$$c_{H^+}^{sys,eq} = \sqrt{K_{Ac} c_{Ac}^{eq}} \tag{6.4}$$

The value of pK_{Ac}, which is defined as the negative of the logarithm of the dissociation constant K_{Ac}, is 3.75 for formic acid and 4.76 for acetic acid (Table 3.7).

Since water is always in excess, an Eley–Rideal type of reaction mechanism [Thom97] can be assumed for the four heterogeneously catalyzed reactions. In this classical mechanism, it is assumed that in a reaction "A + B → Products" one feed component adsorbs on the solid surface (here the ester) and reacts with the other (here water) in the bulk phase. Thus, the rate equation (2.112) can be rewritten for the heterogeneously catalyzed reactions as follows:

$$r^{het}\left(\overline{c}, \overline{q}_{av}\right) = k^{het}\left(q_{av,Es} c_W - \frac{q_{av,Ac} q_{av,Al}}{K_c^{het}} \right) \tag{6.5}$$

In agreement with previous results [Falk02] and for the sake of simplicity, the distribution equilibrium functions $q(c)$ used in this work are assumed to be in the considered concentration range decoupled and linear [Eq. (2.41)]. The following expression should hold under complete equilibrium conditions:

$$r^{hom} = r^{het} = 0 \tag{6.6}$$

It follows in equilibrium:

$$0 = c_{Es}^{eq} c_W^{eq} - \frac{c_{Ac}^{eq} c_{Al}^{eq}}{K_c^{hom}} \quad \text{and} \quad 0 = K_{Es} c_{Es}^{eq} c_W^{eq} - \frac{K_{Ac} c_{Ac}^{eq} K_{Al} c_{Al}^{eq}}{K_c^{het}} \tag{6.7}$$

Therefore, to ensure that the reactions are simultaneously in equilibrium in both phases, the following two relationships must hold:

$$K_c^{\mathrm{hom}} = \frac{c_{Ac}^{eq} c_{Al}^{eq}}{c_{Es}^{eq} c_W^{eq}} \tag{6.8}$$

$$K_c^{\mathrm{het}} = K_c^{\mathrm{hom}} \frac{K_{Ac} K_{Al}}{K_{Es}} \tag{6.9}$$

In addition to the experimentally measured heat flows, $\dot{Q}_{wall}$, input parameters for the analyses were the distribution equilibrium constants K_i (Table 6.2), the reaction equilibrium constants K_c^{hom} (Table 6.3) and K_c^{het} [Eq. (6.9)], the initial liquid-phase compositions of the specific experiments, the reaction enthalpies $\Delta H_r^{\mathrm{hom}}$ and $\Delta H_r^{\mathrm{het}}$ (which were taken identically from the integrals of the heat flows given in Table 6.11), and the liquid fraction ε [Eq. (2.81)]. The free parameters to be determined were the rate constants k^{hom} and k^{het}, and in the case of the heterogeneous model additionally the intraparticle mass-transfer coefficients β_i [Eqs. (4.13) and (4.14)].

A commercially available optimizer based on standard stochastic algorithms provided by Presto [Wulk01] was used to estimate these parameters. After integrating numerically equations (4.13) and (4.14) for the heterogeneous model or equation (4.16) for the pseudohomogeneous model, the time dependences of c_i and q_i were found. The calculated time dependence of the heat flow over the calorimeter wall [Eq. 4.25)] was then compared with the measured one to find the best-fit values of the free parameters k^{hom} and k^{het}.

In the heterogeneous model, the intraparticle mass-transfer coefficients β_i were assumed to be equal for all components. For the runs performed, a value of $\beta = 0.01$ min^{-1} was estimated to be most probable. For values of $\beta \geq 0.25$ min^{-1}, no effect of the mass-transfer resistance remained, and the results were identical to those obtained using the pseudohomogeneous model [Eq. (4.16)] for the same rate constants. The above observations can be seen in Figure 6.9, which shows a typical relationship between the calculated standard deviations of the parametric model estimations using the heterogeneous model and the intraparticle mass-transfer coefficient, β.

Figure 6.10a shows the comparison of simulated heat flows using the heterogeneous model [Eqs. (4.13) and (4.14)] and the pseudohomogeneous model [Eq. (4.16)]. It is obvious that the influence of β is only very small. Consequently, in further calculations, only the pseudohomogeneous model (β infinite) was applied to quantify the reaction rate constants.
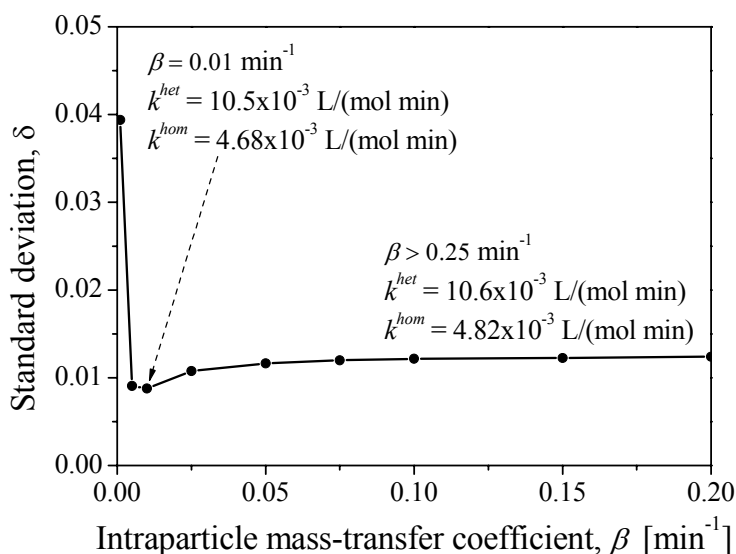
Figure 6.9. Influence of the intraparticle mass-transfer coefficient, β, on the standard deviation of the parametric model estimation using the heterogeneous model [Eqs. (4.13) and (4.14) combined with Eq. (4.25)]. Input data: measured heat flow of the methyl formate hydrolysis, $T = 25\ ^{\circ}C$, $c_{Es_{11}}^{o} = 2.0$ mol/L, Cat1.

An overview of the obtained reaction enthalpies and reaction rate constants is given in Tables 6.11 and 6.12. It can be seen from Table 6.11 that the reaction enthalpies for the hydrolysis of methyl formate and methyl acetate obtained from the calorimetric measurements are considerably lower than those obtained from heats of formation and from the equilibration experiments (Table 6.7). Persuasive reasons for this difference have not been found yet. Figures 6.10b and 6.10c shows comparisons of the measured and the simulated heat flows for hydrolysis of methyl acetate at (a) 25 and (b) 30 $^{\circ}C$ with Cat2. It can be seen that the simulation is in slightly better agreement with the measured heat flows for the reaction at 30 $^{\circ}C$ (Fig. 6.10c) than 25 $^{\circ}C$ (Fig. 6.10b). Figure 6.10d shows a comparison of the measured and simulated heat flows for the hydrolysis of methyl formate at 25 $^{\circ}C$ with Cat1 performed in the calorimeter. In addition, a simulation of this run was also performed with the k^{het} value (14×10^{-3}) determined from the analysis of the chromatograms measured in the fixed-bed reactor.

From Figure 6.10d and the results in Table 6.12, it can be observed that the rate constants quantified from both the chromatograms and the heat flows are in relatively good agreement. This was also demonstrated already earlier in Figure 6.10a. Because of the

higher liquid-phase fraction, the contribution of the homogeneous reaction is more significant in the calorimetric reactor than in the well-packed fixed-bed reactor with the smaller porosity ε. This is also visible in Figure 6.10d, where the contribution of homogeneous reaction is eliminated in one of the curves by setting $k^{hom} = 0$.

Table 6.11. The hydrolysis reactions of methyl formate and methyl acetate conducted in the reaction calorimeter.

Methyl formate hydrolysis (Es_{11}) with Cat1										
Run	T_r	$c_{Es_{11}}^o$	c_W^o	$c_{Es_{11}}^{eq}$	c_W^{eq}	c_{Ac_1,Al_1}^{eq}	V_R	ε	I_{wall}[a]	ΔH_r[b]
	[^{o}C]			[mol/L]			[L]	[-]	[kJ]	[kJ/mol]
B10	25	1.42	49.8	0.24	48.6	1.59	1.11	0.96	3.97	3.03
B11	25	2.00	47.1	0.46	45.5	2.02	1.17	0.96	5.75	3.19
B12	25	2.66	44.9	0.75	42.9	2.55	1.22	0.96	7.08	3.04
Methyl acetate hydrolysis (Es_{12}) with Cat2										
Run	T_r	$c_{Es_{21}}^o$	c_W^o	$c_{Es_{12}}^{eq}$	c_W^{eq}	c_{Ac_2,Al_1}^{eq}	V_R	ε	I_{wall}[a]	ΔH_r[b]
	[^{o}C]			[mol/L]			[L]	[-]	[kJ]	[kJ/mol]
B15	25	2.83	43.8	0.73	41.7	2.10	1.20	0.92	8.30	3.29
B18	30	2.82	43.8	0.73	41.7	2.09	1.01	0.91	6.87	3.25

[a] $I_{wall} = \int \dot{Q}_{wall}(t)dt$

[b] $\Delta H_r = I_{wall} / \left[\left(c_{Es}^o - c_{Es}^{eq} \right) V_R \right]$

Table 6.12. Resulting parameters for the hydrolysis reactions of methyl formate and methyl acetate.

Run	T_r[^{o}C]	k^{het} [L/(mol min)]	k^{hom} [L/(mol min)]
Methyl formate hydrolysis (Es_{11}) with Cat1			
B10	25	12.0 x 10^{-3} (14.0 x 10^{-3})[*]	5.13 x 10^{-3}
B11	25	10.6 x 10^{-3}	4.82 x 10^{-3}
B12	25	10.5 x 10^{-3}	4.55 x 10^{-3}
Methyl acetate hydrolysis (Es_{12}) with Cat2			
B15	25	0.69 x 10^{-3} (0.76 x 10^{-3})[*]	0.11 x 10^{-3}
B18	30	1.34 x 10^{-3}	0.24 x 10^{-3}

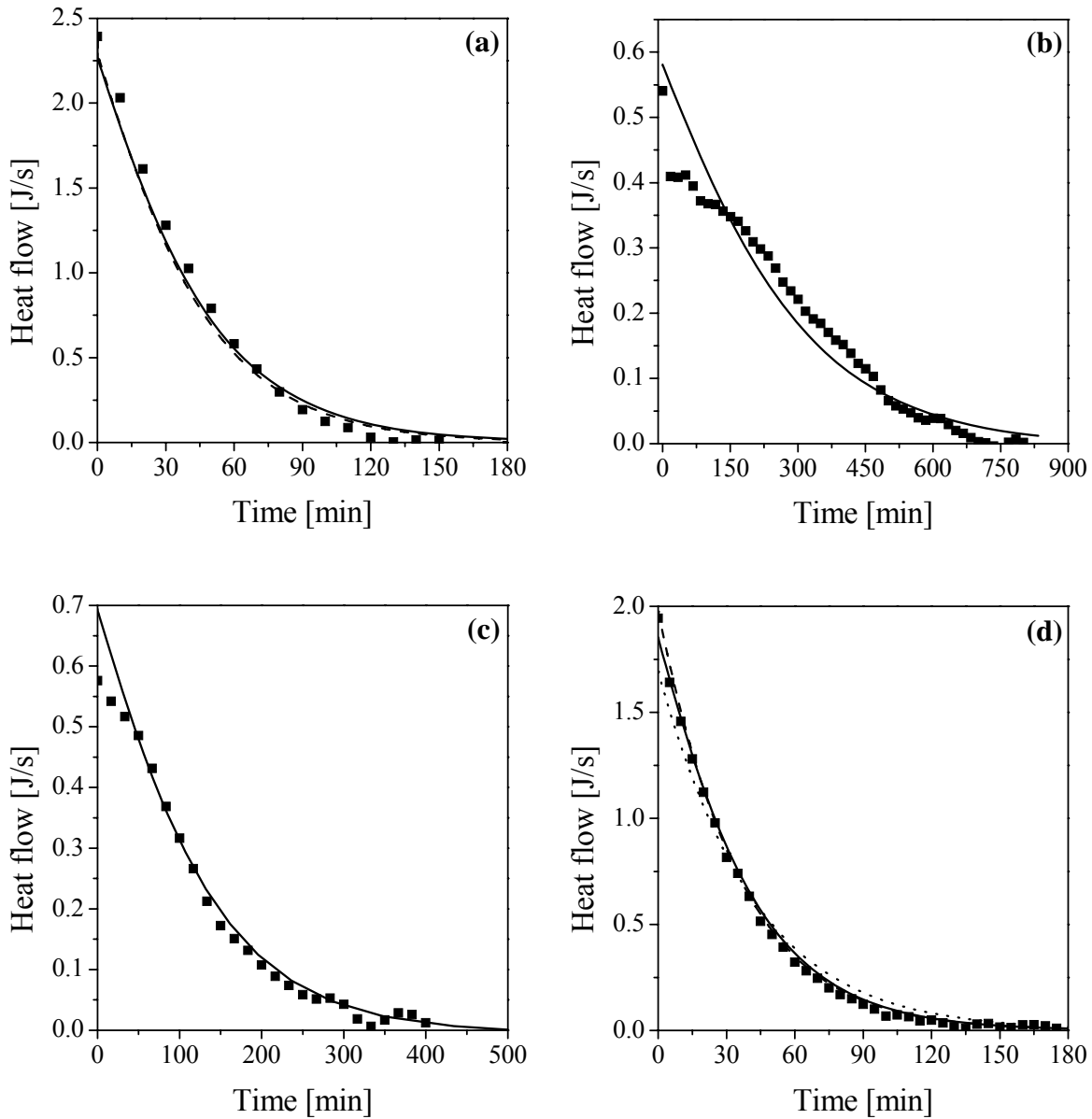[*] Previous results quantified from elution profiles for a chromatographic reactor [Mai04]

Figure 6.10. Comparisons of the simulated (lines) and measured (symbols) heat flows (ideal solution behavior). (**a**) Es_{11}, $T = 25$ °C, $c^o_{Es_{11}} = 2.0$ mol/L, Cat1: (solid) Eqs. (4.13) and (4.14), $\beta = 0.01$ min^{-1}, $k^{het} = 10.5$ x 10^{-3}, $k^{hom} = 4.68$ x 10^{-3} L/(mol min); (dashed) Eq. (4.16), $k^{het} = 10.6$ x 10^{-3}, $k^{hom} = 4.82$ x 10^{-3} L/(mol min). (**b**) Es_{12}, $T = 25$ °C, Cat2, $k^{het} = 0.69$ x 10^{-3}, $k^{hom} = 0.11$ x 10^{-3} L/(mol min), Eq. (4.16). (**c**) Es_{12}, $T = 30$ °C, Cat2, $k^{het} = 1.34$ x 10^{-3}, $k^{hom} = 0.24$ x 10^{-3} L/(mol min), Eq. (4.16). (**d**) Es_{11}, $T = 25$ °C, $c^o_{Es_{11}} = 1.42$ mol/L, Cat1: (solid) $k^{het} = 12.0$ x 10^{-3} and $k^{hom} = 5.13$ x 10^{-3} L/(mol min) [determined from the course of the heat flows, Eq. (4.16)]; (dotted) $k^{het} = 12.0$ x 10^{-3} and $k^{hom} = 0$; (dashed) $k^{het} = 14.0$ x 10^{-3} L/(mol min) and $k^{hom} = 0$ (determined from the shape of the elution profiles [Mai04]).

6.4.3.2 Non-Ideal Solution Behavior

Alternatively, the reaction rate can be expressed in terms of activities as in the following Eqs. (6.10) and (6.11) to take into account the non-idealities of both liquid and solid phases. Again due to the excess of water in the reaction systems, Eley–Rideal type of reaction mechanism [Thom97] can be assumed for the four heterogeneously catalyzed reactions:

$$r^{hom} = k^{hom} c_{H^+} \left(a_{Es}^L a_W^L - \frac{a_{Ac}^L a_{Al}^L}{K_a^{hom}} \right) \tag{6.10}$$

$$r^{het} = k^{het} \left(a_{Es}^S a_W^L - \frac{a_{Ac}^S a_{Al}^S}{K_a^{het}} \right) \tag{6.11}$$

In the above equations, a^L and a^S denote activities in the liquid and solid phases, respectively. The activity coefficient, γ_i, of component i in the liquid phase was calculated using the UNIQUAC model as described in Section 2.4.

Equation (2.39) expressing the relation between the activity in the liquid phase and that in the solid phase as introduced earlier in Section 2.1.2 is now recalled:

$$\ln a_i^L \left(T, p^L, n^L \right) = \ln a_i^S \left(T, p^L, n^S \right) + \pi_{sw} V_{m,i} \qquad i = 1, \ldots, N_c \tag{2.39}$$

where π_{ws} is the swelling pressure of the solid catalyst, and $V_{m,i}$ is the molar volume of component i. Thus, the activity of component i in the solid phase can then be calculated from its activity in the liquid phase using the following equation:

$$a_i^S = a_i^L \exp\left(-\frac{V_{m,i}\pi_{sw}}{RT} \right) \qquad i = 1, \ldots, N_c \tag{6.12}$$

As discussed in Section 2.1.2, the swelling pressure can be expressed in terms of the change in the configurational entropy of the elastic structure and in the volume of the solid phase [Eq. (2.31)]. Therefore, the swelling pressure is somehow related to the distribution equilibrium constants.

To ensure that the reactions are simultaneously in equilibrium in both phases, the following two relationships must hold (similarly to the situation for the ideal solution behavior discussed above [Eq. (6.8)]):

$$K_a^{hom} = \frac{a_{Ac}^{L,eq} a_{Al}^{L,eq}}{a_{Es}^{L,eq} a_{W}^{L,eq}} \qquad\qquad (6.13)$$

$$K_a^{het} = K_a^{hom} \exp\left(-\frac{\pi_{sw}}{RT} \sum_{i=1}^{N_c} \nu_i V_{m,i} \right) \qquad\qquad (6.14)$$

In the present work, a determination of the swelling pressure of the solid catalyst in contact with the liquid reaction mixtures was not carried out. Sainio [Sainio05] studied the swelling pressures of several sulfonated poly(styrene-co-divinylbenzene) cation-exchange resins for similar reaction systems. One of these resins, which has the cross-linked density of 8 wt-%, is similar to Cat1 and Cat2 used in this work. In his work, the dependence of swelling pressure on the swelling ratio was predicted and compared with experimental data. It was found that in any case, the swelling pressure model used in his work yields a better description than the Flory elasticity model and the Gussler–Cohen modification of it that were used by Lode [Lode02] and Mazzotti *et al.* [Mazz97]. Based on his reported results, a value of $\pi_{sw} = 30$ MPa was found for Cat1 and Cat2 in contact with the reaction mixtures used in the present work.

With taking into account the real solution behavior of the liquid and solid phases, reaction rate constants of the two hydrolysis reactions studied in the calorimeter were again quantified by applying the pseudohomogeneous model [Eq. (4.16)] in combination with the energy balance [Eq. (4.25)]. The obtained values of the reaction rate constants are given in Table 6.13, in which the values quantified with the assumption of ideal solution behavior, are also listed for comparison. Figure 6.11 shows how good the agreement between the measured and the simulated heat flows for the hydrolysis of (a) methyl formate at 25 ^{o}C with Cat1, and (b) methyl acetate at 25 and 30 ^{o}C with Cat2 is. It can be seen from the data in shown Table 6.13 that the values of reaction rate constants obtained by taking into account the real solution behavior were always smaller than what obtained by assuming the ideal solution behavior.

Among the four hydrolysis reactions investigated, only the hydrolysis of methyl formate was performed with two different Cat1 and Cat2. The obtained values of k^{het} for the hydrolysis of methyl formate shown in Table 6.13 indicate that this reaction is faster using Cat2 than using Cat1. This is in agreement with the different amounts of sulfonic acid groups on the two catalysts (Section 6.1).

Table 6.13. Reaction rate constants for the hydrolysis reactions of methyl formate and methyl acetate conducted in the reaction calorimeter quantified by using different kinetic models.

			Methyl formate hydrolysis (Es_{11})			
			Ideal solution behavior		Real solution behavior [*]	
		T	$k_{(c)}^{het}$	$k_{(c)}^{hom}$	$k_{(a)}^{het}$	$k_{(a)}^{hom}$
Run	Cat.	[°C]	[L/(mol min)]	[L/(mol min)]	[L/(mol min)]	[L/(mol min)]
B10	Cat1	25	12.0×10^{-3}	5.13×10^{-3}	5.50×10^{-3}	1.17×10^{-3}
B11	Cat1	25	10.6×10^{-3}	4.82×10^{-3}	4.82×10^{-3}	0.88×10^{-3}
B12	Cat1	25	10.5×10^{-3}	4.55×10^{-3}	4.56×10^{-3}	1.01×10^{-3}
B14	Cat2	25	29.9×10^{-3}	3.27×10^{-3}	10.4×10^{-3}	1.08×10^{-3}
			Methyl acetate hydrolysis (Es_{12})			
			Ideal solution behavior		Real solution behavior [*]	
		T	$k_{(c)}^{het}$	$k_{(c)}^{hom}$	$k_{(a)}^{het}$	$k_{(a)}^{hom}$
Run	Cat.	[°C]	[L/(mol min)]	[L/(mol min)]	[L/(mol min)]	[L/(mol min)]
B15	Cat2	25	0.69×10^{-3}	0.11×10^{-3}	0.54×10^{-4}	0.65×10^{-5}
B18	Cat2	30	1.34×10^{-3}	0.24×10^{-3}	0.10×10^{-3}	0.13×10^{-4}

*) Activity coefficients in the liquid phase were calculated using UNIQUAC model; activities in the solid phase were calculated using Eq. (6.12).

To achieve more reliable information about the temperature dependence of the rate constants, experiments at more temperatures than 20 and 30 °C should be done. However, because of limited sensitivity of the calorimeter and the relatively low boiling point of methyl acetate (Table 3.1), the results obtained for experiments at temperatures lower than 20 °C and higher than 30 °C were not precise. Since only the hydrolysis of methyl acetate was conducted in the calorimeter at various temperatures (25 and 30 °C), only the activation energy for that reaction was estimated using different kinetic models [Eqs. (6.2), (6.5) and Eqs. (6.10), (6.11)]. The obtained values of activation energy for the methyl acetate hydrolysis using Cat2 given in Table 6.14 are well comparable with the value of 104.1 kJ/mol reported by Kirbaslar *et al.* [Kirb01], but differ considerably from 69.2 kJ/mol and 66.1 kJ/mol given by Pöpken *et al.* [Pöpken00] and Mazzotti *et al.* [Mazz97a], where the Amberlyst 15 was used.
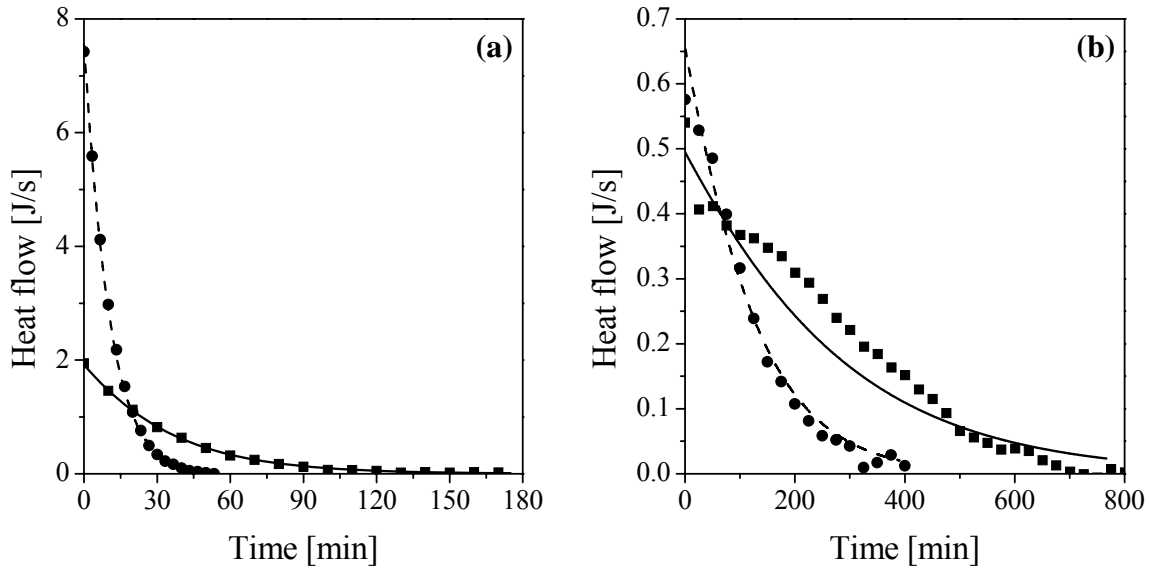
Figure 6.11. Comparisons of the simulated (lines) and measured (symbols) heat flows (real solution behavior, activity coefficients calculated by UNIQUAC and Eq. 6.12). (**a**) (solid): Es_{11}, $T = 25\ ^{\circ}\mathrm{C}$, $c^o_{Es_{11}} = 1.42$ mol/L, Cat1, Eq. (4.16), $k^{\mathrm{het}} = 5.50 \times 10^{-3}$, $k^{\mathrm{hom}} = 1.17 \times 10^{-3}$ L/(mol min); (dashed): Es_{11}, $T = 25\ ^{\circ}\mathrm{C}$, $c^o_{Es_{11}} = 2.03$ mol/L, Cat2, Eq. (4.16), $k^{\mathrm{het}} = 10.4 \times 10^{-3}$, $k^{\mathrm{hom}} = 1.08 \times 10^{-3}$ L/(mol min). (**b**) (solid): Es_{12}, $T = 25\ ^{\circ}\mathrm{C}$, Cat2, Eq. (4.16), $k^{\mathrm{het}} = 0.54 \times 10^{-4}$, $k^{\mathrm{hom}} = 0.65 \times 10^{-5}$ L/(mol min); (dashed): Es_{12}, $T = 30\ ^{\circ}\mathrm{C}$, Cat2, Eq. (4.16), $k^{\mathrm{het}} = 0.10 \times 10^{-3}$, $k^{\mathrm{hom}} = 0.13 \times 10^{-4}$ L/(mol min).

Table 6.14. Activation energy obtained by using the Arrhenius equation for the hydrolysis of methyl acetate catalyzed by Cat2.

Solution behavior	Activation energy, E_A [kJ/mol]	
	Homogeneous reaction	Heterogeneous reaction
Ideal	117.1	99.6
Real*	108.4	94.2

*) activity coefficients in the liquid phase were calculated using UNIQUAC model; activities in the solid phase were calculated using Eq. (6.12).

6.5 Reaction Kinetic Estimation Using Batch Experiments

A conventional approach to the quantification of reaction rates is to measure reactant or product concentrations as functions of time in a batch reactor. To verify the reaction rate constants quantified from measured heat flows and to enlarge the database of the involved reactions as well, in the present work the kinetic experiments for hydrolysis of the four esters were performed also in a conventional batch reactor as described in Section 5.2.4. Hydrochloric acid was used as a homogeneous catalyst, and Cat1 and Cat2 as heterogeneous catalysts. The experiments were conducted at only 25 ^{o}C. The qualitative analysis of the experimental results is given in the following Section 6.5.1, while the quantitative analysis is discussed later in Section 6.5.2.

6.5.1 Qualitative Analysis

At first, to evaluate if temporal development of concentrations correlates with temporal development of reaction heat flows, the measured concentrations of esters in the batch experiments and the measured heat flows in the calorimeter were normalized to the dimensionless parameters c^{norm} and $\dot{Q}^{norm}$, respectively, by the following equations:

$$c^{norm}(t) = \frac{c(t) - c_{end}}{c_o - c_{end}}$$

(6.15)

$$\dot{Q}^{norm}(t) = \frac{\dot{Q}(t) - \dot{Q}_{end}}{\dot{Q}_o - \dot{Q}_{end}}$$

(6.16)

where c_o and c_{end} are the initial and the final concentration, $\dot{Q}_o$ and $\dot{Q}_{end}$ are the initial and the final heat low, respectively. Theoretically, c^{norm} and $\dot{Q}^{norm}$ should be correlative for each reaction.

Figure 6.12a shows typical normalized concentrations of methyl formate together with typical normalized heat flows for the hydrolysis of methyl formate as a function of time. It can be seen that the normalized concentrations agree well with the normalized heat flows. This indicates that for the hydrolysis of methyl formate the temporal development of concentrations and heat flows measured are consistent with theory. In Figure 6.12b is illustrated the comparison of the normalized concentrations of methyl acetate with the normalized heat flows for the hydrolysis of methyl acetate. The figure shows that the agreement between the normalized concentrations and heat flows for the hydrolysis of

methyl acetate is not as good as that for the hydrolysis of methyl formate. This can be due to the poorly measured heat flow for the hydrolysis of methyl acetate as mentioned already in Section 6.4 that there is considerable noise in the measurements for the methyl acetate hydrolysis. This indicates that for reactions with low heat flow, measuring reaction kinetics by using a conventional batch reactor provides more reliable results compared to using a reaction calorimeter. However, to perform such batch reactor measurements more analytical work is needed.
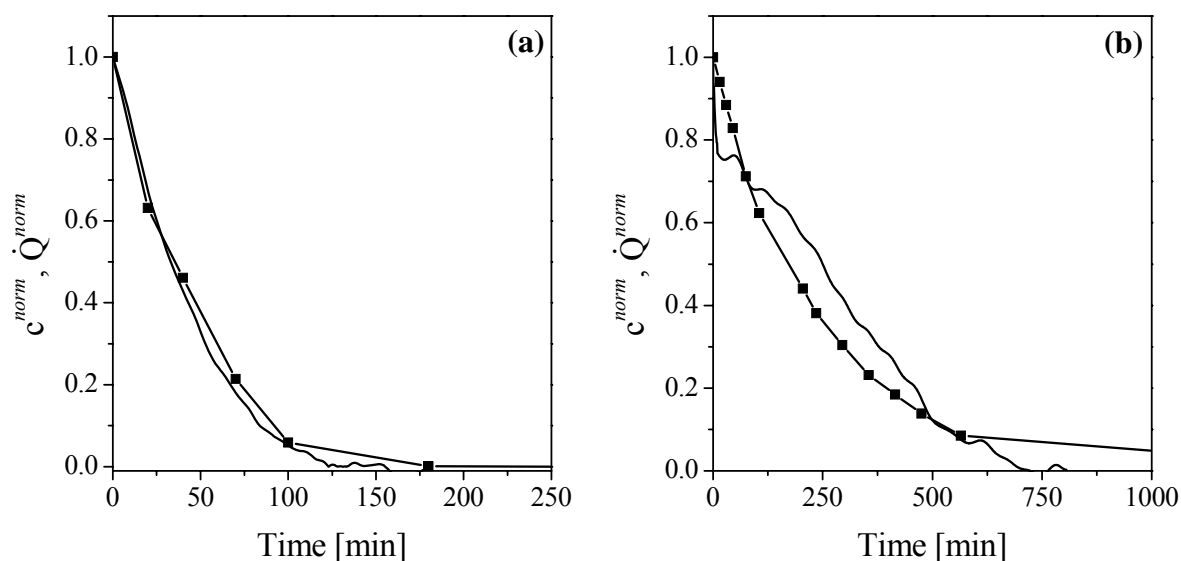

Figure 6.12. Normalized concentrations (lines–symbols) and heat flows measured (lines) for: **(a)** methyl formate hydrolysis, Cat1, $T_r = 25$ ^{o}C, $c^o_{Es_{11}} = 2.0$ mol/L; **(b)** methyl acetate hydrolysis, Cat1, $T_r = 25$ ^{o}C, $c^o_{Es_{12}} = 2.5$ mol/L.

In Figure 6.13, the liquid phase concentrations of esters in a batch reactor for the hydrolysis of the four esters catalyzed by different catalysts at 25 ^{o}C are shown. Hydrochloric acid was used as a homogeneous catalyst with a concentration of 0.025 mol/L. Cat1 and Cat2 were used as heterogeneous catalysts with the same liquid fraction, ε, as used for the experiments performed in the reaction calorimeter. Cat2 was used for all the four reactions, while Cat1 for only the methyl formate hydrolysis. It is apparent from Figure 6.13 that with the liquid fraction between 0.92 and 0.96, the heterogeneous catalysts accelerate the reactions much more than the homogeneous catalyst. It can also be seen that for the same temperature and catalyst loading, the hydrolysis of methyl formate occurs fastest, followed by that of ethyl formate, then methyl acetate and ethyl acetate.
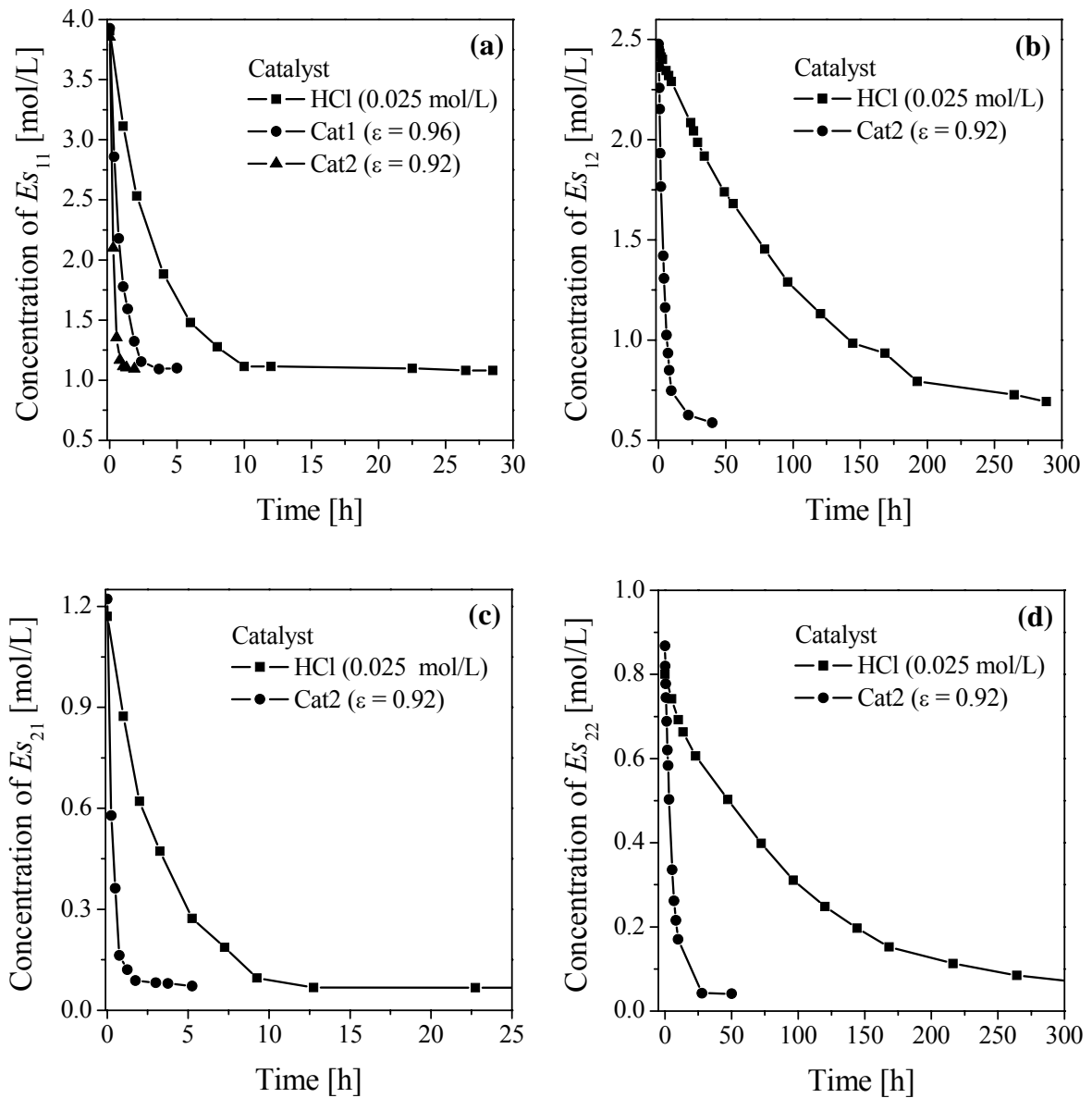
Figure 6.13. Liquid phase concentration of ester in a batch reactor as a function of time for the hydrolysis of the four esters catalyzed by different catalysts at 25 $^{\circ}$C: (**a**) methyl formate, Es_{11}; (**b**) methyl acetate, Es_{12}; (**c**) ethyl formate, Es_{21}; and (**d**) ethyl acetate, Es_{22}.

6.5.2 Estimation of Reaction Rate Constants

To determine the reaction rate constants, an attempt was made to match the simulated and the measured concentration profiles. The pseudohomogeneous model [Eq. (4.16)], which has been used in combination with the energy balance [Eq. (4.25)] to quantify reaction rate constants of the reactions studied in the calorimeter, was applied. All optimization were

run with again a) the assumption of ideal solution behavior [Eqs. (6.2) and (6.5)] and b) with taking into account the real solution behavior [Eqs. (6.10) and (6.11)] for both phases. The activity coefficients, γ_i, of component i in the liquid phase were again calculated using the UNIQUAC model as described in Section 2.4. The activity of component i in the solid phase can be calculated from its activity the liquid phase using Eq. (6.12). The rate constant values for the homogeneous reaction, k^{hom}, obtained from the batch reactions catalyzed by homogeneous hydrochloric acid were used as input values to estimate the heterogeneous reaction rate constants, k^{het}, for the batch reactions catalyzed by Cat1 and Cat2. The determined values of the reaction rate constants for the four hydrolysis reactions are reported in Table 6.15. In the case of assuming ideal solution behavior, Figure 6.14 shows comparisons of the measured and the simulated ester concentrations for the hydrolysis reactions of the four esters at 25 ^{o}C with the homogeneous and heterogeneous catalysts performed in the batch reactor. In addition, simulations of the runs G2 and G6 (see Table 5.8, Section 5.2.4) were also performed with the k^{het} and k^{hom} values determined from the analysis of the measured heat flows. From Figures 6.14a-b and the data shown in Tables 6.13 and 6.15, it can be seen that the rate constants for the hydrolysis of methyl formate quantified from the measured concentration-time profiles (k^{het} = 12.0 x 10^{-3}, k^{hom} = 5.13 x 10^{-3}) agree well with those quantified from the measured heat flows (k^{het} = 12.6 x 10^{-3}, k^{hom} = 3.19 x 10^{-3}). However, the agreement is slightly worse for the hydrolysis of methyl acetate. This can be due to the slightly poor measured heat flow for the methyl acetate hydrolysis at 25 ^{o}C, which has not been also in very good agreement with the simulation as shown already in Figure 6.10a. The values of k^{het} for the hydrolyses of ethyl formate and ethyl acetate given in Table 6.15 agree well with the value of 13.6 x 10^{-3} and 0.75 x 10^{-3} L/(mol min), which were quantified earlier in chromatographic experiments [Mai04]. This is also illustrated in Figures 6.14c-d.

Table 6.15. Reaction rate constants for the hydrolysis reactions of the four esters conducted in the conventional batch reactor at 25 °C quantified by using different kinetic expressions.

| Run | Catalyst | Ideal solution behavior [*] | | Real solution behavior [**] | |
		$k_{(c)}^{het}$ [L/(mol min)]	$k_{(c)}^{hom}$ [L/(mol min)]	$k_{(a)}^{het}$ [L/(mol min)]	$k_{(a)}^{hom}$ [L/(mol min)]
		Methyl formate hydrolysis, Es_{11}			
E1	HCl	-	3.19×10^{-3}	-	1.17×10^{-3}
E2	Cat1	12.6×10^{-3}	3.19×10^{-3}	4.67×10^{-3}	1.17×10^{-3}
E3	Cat2	27.1×10^{-3}	3.19×10^{-3}	9.73×10^{-3}	1.17×10^{-3}
		Methyl acetate hydrolysis, Es_{12}			
E5	HCl	-	0.10×10^{-3}	-	0.77×10^{-5}
E6	Cat2	0.99×10^{-3}	0.10×10^{-3}	0.72×10^{-4}	0.77×10^{-5}
		Ethyl formate hydrolysis, Es_{21}			
E8	HCl	-	2.98×10^{-3}	-	1.21×10^{-3}
E9	Cat2	13.7×10^{-3}	2.98×10^{-3}	4.59×10^{-3}	1.21×10^{-3}
		Ethyl acetate hydrolysis, Es_{22}			
E10	HCl	-	0.12×10^{-3}	-	1.22×10^{-5}
E11	Cat2	0.75×10^{-3}	0.12×10^{-3}	9.40×10^{-5}	1.22×10^{-5}

[*]) Pseudohomogeneous model: Eq. (4.16); kinetic expressions: Eqs. (6.2) and (6.5).

[**]) Pseudohomogeneous model: Eq. (4.16); kinetic expressions: Eqs. (6.10) and (6.11); activity coefficients in the liquid phase were calculated using UNIQUAC model; activities in the solid phase were calculated using Eq. (6.12).
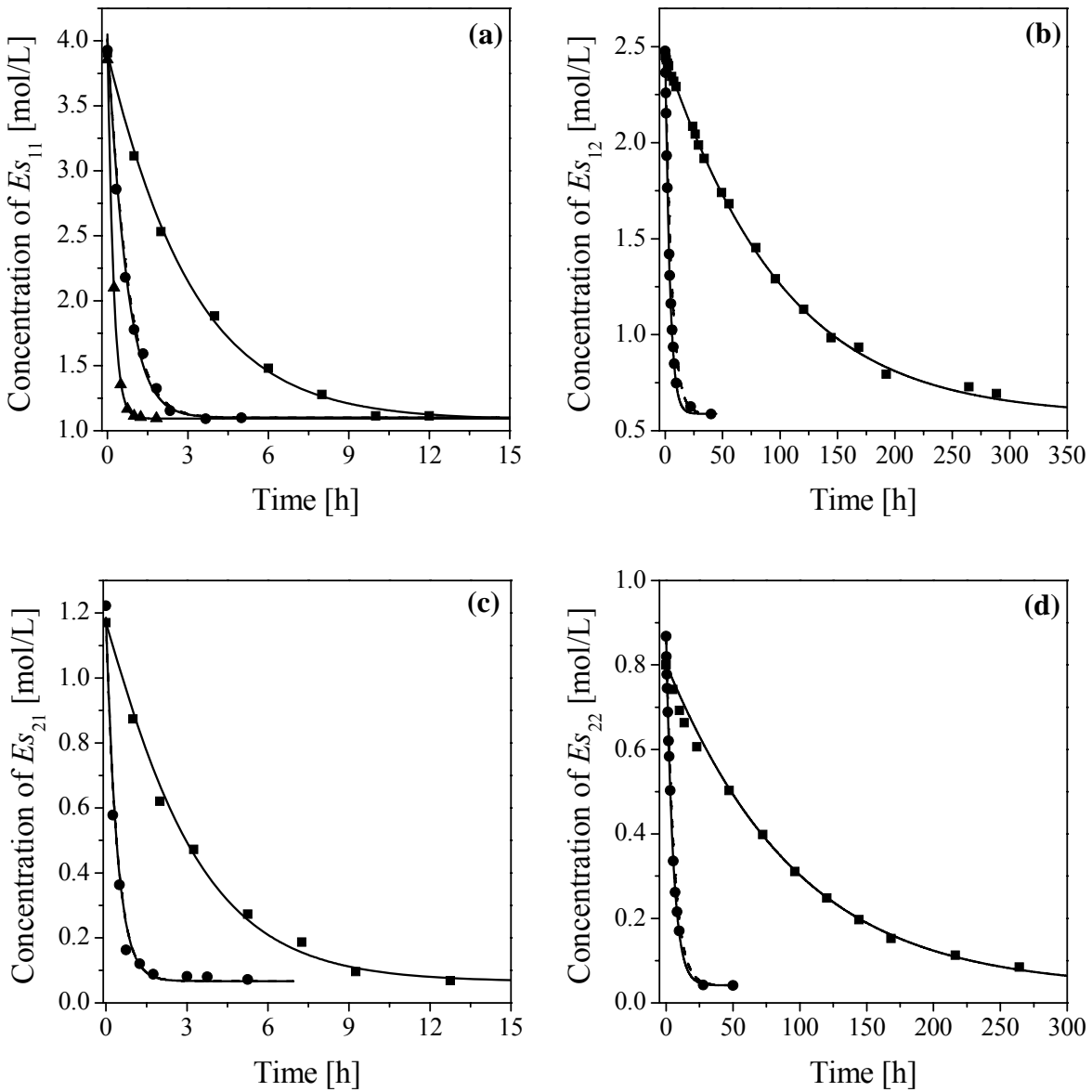
Figure 6.14. Comparisons of the simulated (solid lines – ideal solution behavior) and measured (symbols) ester concentrations for the hydrolysis reactions of the four esters at 25 °C performed in the batch reactor. (**a**) Es_{11}: (■) homogeneous catalyst; (●) Cat1, (dashed line) calculated with the k^{het} and k^{hom} values determined from the analysis of the heat flows; (▲) Cat2. (**b**) Es_{12}: (■) homogeneous catalyst; (●) Cat2, (dashed line) calculated with the k^{het} and k^{hom} values determined from the analysis of the heat flows. (**c**) Es_{21}: (■) homogeneous catalyst; (●) Cat2, (dashed line) calculated with the k^{het} values determined from the chromatograms. (**d**) Es_{22}: (■) homogeneous catalyst; (●) Cat2, (dashed line) calculated with the k^{het} values determined from the chromatograms.

6.6 Error Evaluation

No detailed error analysis so far in this work has been performed. This would require a complex propagation analysis. Thus, despite of all activities there is still considerable uncertainty in determining the parameters. This could be due to model and/or measurement errors.

Possible sources of error in the model include the underlying assumptions of isothermal conditions, perfect mixing, no heat losses, no heat generated by the stirrer, and so on.

The uncertainty can also be due to errors in the measurement of heat flows with the reaction calorimeter and the analysis of reaction mixtures with the gas chromatography system. For calorimetric measurements, a major limitation to successful process control is the inability to achieve real-time quantitative calorimetry. This is in part due to the operating principle of the calorimeter, in which the measured heat signal is calculated from the temperature difference between the reaction contents and the jacket oil and the heat transfer coefficient. As discussed in Section 4.1.4, the latter frequently varies during a reaction due to changes in composition, volume, and density, and is difficult to determine accurately during the process.

The errors of GC measurements are essentially related to the data acquisition system, the injection of samples, the measurement of the peak data, and the stability of the gas chromatography.

6.7 Model Validation

Above a simple mathematical model describing the essential features of thermodynamics and kinetics of heterogeneously catalyzed ester hydrolysis reactions was proposed. The analysis shows that the influence of internal mass-transfer limitations in the applied resin particles is only very small. Therefore, a pseudohomogeneous model [Eq. (4.16)] can be used in combination with the energy balance [Eq. (4.25)] to quantify the reaction rate constants. Subsequently, the rate constants of the reactions investigated to establish kinetic expressions have been quantified from the measured heat flows. As a result of the work presented above the following model and parameters were suggested:
- mass balances [Eq. (4.16)]
- energy balance [Eq. (4.25)]
- parameters (Tables 6.11 and 6.12)

The aim of model validation is to ensure that the model used can describe properly the essential features of the reaction calorimeter, and can generalize well. The aim also includes ensuring that the reaction rate constants quantified are reliable. These mean that, with the energy balance and the quantified parameters, the model can predict properly the reaction heat flows with respect to different conditions or systems. They could be different runs of the ester hydrolysis reactions with consideration of the same respective catalyst and temperature but different initial compositions or runs of corresponding esterification reactions at the same conditions. In addition, several chromatograms recorded from the chromatographic experiments for the hydrolysis of ester pulses can also be used to validate the rate constants quantified.

In order to validate the model and the obtained rate constants, several experiments of the esterification of formic acid and of acetic acid with methanol were performed in the calorimeter. In principle, the rate constant of an esterification of an acid with an alcohol can be calculated from the rate constant and the equilibrium constant of the corresponding ester hydrolysis as defined in the following equation:

$$k_{esterification} = \frac{k_{hydrolysis}}{K_{eq,hydrolysis}} \qquad\qquad (6.17)$$

Using Eq. (6.17) and the obtained values of the rate constants for the hydrolysis of methyl formate and methyl acetate (runs G10 and G15, Table 6.12), the rate constants of the corresponding esterification reactions are found to be a) $k^{het} = 54.5 \times 10^{-3}$, $k^{hom} = 23.3 \times 10^{-3}$ L/(mol min) (for the esterification of formic acid with methanol), and b) $k^{het} = 4.93 \times 10^{-3}$, $k^{hom} = 0.78 \times 10^{-3}$ L/(mol min) (for the esterification of acetic acid with methanol). Examples of calculating the heat flows for the esterifications of formic acid and of acetic acid with methanol with these obtained values are given in Figure 6.15. It is shown in Figure 6.15 that the agreement between the calculated and measured heat flows for both esterifications of formic acid and of acetic acid with methanol is very good. This validates both the suggested model and the quantified parameters.

The reason of the unusual behavior between 200–400 min of the measured heat flow for the esterification of acetic acid with methanol (Figure 6.15b) is not clear. This should be examined in the future work.
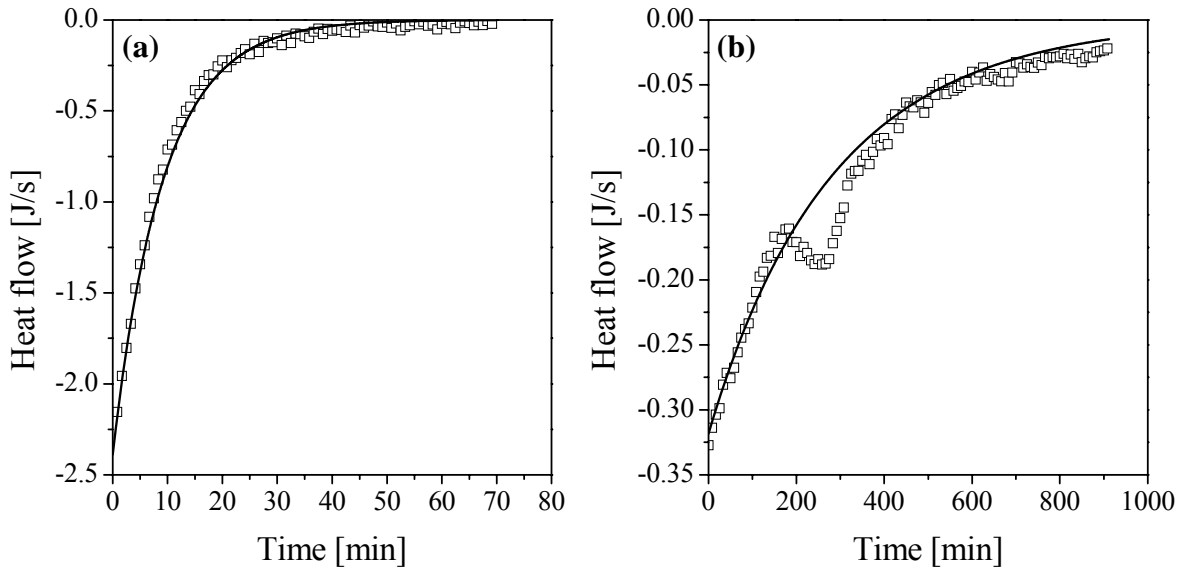
Figure 6.15. Comparisons of the heat flows calculated back (lines) using the obtained values of k^{het} and k^{hom}, and the measured results (symbols) for the esterification of (**a**) formic acid, and (**b**) acetic acid with methanol catalyzed by Cat2 at 25 ^{o}C. Ideal solution behavior was assumed.

Alternatively, chromatographic experiments for the hydrolysis of ester pulses were used to validate the obtained rate constants. For this, examples of simulating the chromatograms using the obtained rate constants $k_{Es_{11}}^{het} = 12.0 \times 10^{-3}$ and $k_{Es_{12}}^{het} = 0.69 \times 10^{-3}$ (Table 6.12) for the hydrolysis of methyl formate and methyl acetate pulses are given together with the recorded chromatograms in Figure 6.16. To perform the simulations, a new model for the chromatographic fixed-bed reactor is needed. This model was already reported by Mai *et al*. (2004) [Mai04]. The results shown in Figure 6.16a are for simulations performed for two different flow rates for the hydrolysis of methyl formate at 25 ^{o}C in the column packed with Cat1. In addition, a simulation performed for the hydrolysis of methyl acetate at 25 ^{o}C in the column packed with Cat2 is shown in Figure 6.16b. It can be seen that the simulated chromatograms using the rate constants quantified from the measured heat flows for the both hydrolysis reactions agree well with the measured ones. This again validates the obtained rate constants.
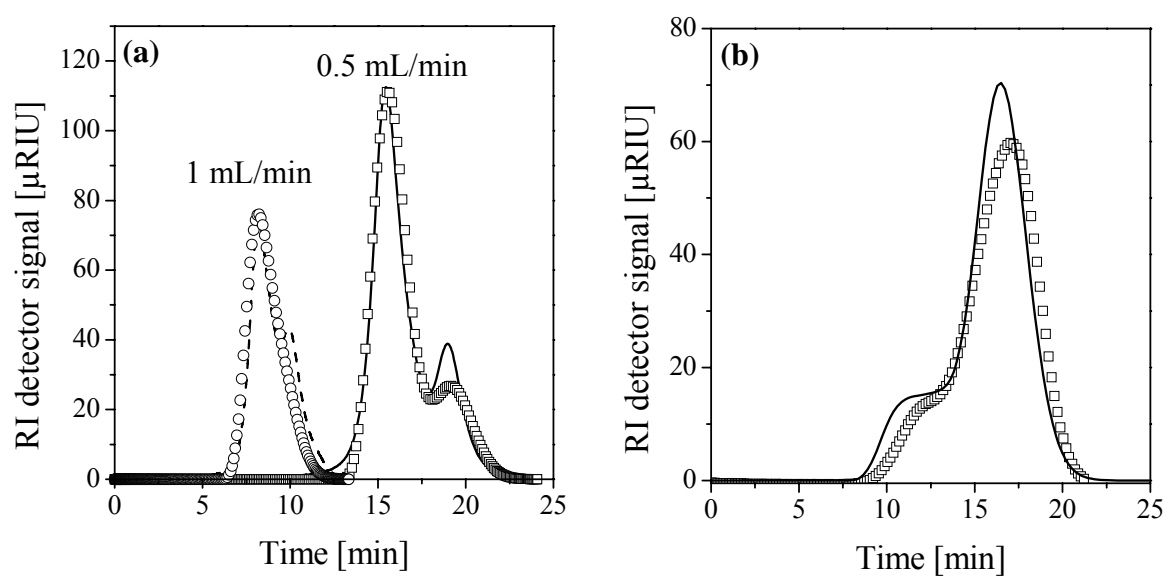
Figure 6.16. Comparisons of the chromatograms simulated (lines) using the obtained rate constants (Table 6.12) and the measured results (symbols) for the hydrolysis of (**a**) methyl formate using Cat1 at 25 ^{o}C, and (**b**) methyl acetate using Cat2 at 25 ^{o}C.

Summary and Conclusions

The purpose of this work was to enlarge the database regarding heterogeneously catalyzed hydrolysis reactions of esters. These reactions are potential candidates to be carried out successfully in chromatographic reactors, where the reaction is performed simultaneously with a chromatographic product separation. To this end, an analysis of thermodynamics and kinetics of the hydrolysis of four esters was done, namely methyl formate, methyl acetate, ethyl formate, and ethyl acetate with an acidic ion-exchange resin as a solid catalyst.

The chemical reaction equilibria of the four hydrolysis reactions were studied experimentally. The influence of the solid catalyst on the liquid-phase equilibrium compositions in a batch reactor was measured. Regarding the experimental investigation of the reaction kinetics of the four reactions a calorimetric technique was employed. Reaction rate constants were quantified from transients of measured heat flows. Besides, these constants were also quantified from the concentration profiles obtained in conventional batch experiments. Idealities and non-idealities of both liquid and polymer solutions were taken into account during data analysis.

The distribution equilibrium constants of the relevant components (esters, acids and alcohols) on the catalysts were available from separately performed chromatographic fixed-bed reactor experiments. It was found that in an excess of water the acids elute first, followed by the alcohols and then the esters. The study also revealed that a linear adsorption isotherm model [Eq. (2.41)] can be adequately applied to quantify the equilibria for the components that are present in the liquid phase at low concentrations (Section 6.2).

The reaction equilibrium constants of the four hydrolysis reactions were determined from the measured equilibrium compositions in a conventional reactor. In the case that more than one ester is present in an initial mixture with water, aside from the hydrolysis of esters, in principle transesterification reactions can also take place. However, the obtained equilibrium compositions show that at a given temperature, the equilibrium constant of the hydrolysis of a certain ester is almost the same when another ester is present in the mixture. The influence of temperature on the equilibrium constants of the four hydrolysis reactions was studied as well. It was shown that a temperature increase shifts the reaction equilibria to the product side. This is due to the fact that the hydrolysis reaction is endothermal (Table 3.4) and in agreement with Le Chatelier's principle.

The influence of the amount of solid catalyst on the liquid-phase equilibrium composition in a batch reactor was studied. Equilibrium compositions calculated from the model are in agreement with that measured experimentally. It was found that the selective adsorption of components on the catalyst has an effect on the liquid phase equilibrium composition in a batch reactor (Table 6.8).

Simplified mathematical models describing the essential features of the reaction calorimeter were developed and applied. An initial analysis shows that the influence of intraparticle mass transfer limitations is very small. Therefore, a simple pseudohomogeneous model can be applied to describe the processes taking place in the batch reactor and/or calorimeter. Kinetic expressions for the four ester hydrolysis reactions were established. The free parameters were quantified from heat flow transients measured in the calorimeter. Aside from using the kinetic expressions based on concentrations, the kinetic parameters were also quantified using the kinetic expressions based on activities to take into account non-idealities of both liquid and solid phases. The results prove that because of the large liquid-phase fraction, the contribution of the homogeneous reaction is significant in the calorimetric reactor, compared to well-packed fixed-bed reactors with a higher solid-phase fraction. Regarding the quantification of reaction rate constants, this work demonstrated that heat flow signals measured with reaction calorimeters can provide a rapid method for determining rate constants of simple reactions, provided the sensitivity of the device is sufficient. In case of the hydrolysis reactions methyl formate and methyl acetate, the reaction rate constants quantified from heat flow signals agree well with that quantified using conventional batch reactor and fixed-bed chromatographic reactor experiments.

The results obtained further reveal interesting tendencies concerning the changes of reaction rate constants and distribution equilibrium constants relevant for the hydrolysis reactions of the four different esters studied. The hydrolysis of methyl formate is the fastest

reaction, followed by the hydrolysis of ethyl formate and the hydrolysis of methyl acetate. The slowest reaction is the hydrolysis of ethyl acetate, which makes this reaction most attractive for applying a chromatographic reactor capable to separate ethanol and acetic acid.

The presented data could prove useful in the design and the optimization of chromatographic reactors (CR) and simulated moving bed reactors (SMBR).

In further work, non-isothermal effects must be further taken into account in the reactor analysis in more detail.

Nomenclature

Latin Symbols

Symbol	Unit	Description
a_i	mol/L	Activity of component i
a_i^L	mol/L	Activity of component i in the liquid phase
a_i^S	mol/L	Activity of component i in the solid phase
a_{ij}^u	–	UNIQUAC interaction parameters
A	kJ	Helmholtz free energy
A_W	m^2	Heat transfer area
b_i	L/mol	Adsorption isotherm parameters
c	mol/L	Liquid-phase concentration
c^{norm}	–	Normalized concentration
c_p	J/(kg K)	Specific heat capacity
c_p^o	J/(kg K)	Standard specific heat capacity
d_R	m	Diameter of the stirrer
Δc_p^o	kJ/(kg K)	Standard heat capacity change of reaction
ΔG_f^o	J/mol	Standard Gibbs free energy of formation
ΔG_r	J/mol	Gibbs free energy change of reaction
ΔG_r^o	J/mol	Standard Gibbs free energy change of reaction
ΔH_{ads}	J/mol	Heat of adsorption
ΔH_f^o	J/mol	Standard enthalpy of reaction
ΔH_r	J/mol	Reaction enthalpy
ΔH_r^o	J/mol	Standard reaction enthalpy
ΔH_{st}	J/mol	Isosteric heat of adsorption
ΔS_r	J/(mol K)	Entropy change of reaction
ΔS_r^o	J/(mol K)	Standard entropy change of reaction
E_A	J/mol	Activation energy
f_i	bar	Fugacity of component i in solution

f_i^o	bar	Standard fugacity of component i
$\dot{F}$	g/s	Feed rate
g	J/mol	Molar Gibbs free energy
g_i	J/mol	Partial molar Gibbs free energy
g^C	J/mol	Combinatorial part of excess Gibbs free energy
g^E	J/mol	Molar excess Gibbs free energy
g_i^E	J/mol	Partial molar excess Gibbs free energy
g^R	J/mol	Residual part of excess Gibbs free energy
G	J	Gibbs free energy
G^E	J	Excess Gibbs free energy
H	J	Enthalpy
H_i^o	J	Standard enthalpy of component i
h_j	J/(m²sK)	Heat-transfer coefficient for the jacket side
h_r	J/(m²sK)	Heat-transfer coefficient for the reactor side
k	L/(mol min)	Reaction rate constant
k_o	L/(mol min)	Pre-exponential factor
k^{het}	L/(mol min)	Rate constant of heterogeneously catalyzed reaction
$k_{(a)}^{het}$	L/(mol min)	Rate constant of heterogeneously catalyzed reaction in real polymer solutions
$k_{(c)}^{het}$	L/(mol min)	Rate constant of heterogeneously catalyzed reaction in ideal polymer solutions
k^{hom}	L/(mol min)	Rate constant of homogeneously catalyzed reaction
$k_{(a)}^{hom}$	L/(mol min)	Rate constant of homogeneously catalyzed reaction in real liquid solution
$k_{(c)}^{hom}$	L/(mol min)	Rate constant of homogeneously catalyzed reaction in ideal liquid solution
K	–	Reaction rate constant
K_i	–	Constant describing the distribution equilibrium
K_a	–	Activity-based reaction equilibrium constant
K_c	–	Concentration-based reaction equilibrium constant
L	m	Thickness of the reactor wall
M	g, kg	Mass
M_i	g/mole	Molar mass of component i
n_i	–	Mole number of component i
n_i^L	–	Mole number of component i in the liquid phase
n_i^S	–	Mole number of component i in the solid phase
N_c	–	Number of components
Ne	–	The Newton number

N_R	–	Number of reactions
p	bar, Pa	Pressure
p^o	bar, Pa	Pressure at standard state
p^L	Pa	Pressure in the liquid phase
p^S	Pa	Pressure in the solid phase
q	mol/L	Loading on the solid phase
q_{av}	mol/L	Average loading on the solid phase
$q_{s,i}$	mol/L	Saturation loading capacity on the solid phase
q_i^u	–	Pure-component molecular-structure constants depending on external surface areas (UNIQUAC)
q^*	mol/L	Equilibrium loading on the solid phase
$\dot{Q}$	J/s	Heat flow
$\dot{Q}_c$	J/s	Heat flow due to the calibration heater
$\dot{Q}_{chem}$	J/s	Heat flow due to chemical reactions
$\dot{Q}_{dos}$	J/s	Heat flow caused by dosing
$\dot{Q}_{loss}$	J/s	Heat lost to the surroundings
$\dot{Q}_{mix}$	J/s	Heat low occurring due to non ideal mixing of different fluids
$\dot{Q}^{norm}$	–	Normalized heat flow
$\dot{Q}_{phase}$	J/s	Heat flow due to phase change processes
$\dot{Q}_{stir}$	J/s	Heat evolved by the stirrer
$\dot{Q}_{tot}$	J/s	Total heat flow
$\dot{Q}_{transfer}$	J/s	Heat transfer between the liquid and the solid phase
$\dot{Q}_{wall}$	J/s	Heat flow over calorimeter wall
r	mol/(L min)	Reaction rate
r^{het}	mol/(L min)	Rate of heterogeneously catalyzed reaction
r^{hom}	mol/(L min)	Rate of homogeneously catalyzed reaction
$r_i^{overall}$	mol/(L min)	Overall rate of transformation of component i
r_i^u	–	Pure-component molecular-structure constants depending on molecular size (UNIQUAC)
R	J/(mol K)	Universal gas constant
$\mathfrak{R}$	–	Proportionality constant dependent on temperature and pressure
S	J/K	Entropy
S^{el}	J/K	Entropy of the elastic structure
S^L	J/K	Entropy of the liquid phase

S^S	J/K	Entropy of the solid phase
t	min	Time coordinate
t_R	min	Retention time
T	K	Temperature
T_j	K	Jacket temperature
T_r	K	Reactor temperature
T_W	K	Temperature of the reactor wall
U	J	Internal energy
U^{el}	J	Internal energy of the elastic structure
U^L	J	Internal energy of the liquid phase
U^S	J	Internal energy of the solid phase
U_W	J/(m^{2}sK)	Overall heat-transfer coefficient for the reactor wall
V	m^3, L	Volume
V^{el}	m^3, L	Volume of the elastic structure
V^L	m^3, L	Volume of the surrounding liquid
$V^{L,o}$	m^3, L	Total volume of the liquid including the volume of liquids in the solid phase
V^S	m^3, L	Volume of the solid phase
$V^{S,o}$	m^3, L	Volume of the unswollen undeformed solid sample
V_m	m^3/mol, L/mol	Molar volume
V_R	m^3, L	Reactor volume
V_{Re}^{eq}	m^3, L	Volume of resin at equilibrium
V_{Re}^{o}	m^3, L	Volume of dry resin
W	J	Work
x	–	Mole fraction
z	–	Coordination number

Greek Symbols

Symbol	Unit	Description
α	–	Deformation factor
β	min^{-1}	Internal mass transfer coefficient
γ	–	Activity coefficient
ε	–	Liquid fraction or porosity
θ	–	Area fraction
λ_W	J/(m^{2}sK)	Heat conduction coefficient through the reactor wall
μ	J/mol	Chemical potential

v	–	Stoichiometric coefficient
ξ	mol	Reaction extent
π_{sw}	Pa	Swelling pressure
ρ	g/L	Density
ρ_r	g/L	Density of the reaction mixtures
τ	N/m^2	Nominal stress
φ	–	Number of phases
Φ	–	Segment fraction

Superscripts and Subscripts

a	activity (real solution)
A	activation
Ac	acid
ads	adsorption
av	average
c	concentration (ideal solution), component or calibration
C	combinatorial
$chem$	chemical
dos	dosing
E	excess
el	elastic structure
end	end, final
eq or $*$	equilibrium
ext	external
f	formation
het	heterogeneous
hom	homogeneous
i	ith component
inj	injection
j	jth reaction or jacket
L	liquid phase
$loss$	loss
m	molar
mix	mixing
mod	modified
$norm$	normalized
$phase$	phase

r, R	reaction, reactor, retention or residual
Re	resin
s	saturation
S	solid phase, polymer phase
st	isosteric
stir	stir
sw	swelling
sys	system
tot	total
transfer	transfer
u	UNIQUAC
W, wall	wall
0	initial or standard state

References

[Abra75]   Abrams, D.S. and Prausnitz, J.M., Statistical Thermodynamics of Liquid Mixtures: A New Expression for the Excess Gibbs Energy of Partly or Completely Miscible Systems. *AIChE J.*, **1975**, *21*, 116–128.

[Afee05]   Afeefy, H.Y.; Liebman, J.F. and Stein, S.E., "Neutral Thermochemical Data" in *NIST Chemistry WebBook, NIST Standard Reference Database Number 69*, Eds. Linstrom, P.J. and Mallard, W.G., June 2005, National Institute of Standards and Technology, Gaithersburg MD, 20899 (http://webbook.nist.gov).

[Ander66] Andersen, H.M., Isothermal Kinetic Calorimeter Applied to Emulsion Polymerization. *Journal of Polymer Science Part A-1*, **1966**, *4*, 783–791.

[Ander69] Andersen, H.M., Polymerization Rates by Calorimetry II. *Journal of Polymer Science Part A-1*. **1969**, *7*, 2889–2896.

[Ander78] Anderson, T.F. and Prausnitz, J.M., *Ind. Eng. Chem. Process Des. Dev.*, **1978**, *17*, 552–561.

[Atki02]   Atkins, P.W. and Paula, J.D., *Atkins's Physical Chemistry*; Oxford Univ. Press: Oxford, U.K., 2002.

[Bala69]   Balashov, M.I.; Serafimov, L.A. and L'Vov, S.V., Hydrolysis of Methyl Acetate in Concentrated Solutions in Presence of Sulfonated Cation Exchanger. *Zn Prikl Khim*, **1969**, *42* (8), 1865–1871.

[Ball00]   Balland, L.; Estel, L.; Cosmao, J.M. and Mouhab, N., A genetic algorithm with decimal coding for the estimation of kinetic and energetic parameters. *Chemometrics and Intelligent Laboratory Systems*, **2000**, *50* (1), 121–135.

[Ball02]   Balland, L.; Mouhab, N.; Cosmao, J.M. and Estel, L., Kinetic parameter estimation of solvent-free reactions: application to esterification of acetic anhydride by methanol. *Chem. Eng. Process.*, **2002**, *41*, 395–402.

[Barin89]   Barin, I. and Sauert, F., *Thermochemical Data of Pure Substances*; Verlag Chemie: Weinheim, Germany, 1995.

[Beck68]   Becker, F., Thermokinetische Messmethoden. *Chemie Ingenieur Technik*, **1968**, *19*, 933–980.

[Bell55]   Bell, R.P.; Dowding, A.L. and Noble, J.A., The kinetics of the ester hydrolysis in concentrated aqueous acids. *Journal of the Chemical Society*, London, **1955**, part III, 3106–3110.

[Bocek69]   Bocek, P.; Novak, J. and Janak, J., *J. Chromatogr.,* **1969**, *42*, 1.

[Bolm83]   Bolme, M.W. and Lange, S.H., The Liquid Chromatographic Reactor for Kinetic Studies. *The Journal of Physical Chemistry*, **1983**, *87*, 18.

[Borr05]   Borren, T. and Fricke, J., Chromatographic Reactors. In: *Preparative Chromatography of Find Chemicals and Pharmaceutical Agents*, edited by Schmidt-Traub, H.; Wiley-VCH Verlag GmbH & Co. KGaA.: Weinheim, Germany, 2005.

[Butt00]   Butt, J. B., *Reaction Kinetics and Reactor Design*; Marcel Dekker: New York, USA, 2000.

[Chemis]   Chemisens, www.chemisens.com

[Cho80a]   Cho, B.K.; Carr, Jr.; Robert, W. and Aris, R., Continuous Chromatographic Reactors. *Chem. Eng. Sci.*, **1980**, *35* (1/2), 74–81.

[Cho80b]   Cho, B.K.; Carr, Jr.; Robert, W. and Aris, R., A New Continuous Flow Reactor for Simultaneous Reaction and Separation. *Sep. Sci. and Techn.*, **1980**, *15* (3), 679–696.

[Clark71]   Clarke, A., and Grant, D.W. in *Gas Chromatography 1970*, R. Stock Ed., The Institute of Petroleum: London, UK, 1971, p. 189.

[Conn90]   Connors, K.A., *Chemical Kinetics: the Study of Reaction Rates in Solution*; VCH: New York, USA, 1990.

[Coon33]   Coon, E.D. and Daniels, F., An isothermal calorimeter for slow reactions, *J. Phys. Chem.*, **1933**, *37*, 1–12.

[CRC05]   *CRC Handbook of Chemistry and Physics, Internet version 2005*; David R. Lide, ed., <http://www.hbcpnetbase.com>, CRC Press, Boca Raton, FL, 2005.

[Do98]   Do, D.D., *Adsorption Analysis: Equilibrium and Kinetics*, Imperial College Press: London, UK, 1998.

[Du99]   Du, Y. and Wang, L., Kinetic Study on Hydrolysis of Methyl Acetate. *Journal of Fuzhou University (Natural Science)*, **1999**, *27* (4), 98–102.

[Dyer02]   Dyer, U.C.; Henderson ,D.A.; Mitchel, M.B. and Tiffin, P.D., Scale-Up of a Vilsmeier Formylation Reaction: Use of HEL Auto-MATE and Simulation Techniques for Rapid and Safe Transfer to Pilot Plant from Laboratory. *Organic Process Research & Development*, **2002**, *6*, 311–316.

[Falk99]   Falk, T. and Seidel-Morgenstern, A., Comparison between a Fixed-Bed Reactor and a Chromatographic Reactor. *Chem. Eng. Sci.* **1999**, *54*, 1479–1485.

[Falk02]   Falk, T. and Seidel-Morgenstern, A., Analysis of a Discontinuously Operated Chromatographic Reactor. *Chem. Eng. Sci.* **2002**, *57*, 1599–1606.

[Flory53] Flory, P., *Principles of Polymer Chemistry*; Cornell University Press: Ithaca, NY, 1953.

[Gelo03]   Gelosa, D.; Ramaioli, M.; Valente; and Morbidelli, M. Chromatographic Reactors: Esterification of Glycerol with Acetic Acid Using Aciduc Polymeric Resins. *Ind. Eng. Chem. Res.* **2003**, *42*, 6536–6544.

[Gill67]   Gill, J.M.; Baumann, F. and Tao, F., *Previews and Reviews*, Varian Aerograph, August 1967.

[Gmeh02]   Gmehling, J.; Onken, U. and Arlt, W., *Vapor-Liquid Equilibrium Data Collection,* Chemistry Data Series, vol. I, parts 1-8, DECHEMA, Frankfurt/Main, 2002.

[Goed69]   Goedert, M. and G. Guiochon, *J. Chromatogr. Sci.,* **1969**, *7*, 323.

[Goed71]   Goedert, M. and Guiochon, G., *Chim. Anal.,* **1971**, *53*, 214.

[Goed73a] Goedert, M. and Guiochon, G., *Chromatographia,* **1973**, *6*, 116.

[Goed73b] Goedert, M. and Guiochon, G., *J. Chromatogr. Sci.,* **1973**, *11*, 326.

[Goed73c] Goedert, M. and Guiochon, G., *Chromatographia,* **1973**, *6*, 76.

[Goto83]   Goto; Shigeo; Teshima and Hideo, Kinetics Studies on Ion-Exchange Resins. *Memoirs of the Faculty of Engineering, Nagoya University*, **1983**, *35* (2), 254–300.

[Grant71] Grant, D.W. and Clarke, A., *Anal. Chem.,* **1971**, *43*, 1951.

[Grop06]   Grop, S. and Hasse, H., Reaction Kinetics of the Homogeneously Catalyzed Esterification of 1-Butanol with Acetic Acid in a Wide Range of Initial Compositions. *Ind. Eng. Chem. Res.*, **2006**, *45*, 1869–1874.

[Guio71]   Guiochon, G.; Geodert, M. and Jacob, L. in *Gas Chromatography 1970*, R. Stock Ed., The Institute of Petroleum: London, UK, 1971, p. 160.

[Guio88]   Guiochon, G. and Guillemin, C.L., *Quantitative Gas Chromatography for laboratory analyses and on-line process control*; Elsevier: Amsterdam, The Netherlands, 1988.

[Günth06] Günther W. H. Höhne, Thermal Analysis and Calorimetry. In: *Ullmann's Encyclopedia of Industrial Chemistry*, 7th ed., Electronic Release 2006; Wiley-VCH Verlag GmbH & Co. KGaA.: Weinheim, Germany.

[Harri03] Harriott, P., *Chemical Reactor Design*; Marcel Dekker: New York, USA, 2003.

[Hass00]   Hansen, D. L. Calorimetric Measurement of the Kinetics of Slow Reactions. *Ind. Eng. Chem. Res*. **2000**, *39*, 3541–3549.

[HEL]   HEL, www.helgroup.co.uk

[Hemm84]   Hemminger, W. and Höhne, G., *Calorimetry: Fundamentals and Practice*; Verlag Chemie: Weinheim, 1984.

[Hent79]   Hentschel, B., Ein automatisches, kontinuierlich registrierendes isothermes Kalorimeter - insbesondere zur Bestimmung der Polymerisationskinetik. *Chemie Ingenieur Technik*, **1979**, *51* (8), 823.

[Hine74]   Hine, J. and Klueppet, A.W., Structural effects on rates and equilibria. XVIII. Thermodynamic stability of ortho esters, *J. Am. Chem. Soc.*, **1974**, *96*, 2924–2929.

[Hiwa04]   Hiwale, R.S.; Bhate, N.V.; Mahajan, Y.S. and Mahajani, S.M., Industrial Applications of Reactive Distillation: Recent Trends. *International Journal of Chemical Reactor Engineering*, **2004**, *2*.

[Indu93]   Indu, B.; Ernst, W.R. and Gelbaum, L.T., Methanol-Formic Acid Esterification Equilibrium in Sulfuric Acid Solutions: Influence of Sodium Salt. *Ind. Eng. Chem. Res.*, **1993**, *32*, 981–985.

[Jaku92]   Jakubith, M., *Memofix–Chemie und Chemietechnik*; VCH Verlagsgesellschaft: Weinheim, 1992.

[Jecko67]   Jecko, G. and Reynaud, B., *Rev. Metal.*, **1967**, *64*, 681.

[Jeng92]   Jeng, C.Y. and Langer, S.H., Reaction Kinetics and Kinetic Processes in Modern Liquid Chromatographic Reactors. *Journal of Chromatography*, **1992**, *589*, 1–30.

[Kaiser69] Kaiser, R., *Methodes Phys. Anal.,* **1969**, *5*, 357.

[Karl87a]   Karlsen, L.G. and Villadsen, J., Isothermal Reaction Calorimeters - I a Literature Review. *Chem. Eng. Sci.,* **1987**, *42* (5), 1153–1164.

[Köhl72]   Köhler, W.; Riedel, O. and Scherer, H., Ein mit Heizpulsen gesteuertes isothermes Kalorimeter. Teil I: Aufbau und Messanordnung. *Chemie Ingenieur Technik*, **1972**, *44* (21), 1216–1218.

[King69]   King, W.H. and Dupre, G.D., *Anal. Chem.*, **1969**, *41*, 1936.

[Kirb01]   Kirbaslar, S.I.; Baykal, Z.B.; Dramur, U., Esterification of Acetic Acid with Ethanol Catalyzed by Ion-Exchange Resin. *Turk. J. Engin. Environ. Sci.,* **2001**, *25*, 569–577.

[Land91]   Landau, R. N.; Williams, L. R. Reaction Calorimetry: A Powerful Tool. *Chem. Eng. Prog*. **1991**, *87* (12), 65–69.

[Land94]   Landau, R.N.; Blackmond, D.G. and Tung, H.H. Calorimetric Investigation of an Exothermic Reaction: Kinetic and Heat Flow Modelling. *Ind. Eng. Chem. Res.*, **1994**, *33*, 814–820.

[Land96]   Landau, R.N., Expanding the role of reaction calorimetry. *Thermochimica Acta*, **1996**, *289* (2), 101–126.

[Lange99] *Lange's Handbook of Chemistry - 15th ed.*, ed. Dean, J. A; McGraw-Hill, 1999.

[LeBl96]   LeBlond, C.; Wang, J.; Larsen, R.D.; Orella, C.J.; Forman, A.L.; Landau, R.N.; Laquidara, J.; Sowa, J.R.; Blackmond, D.G. and Sun, Q.K., Reaction calorimetry as an insitu kinetic tool for characterizing complex reactions. *Thermochimica Acta*, **1996,** *289* (2), 189–207.

[Leve99]   Levenspiel, O., *Chemical Reaction Engineering*; John Wiley & Sons: New York, USA, 1999.

[Lode02]   Lode, F., *A Simulated Moving Bed Reactor (SMSR) for Esterifications*. Diss. ETH Nr. 14350, Shaker Verlag, Aachen 2002.

[Lode03]   Lode, F.; Francesconi, G.; Mazzotti, M. and Morbidelli, M., Synthesis of Methylacetate in a Simulated Moving-Bed Reactor: Experiments and Modeling. *AIChE Journal*, **2003**, *49* (6), 1516–1524.

[Mai04]   Mai, P.T.; Vu, T.D.; Mai, K.X. and Seidel-Morgentern, A., Analysis of Heterogeneously Catalyzed Ester Hydrolysis Performed in a Chromatographic Reactor and in a Reaction Calorimeter. *Ind. Eng. Chem. Res.,* **2004**, *43*, 4691–4702.

[Matlab]   http://www.mathworks.com

[Maur96]   Maurer, G. and Prausnitz J.M., Thermodynamics of Phase Equilibrium for systems Containing Gels. *Fluid Phase Equilibria*, **1996**, *115*, 113–133.

[Mazz97a] Mazzotti, M., Neri, B., Gelosa, D., Kruglov, A., Morbidelli, M., Kinetics of Liquid-Phase Esterification Catalyzed by Acidic Resins. *Ind. Eng. Chem. Res.,* **1997**, *36*, 3–10.

[Mazz97b] Mazzotti, M.; Neri, B.; Gelosa, D.; Morbidelli, M. Dynamics of a Chromatographic Reactor: Esterification Catalyzed by Acidic Resins. *Ind. Eng. Chem. Res.* **1997**, *36*, 3163–3172.

[Meek68] Meeks, M.R. An Analog Computer Study of Polymerization Rates in Vinyl Chloride Suspensions. *Polymer Engineering and Science*, **1968**, *9* (2), 141–151.

[Merck05] Merck AG, Chemikalien und Reagenzien für das chemische Labor, Darmstadt, 2005.

[Mettler] Mettler Toledo, www.mt.com

[Miss99] Missen, R.W.; Mims, C.A. and Saville, B.A., *Introduction to Chemical Reaction Engineering and Kinetics*; John Wiley & Sons: Chichester, U.K., 1999.

[Myers65] Myers, A.L. and Prausnitz, J.M. Thermodynamics of Mixed-Gas Adsorption. *AIChE Journal*, **1965**, *11* (1), 121–127.

[Neve02] Nevers, N.D., *Physical and Chemical Equilibrium for Chemical Engineering*; John Wiley & Sons: New York, USA, 2002.

[Newl36] Newling, W.B.S. and Hinshelwood, C.N., The kinetics of the acid and the alkaline hydrolysis of esters. *Journal of the Chemical Society*, London, **1936**, part II, 1357–1361.

[Nilss82] Nilsson, H.; Solvegren C.; Toernell, B., A Calorimetric Reactor System for Kinetic Studies of Heterogeneous Polymerizations. *Chemica Scripta*, **1982**, *19*, 164–171.

[O´con05] O´connell, J.P. and Haile, J.M., *Thermodynamics: Fundamentals for Applications*; Cambridge University Express: New York, USA, 2005.

[Pastré00] Pastré, J., *Beitrag zum erweiterten Einsatz der Kalorimetrie in frühen Phasen der chemischen Prozessentwicklung*; ETH Zürich, Diss. ETH Nr. 13840, 2000.

[Pastré01] Pastré, J.; Zogg, A.; Fischer, U. and Hungerbühler, K., Determination of Thermodynamical and Kinetic Parameters using a small Power Compensation Calorimeter with and integrated FTIR Probe. *Organic Process Research & Development*, **2001**, *5* (2), 158–166.

[Pauer99]   Pauer, W.; Tchonkou, J.P.; Moritz, H.U. and Brown, D., Ein neues isothermes Wärmebilanzkalorimeter. *Workshop Reaktionskalorimetrie*, **1999**, DECHEMA e.V., Frankfurt.

[Perry99]   *Perry's Chemical Engineers' Handbook - 7th ed.*, eds. Perry, R.H.; Grenn, D.W. and Maloney, J.O.; McGraw-Hill, 1999.

[Poll01]   Pollard, M., Process Development Automation: An Evolutionary Approach. *Organic Process Research & Development*, **2001**, *5*, 273–282.

[Pöpk00]   Pöpken, T.; Götze, L. and Gmehling, J., Reaction Kinetics and Chemical Equilibrium of Homogeneously and Heterogeneously Catalyzed Acetic Acid Esterification with Methanol and Methyl Acetate Hydrolysis. *Ind. Eng. Che. Res.*, **2000**, *39*, 2601–2611.

[Pöpk01]   Pöpken, T.; Steinigeweg, S. and Gmehling, J., Synthesis and Hydrolysis of Methyl Acetate by Reactive Distillation Using Structured Catalytic Packings: Experiments and Simulation. *Ind. Eng. Che. Res.*, **2001**, *40*, 1566–1574.

[Prau99]   Praunitz, J.M.; Lichtenthaler, R.N. and Gomes de Azevedo, E., *Molecular Thermodynamics of Liquid-Phase Equilibria*; Prentice Hall PTR, New Jersey, Third Edition, 1999.

[Radke72]   Radke, C.J. and Prausnitz, J.M. Thermodynamics of Multi-Solute Adsorption from Dilute Liquid Solutions. *AIChE Journal*, **1972**, *18* (4), 761–768.

[Raja78]   Rajamani; Kuppuswami; Shenoy; Subhash, C.; Rao; Musti, S. and Manthripragada, G., Kinetics of the Hydrolysis of Ethyl Acetate Catalysed by Cation-Exchange Resin. *J. Appl. Chem. Biotechnol.*, **1978**, *28* (11), 699–708.

[Regen83]   Regenass, W., Thermische Methoden zur Bestimmung der Makrokinetik. *Chimia*, **1983**, *37* (11), 430–437.

[Regen97]   Regenass, W., The Development of Stirred-Tank Heat Flow Calorimetry as a Tool for Process Optimization and Process Safety. *Chimia*, **1997**, *51* (5), 189–200.

[Reid87]   Reid, R.C.; Prausnitz, J.M. and Poling, B.E., *The Properties of Gases and Liquids*; McGraw-Hill: New York, USA, 1987.

[Reut89]   Reutmann, W. and Kieczka, H., „Formic acid", in: *Ullmann's Encyclopedia of Industrial Chemistry*, 7th ed., Electronic Release 2006; Wiley-VCH Verlag GmbH & Co. KGaA.: Weinheim, Germany.

[Ruth84]   Ruthven, D.M., *Principles of Adsorption and Adsorption Processes*; John Wiley & Sons: New York, USA, 1984.

[Sainio04] Sainio, T.; Laatikainen, M. and Paatero, E., Phase Equilibrium in Solvent Mixture-Ion Exchange Resin Catalyst Systems. *Fluid Phase Equilibria.* **2004**, *218*, 269–283.

[Sainio05] Sainio, T., *Ion-Exchange Resins as Stationary Phase in Reactive Chromatography*. Diss. Lappeenranta University of Technology, Acta Universitatis Lappeenrantaensis 218, Lappeenranta, 2005.

[Sand99]   Sandler, S.I., *Chemical and Engineering Thermodynamics*; John Wiley & Sons: New York, USA, 1999.

[Sard79]   Sardin, M.; Villermaux, J. Esterification catalysee par une resine echangeuse de cation dans un reacteur chromatographique. *Nouv. J. Chim.* **1979**, *3*, 225–235.

[Sato87]   Sato, T.; Hohnosu, S. and Hartwig, J.F., Adsorption of Butachlor to Soils. *J. Agric. Food Chem.* **1987**, *35*, 397–402.

[Schild81] Schildknecht, J., Reaction Calorimeter for Applications in Chemical Process Industries: Performance and Calibration. *Thermochimica Acta*, **1981**, *49*, 87–100.

[Schle97]   Schlegel, M. and Löwe, A., A Reaction Calorimeter with Compensation Heater
            and Differential Cooling. *Chem. Eng. Process.*, **1997**, *37*, 61–67.

[Schu39]   Schultz, R.F, *Journ. Am. Chem. Soc.*, **1939**, *61*, 1443–1447.

[Schm98]   Sschmidt, L.D., *The Engineering of Chemical Reactions*; Oxford University
            Express: New York, USA, 1998.

[Semp98]   Sempere, J.; Nomen, R.; Rodriguez, J.L. and Papadaki, M., Modeling of the
            reaction of N-oxidation of 2 methylpyridine using hydrogen peroxide and a
            complex metal catalyst, *Chem. Eng. Sci.*, **1998**, *37*, 33–46.

[Shah54]   Shah, P.N. and Amis, E.S., The dielectric constant and salt effects upon the
            acid hydrolysis of ethyl formate. *Analytica Chimica Acta*, **1954**, *11*, 401–411.

[Simm00]   Simms, C. and Singh, J., Rapid Process Development and Scale-Up Using A
            Multiple Reactor System. *Organic Process Research & Development*, **2000**, *4*,
            554–562.

[Singh97]   Singh, J., Reaction Calorimetry for Process Development: Recent Advances.
            Process Safety Progress, **1997**, *16* (1), 43–49.

[Silva06]   Silva, V.M.T.M. and Rodrigues, A.E, Kinetic studies in a batch reactor using
            ion exchange resin catalysts for oxygenates production: Role of mass transfer
            mechanisms. *Chemical Engineering Science*, **2006**, *61*, 316–331.

[Smith81]   Smith, J.M., *Chemical Engineering Kinetics*; McGraw-Hill: New York, USA,
            1981.

[Smith82]   Smith, W.R. and Missen, R.W., *Chemical Reaction Equilibrium Analysis:
            Theory and Algorithms*; John Wiley: New York, USA, 1982.

[Smith96]   Smith, J.M.; Van Ness, H.C. and Abbott, M.M., *Introduction to Chemical
            Engineering Thermodynamics*; McGraw-Hill: New York, USA, 1996.

[Song98]   Song, W.; Venimadhavan, G.; Manning, J.M.; Malon, M.F.; Doherty, M.F.,
            Measurement of Residue Curve Maps and Heterogeneous Kinetics in Methyl
            Acetate Synthesis. *Ind. Eng. Chem. Res.* **1998**, *37*, 1917.

[Sund05]   Sundmacher, K.; Kinle, A. and Seidel-Morgenstern, A., *Integrated Chemical Processes: Synthesis, Operation, Analysis, and Control*; Wiley-VCH Verlag: Weinheim, Germany, 2005.

[Stapp02] Stappers, F.; Broeckx, R.; Leurs, S.; Den Bergh, L.V.; Agten, J.; Lambrechts, A.; Van den Heuvel, D. and De Smaele, D., Development of a Safe and Scalable Amine-to-Nitrone Oxidation: A Key Step in the Synthesis of R107500. *Organic Process Research & Development*, **2002**, *6*, 911–914.

[Stoye06] Stoye, D., Solvents. In: *Ullmann's Encyclopedia of Industrial Chemistry*, 7th ed., Electronic Release 2006; Wiley-VCH Verlag GmbH & Co. KGaA.: Weinheim, Germany.

[Stull69] Stull, D.R.; Westtrum, E.F. and Sinke, G.C., *The Chemical Thermodynamics of Organic Compounds*; John Wiley & Sons: New York, USA, 1969.

[Systag]   Systag, www.systag.ch

[Thom97]   Thomas, J.M. and Thomas, W.J., *Principles and Practice of Heterogeneous Catalysis*; VCH Verlag: Weiheim, Germany, 1997.

[Tomi98]   Tominaga, H. and Tamaki, M., *Chemical Reaction and Reactor Design*; John Wiley & Sons: Chichester, U.K., 1998.

[Ubrich99] Ubrich, O.; Srinivasan, B.; Lerena, P.; Bonvin, D. and Stoessel, F., Optimal feed profile for a second order reaction in a semi-batch reactor under safety constraints.
           Experimental Study, Journal of Loss Prevention in the Process Industries, **1999**, *12* (6), 485–493.

[Vilcu94] Vilcu, N. and Meltzer, V., Thermokinetics of the Ethyl Acetate Acid and Alkaline Hydrolysis by Differential Scanning Calorimeter. *Journal of Thermal Analysis*, **1994**, *41* (6), 1335–1341.

[Vu03]   Vu, T.D., *Investigation of Heterogeneous Catalyzed Ester Hydrolysis in a Chromatographic Reactor*; Ph.D. work in preparation, University of Magdeburg, started 2003.

[Vu06]   Vu, T.D.; Mai, P.T.; Kienle, A. and Seidel-Morgenstern, A.; Analysis of Temperature Effects on Ester Hydrolysis Reactions in a Fixed-Bed Chromatographic Reactor. *Poster, ISCRE 19th*, **2006**, Potsdam, Germany.

[West84]   Westerterp, K.R.; Van Swaaij, W.P.M. and Beennackers, A.A.C.M., *Chemical Reactor Design and Operation*; Wiley: Chichester, U.K., 1984.

[Weth74]   Wetherold, R.G.; Wissler, E.H.; Bischoff, K.P. and Kenneth, B., An Experimental and Computational Study of the Hydrolysis of Methyl Formate in a Chromatographic Reactor. *Advances in Chemistry Series*, **1974**, *13*, 181–190.

[Willi99]   Williams, P.A. and Dyer, A., *Advances in Ion Exchange for Industry and Research*; The Royal Society of Chemistry: Cambridge, UK, 1999.

[Wulk01]   Wulkow, M., *Manual of "Presto - Simulation of Kinetic Models"*; Computing in Technology GmbH: Rastede, Germany, 2001.

[Yu04]   Yu, W.; Hidajat, K. and Ray, A.K., Determination of Adsorption and Kinetic Parameters for Methyl Acetate Esterification and Hydrolysis Reaction Catalyzed by Amberlyst 15. *Applied Catalysis A: General*, **2004**, *260* (2), 191–205.

[Zeton] Zeton-Altamira, www.zetonaltamira.com

[Zogg93]   Zogg, M., *Einführung in die Mechanische Verfahrenstechnik*; B. G. Teubner, Stuttgart, 3rd edition, 1993.

Appendix A

Antoine Equation

Numerous mathematical formulas relating the temperature and pressure of the gas phase in equilibrium with the condensed phase have been proposed. The Antoine equation gives good correlation with experimental values for most substances. The Antoine equation is expressed as [Lang99]:

$$\log p = A - \frac{B}{T + C}$$
(A-1)

where p and T are the pressure and temperature of the gas phase in equilibrium with the condensed phase, respectively; A, B, and C are arbitrary constants to be obtained from the experimental data.

A simpler equation is the Clausius-Clapeyron equation as shown in Eq. (A-2). However, the Clausius-Clapeyron equation gives a perfect representation of the experimental data for only substances whose p versus $1/T$ plots are straight lines.

$$\log p = A - \frac{B}{T}$$
(A-2)

In fact, most substances produce a slightly curved vapor pressure line. The Antoine equation introduces a third arbitrary constant, C, to represent that curvature. There is no theoretical basis for introducing the third constant; it is simply the most successful simple way to modify the Clausius-Clapeyron equation, improving its ability to fit experimental data.

Values of Antoine constants A, B, and C for methyl formate are given in Table A-1. Using these constants' values and temperature, T, in $^{\circ}C$, the vapor pressure, p, is obtained in Torr (1 Torr = 133.322 Pa) by Eq. (A-1).
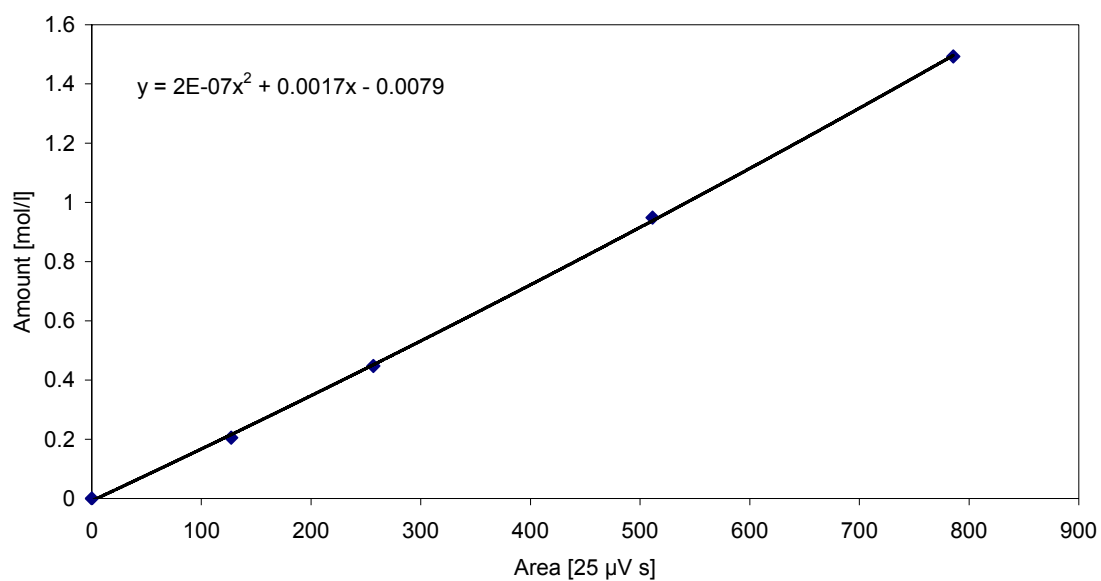
Table A-1. Antoine constants for methyl formate [Jaku92]

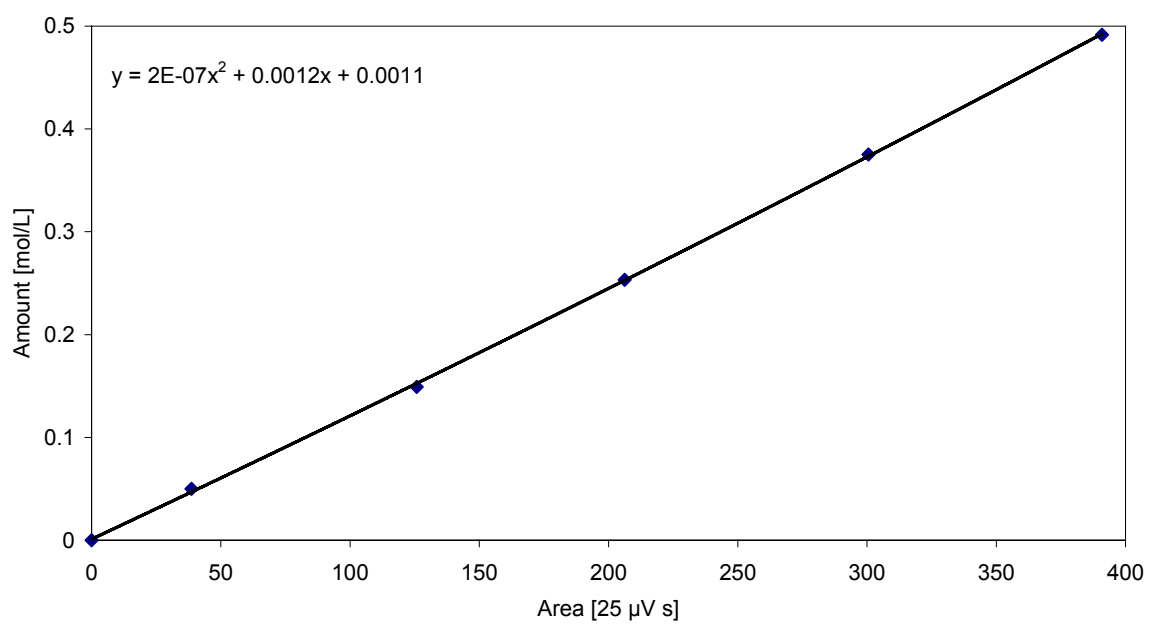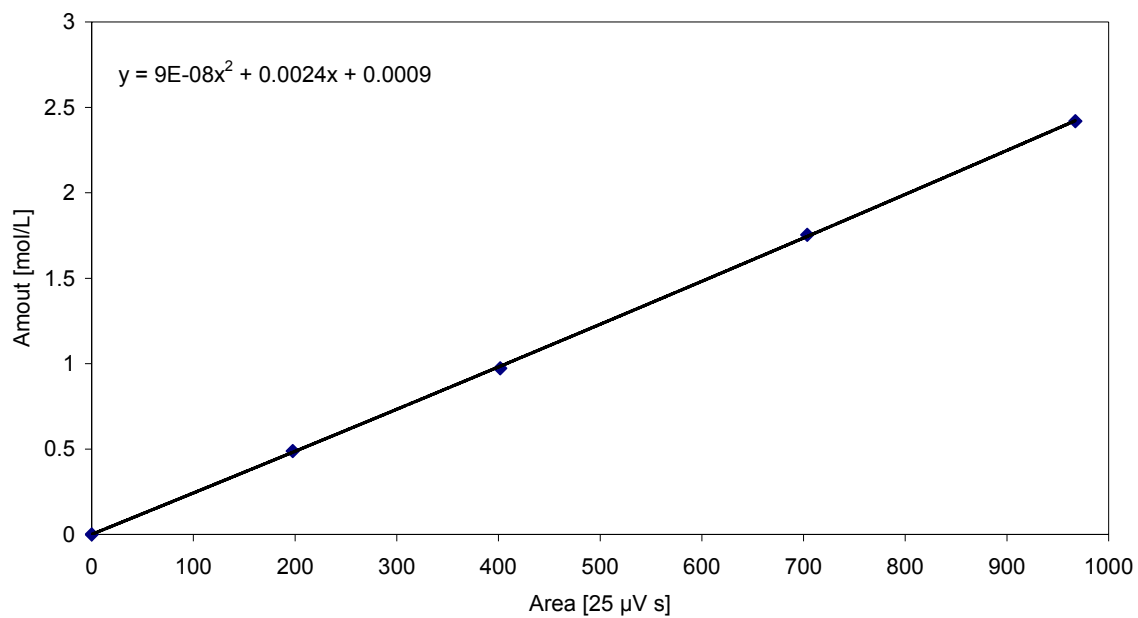| Substance	*A*	*B*	*C*
Methyl formate	3.02742	3.018	-11.880
Methyl acetate	7.0652	1157.63	219.73
Ethyl formate	7.009	1123.94	218.2
Ethyl acetate	7.10179	1244.95	217.88
Methanol	7.8975	1474.08	229.13
Ethanol	8.32109	1718.1	237.52
Formic acid	7.5818	1699.2	260.7
Acetic acid	7.38782	1533.313	22.309

Appendix B

GC Calibration curves

Methyl formate

$$y = 2E\text{-}07x^2 + 0.0017x - 0.0079$$

Methyl Acetate

$$y = 3E\text{-}07x^2 + 0.0013x + 0.0052$$

Ethyl Formate

$y = 2E\text{-}07x^2 + 0.0014x + 0.0011$

Ethyl Acetate

$y = 2E\text{-}07x^2 + 0.0012x + 0.0011$

Methanol

$y = 9E\text{-}08x^2 + 0.0024x + 0.0009$

Ethanol

$y = 8E\text{-}08x^2 + 0.0018x + 0.003$

Formic Acid

$y = -2E-07x^2 + 0.0024x + 0.0077$

Acetic Acid

$y = 1E-08x^2 + 0.0017x + 0.0054$
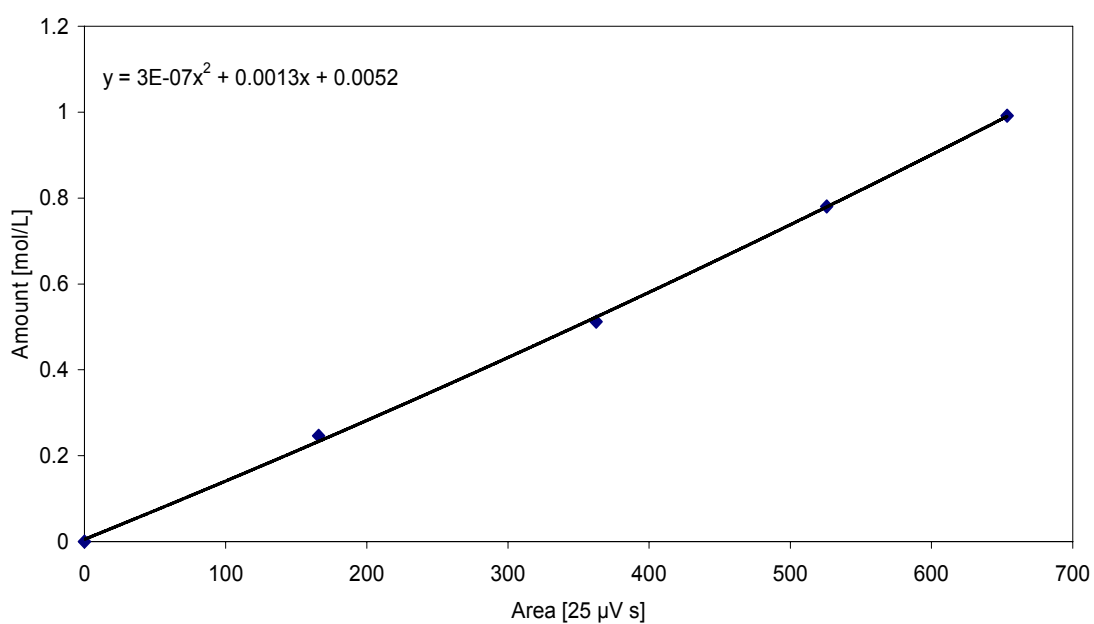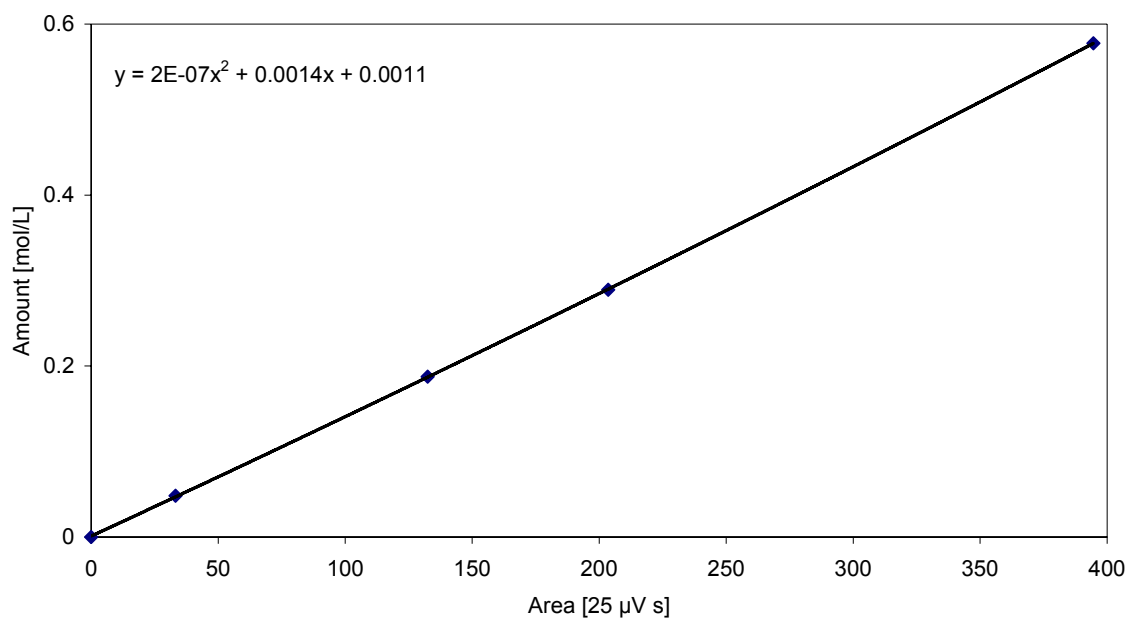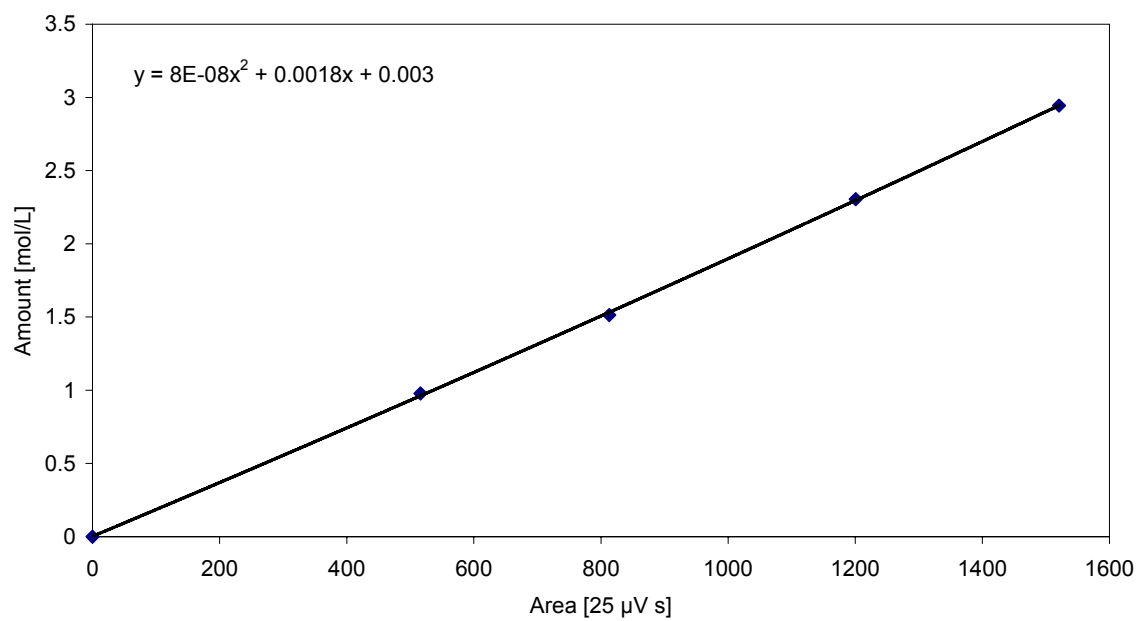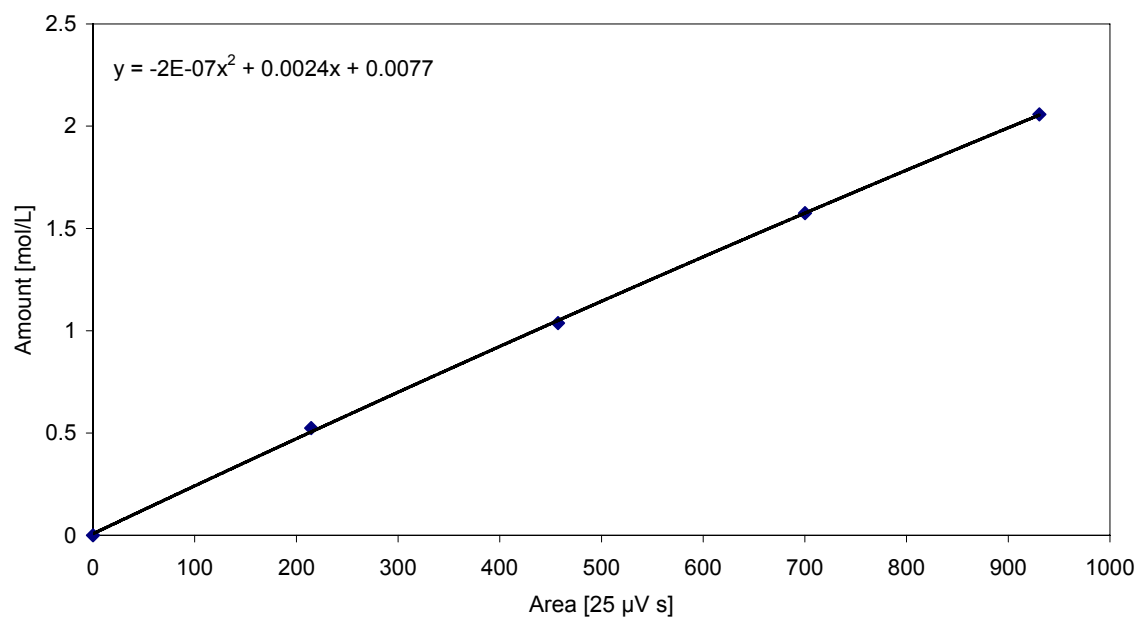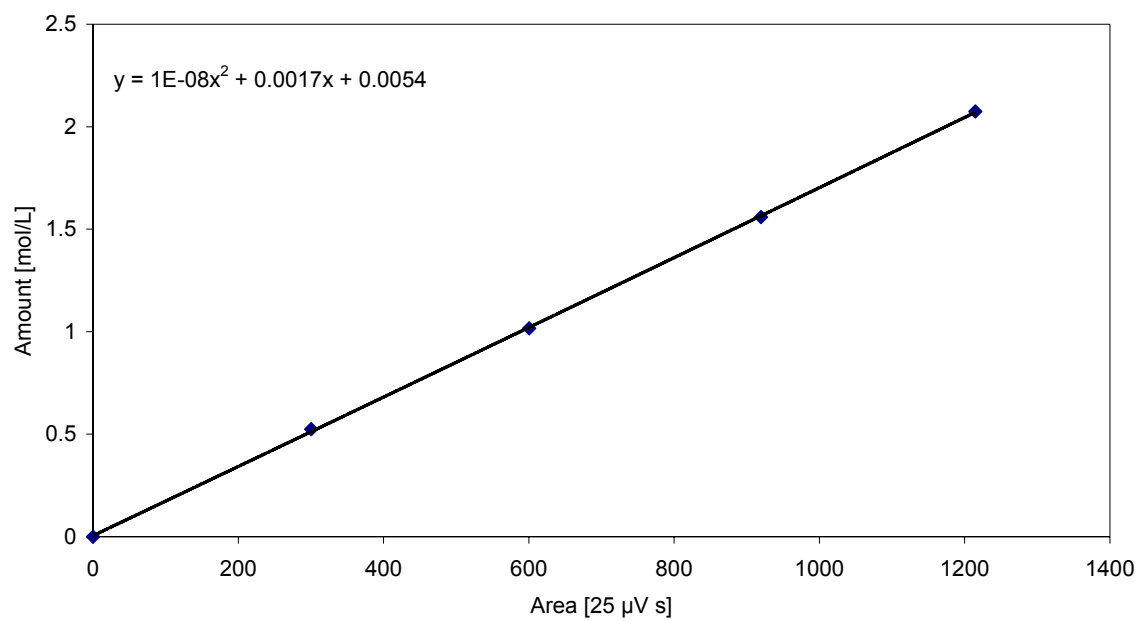
Lebenslauf

Persönliche Daten

Thanh-Phong Mai
55/4 Hung Vuong Str.
Dalat – Vietnam

Geburtstag	03/02/1972
Geburtsort	Ha-Tinh, Vietnam
Familienstand	ledig
Staatsangehörigkeit	vietnamesisch

Ausbildung

01/2002 – 12/2006:   Promotion am Institut für Verfahrenstechnik
an der Otto-von-Guericke-Universität Magdeburg
Promotionsthema: Experimental investigation of heterogeneously
catalyzed hydrolysis of esters

01/1998 – 09/1999:   Master of Engineering in Environmental Engineering
at Asian Institute of Technology, Bangkok, Thailand
Thesis topic: Modeling in water quality management: a case study
of the West Lake in Hanoi

10/1989 – 06/1994:   Bachelor of Chemical Engineering
at Hanoi University of Technology, Hanoi, Vietnam
Thesis topic: Analysis of dehydrogenation of furfurol using
metal oxide catalysts

Berufserfahrung

seit 01/2000:   Lecturer
at Faculty of Chemical Engineering
Hanoi University of Technology, Hanoi, Vietnam

01/1995 – 12/1997:   Quality Officer/ Internal Auditor
at the Institute for Standard and Quality
Ho Chi Minh City, Vietnam